Surge and Flood Modeling for Miami-Dade County (Task 2.10)

Submitted as Part of

2015 Validation of Ocean Outfall Legislation Compliance Plan

Prepared for

Miami-Dade Water and Sewer Department

June 2015

Executive Summary

Purpose

This report applies the projections of changes in sea level rise (SLR) and precipitation to estimate the resulting surge elevations and inland flood maps for specified climate events, which will be used by other components of the Miami-Dade Water and Sewer Department (WASD) program to develop wastewater facility hardening plans.

Background

Surge Modeling Approach and Assumptions

The purpose of the surge modeling is to provide surge boundary conditions to drive the flood model to assess flood propagation inland. The surge model, which couples waves, tides, and meteorologically induced surges, covers the entire North Atlantic stretching from Newfoundland to South America. The mesh resolution is refined progressively landward to resolve bathymetric details in the project vicinity.

Based on a review of hurricane climatology of the southeast coast of Florida within which the project site is located, Hurricane Andrew generated the largest surge event along the project coastline and was selected as the base hurricane set. A strategy of parallel shifts (north-south direction) in the historical track was adopted to derive the largest surge elevation at each of WASD's three wastewater treatment plants. The peak surge elevations extracted from Federal Emergency Management Agency (FEMA) transects were combined by selecting the maximum of the three track-based results. The composite modeled peak surge elevations were pegged to FEMA's Stillwater elevations to derive the 100 year (yr) surge elevations under specified SLR scenarios using linear scaling.

Two SLR projections of 1.23 meters (m) and 0.93 m in the year 2075 were adopted, based on preliminary guidance from the Southeast Florida Climate Compact. The results of the 1.23 m SLR scenario were applied as surge boundary conditions in flood modeling while the results of the 0.93 m SLR scenario were used to support the use of linear scaling of the 1.23 m SLR scenario results for other SLR projections as a first order estimate.

Flood Modeling Approach and Assumptions

Rapid flood inundation assessment was conducted for Miami-Dade County, with a focus on areas covered by the critical assets of the Ocean Outfall Legislation Program. The three modeling scenarios developed for inland inundation modeling include:

1. Hurricane Andrew (1992), based on measured coastal surge levels and measured rainfall
2. 100-year flood condition, based on FEMA 1 percent coastal flood elevation and estimated current 100-year precipitation
3. 100-year flood condition, based on FEMA 1 percent coastal flood elevation coupled with projected SLR in 2075 given by SE FL Climate Compact, and projected 2075 100-year precipitation.

Key Findings and Recommendations

In addition to providing surge boundary conditions for the flood model, the following findings from the surge modeling component are noteworthy:

1. SLR in the offshore does not translate in a linear fashion along the coast as the resulting water level surface appears to be affected by local shoreline planform and bathymetric features. For the Biscayne Bay, the largest peak water level amplification occurs near the central portion of the Bay.

2. SLR changes offshore can be approximated along the coast using a linear scaling approach, as demonstrated by comparing the modeled 0.93 meter SLR results and those based on linear scaling using the results of the modeled 1.23 meter SLR and without SLR scenarios but with slight tendency toward under-prediction.

For the flood modeling component, the 100-year inundation results are presented in Figure ES-1, while results for the 100-year scenario with climate change and SLR conditions are presented in Figure ES-2.

The future 100-year inundation map shows broad and significant flooding throughout the WASD area.

For each simulation flood inundation depth grids, flood inundation water elevation grids, and flow direction shapefiles were used to estimate projected flooding depths at critical WASD facilities, as discussed in a separate report.

FIGURE ES-1
100-year Depth Grid

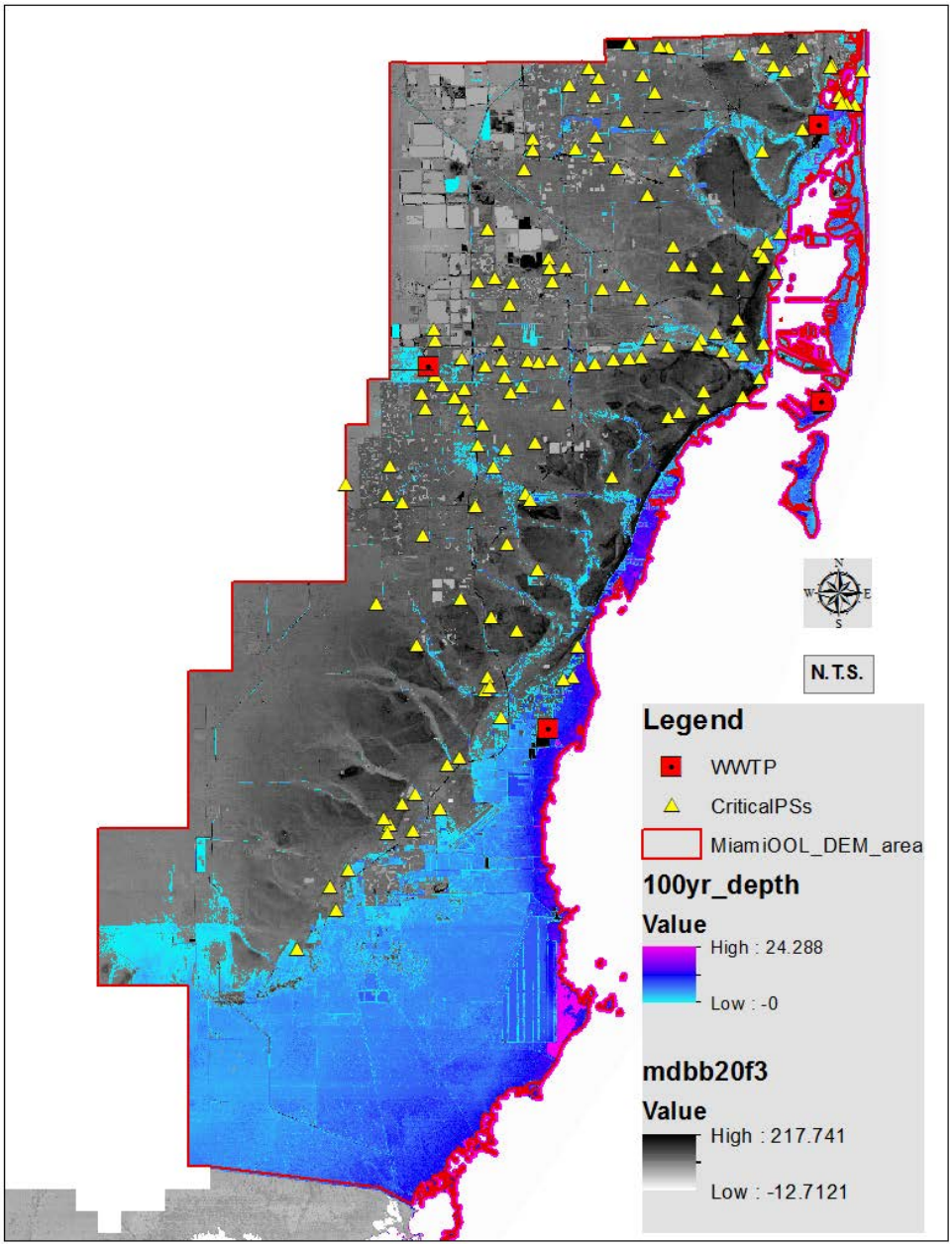

FIGURE ES-2

Future 100-year with Climate Change and Sea Level Rise Depth Grid

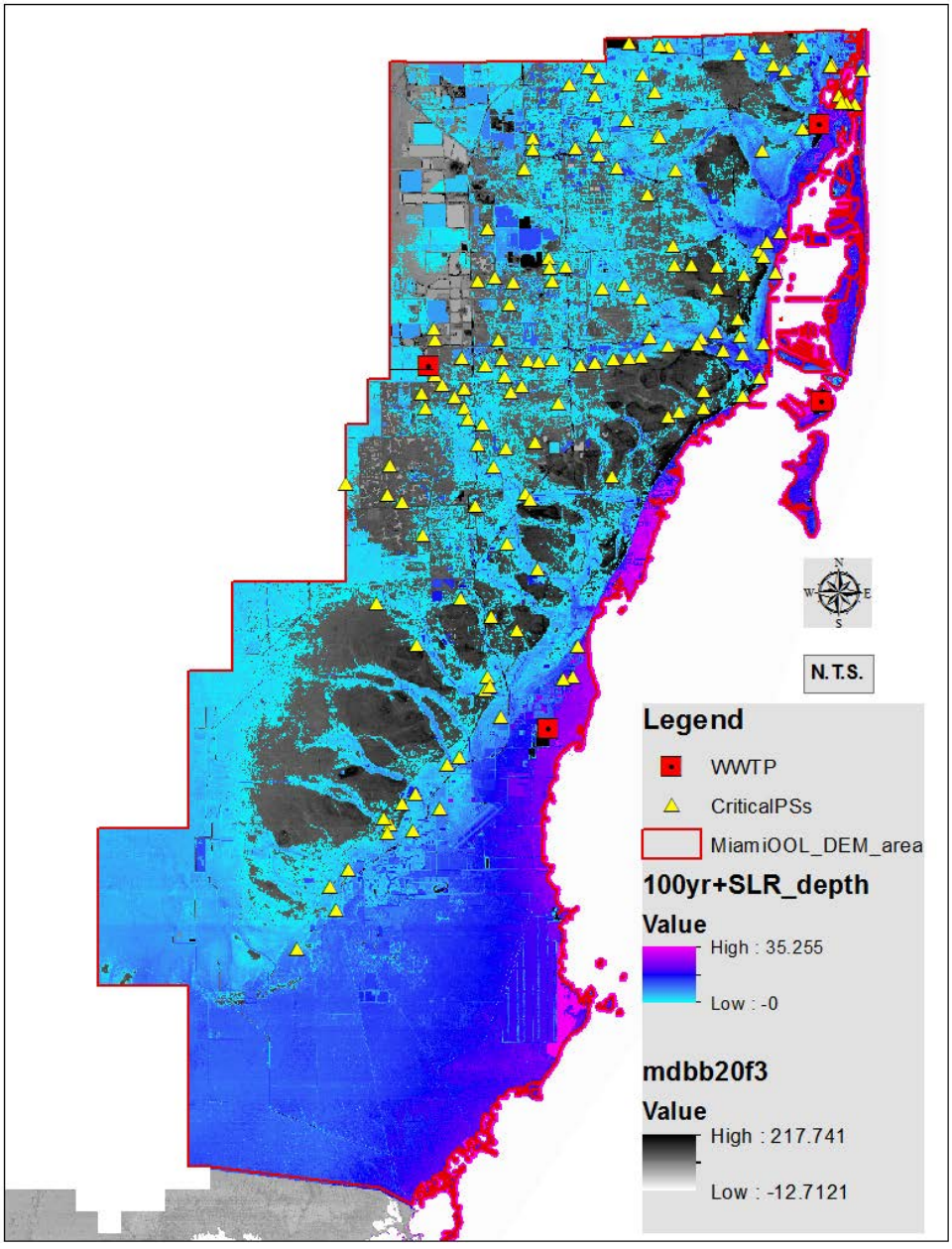

Recommended Next Steps

The modeled outputs from the surge modeling component are consistent with FEMA's Stillwater elevations. However, these are not directly comparable to FEMA's Base Flood Elevations (BFEs) that includes wave height effects. While a first order estimate of future BFEs incorporating the effect of SLR can be made by assuming the same degree of wave height effects used in FEMA's BFEs, it is conceivable that a larger wave height effect may result in the future due to the larger water depths resulting from SLR. This increase in wave height effect in the future can be reasonably assessed by comparing the wave height results of the no-SLR and SLR scenario runs. By pegging the modeled no-SLR wave heights to the published FEMA's wave heights corresponding to FEMA's BFEs in FEMA's FIS, the increased wave heights for the SLR scenario can be estimated using linear scaling as was done for the 100yr plus SLR Stillwater elevations. The wave height attenuation overland can then be estimated using FEMA's WHAFIS (Wave Height Analysis for Flood Insurance Studies) to derive the BFEs corresponding to the future SLR condition.

As yet, the non-linear amplification in the peak water level under the SLR scenario has not been adequately investigated. By expanding the surge scenarios to include other SLR scenarios and hurricane track trajectories to complement the available result sets, the resulting comparison of amplification as a function of SLR magnitudes and hurricane track trajectories may illuminate the causative mechanisms.

The 100-year simulation results do show less flooding than the current FEMA Flood Zone maps for the area. The modeling methods are different however, and it is important to recognize that the mapping presented has been developed through simplified methods that do not explicitly model the detailed canal and drainage network in the area.

It is recommended that the inland flood inundation models be refined to address these limitations by explicitly including the following hydraulic details.

- Include a more detailed resolution of the hydraulic calculation grids to improve the representation of the flood flow mechanisms and increase the accuracy/precision of stage results
- Enhanc the representation of canals to improve the model's performance in simulating the inland flood mechanisms and potential interconnected flood flow routes between canal subwatersheds

Contents

Appendix

Tables

Figures

Acronyms and Abbreviations

°C	degrees Celsius
2-D	two dimensional
CDWWTP	Central District Wastewater Treatment Plant
DEM	Digital Elevation Map
FDEP	Florida Department of Environmental Protection
FEMA	Federal Emergency Management Agency
flood model	flood propagation/inundation model
FM	flexible mesh
HWM	High Water Mark
mgd	million gallons per day
m/s	meter(s) per second
NGVD	National Geodetic Vertical Datum
NHC	National Hurricane Center
NOAA	National Oceanic and Atmospheric Administration
SDWWTP	South District Wastewater Treatment Plant
SLR	sea level rise
surge model	2-D depth-averaged regional hydrodynamic model
SW	Spectral Wave
TC	tropical cyclone
TM	technical memorandum
WASD	Miami-Dade Water and Sewer Department
WDWWTP	West District Wastewater Treatment Plant
yr	year

SECTION 1

Project Description

1.1 Project Background

Incorporating climate risks and vulnerabilities is key to developing a robust facility hardening plan and designs for the Ocean Outfall Legislation (OOL) program. The climate risks and vulnerabilities entails two parallel activities:

- Assess projected climate change for key climate variables
- Define critical assets

There are at least four key climate variables that could affect planning for Miami-Dade Water and Sewer Department (WASD's) OOL program: sea level rise (SLR), storm surge, precipitation, and wind. Coastal facilities are potentially subject to flooding from SLR and surge, while inland facilities (e.g., WDWWTP and some pump stations) are potentially subject to flooding from increased precipitation intensity, especially if coupled with SLR impacting tailwater conditions in drainage canals.

This report applies the projections of changes in SLR and climate change to estimate the resulting surge elevations and inland flood maps for specified climate events, which will be used by other components of the program to develop facility hardening plans. The report includes a brief review of tropical cyclone (TC) climatology, and the selection of a historical hurricane event as the base event to drive hurricane-induced surge and flood propagation into the project area of a specified return period (100 years [yrs] in this case). The impacts of future climate change on the surge and flood propagation are assessed by incorporating the associated climate changes into the simulation of the same base historical hurricane using appropriate scaling of the Federal Emergency Management Agency's (FEMA's) 100-yr Stillwater elevations.

1.2 Brief Overview of Hurricane Climatology

A brief account of the hurricane landfalls and their impacts on the southeast coast of Florida, specifically Miami-Dade County, is summarized from the National Oceanic and Atmospheric Administration (NOAA) 2013 and (Landsea, et.al. 2004) as presented below:

a. 1926 Great Miami Hurricane

   The first well-documented storm surge was associated with the 1926 Great Miami Hurricane, which made landfall at Miami on September 18, 1926 as a Category 4 hurricane. The resulting storm surge was estimated at 8 to 11 feet from Miami Beach to downtown Miami, with values perhaps as high as 15 feet in Coconut Grove. It is thought that many of the reported fatalities in South Florida were because of the storm surge.

   A series of major hurricanes struck mainland southern Florida in the 1940s, producing storm surges of several feet in depth along the southeast and southwest coasts, but nothing as severe as the hurricanes of the 1920s.

b. 1992 Hurricane Andrew

   It was not until 1992 when Southeast Florida experienced its next major hurricane. Hurricane Andrew struck southern Miami-Dade County on August 24, 1992 as a Category 5 storm. In a 1992 post-storm analysis, the maximum 1-min surface winds estimated at 125 knot (64 meters per second [m/s], 144 miles per hour). This original assessment was primarily based on an adjustment of aircraft reconnaissance flight-level winds to the surface. Based on recent advancements in the understanding of the eyewall wind structure of major hurricanes, the official intensity of Andrew was adjusted upward for

five days during its track across the Atlantic Ocean and Gulf of Mexico by the National Hurricane Center (NHC) Best Track Change Committee. In particular, Andrew is now assessed by the NHC to be a Saffir-Simpson Hurricane Scale Category 5 hurricane (the highest intensity category possible) at its landfall in southeastern Florida, with maximum 1 min winds of 145 knot (75 m/s, 167 miles per hour). This makes Andrew only the third Category 5 hurricane to strike the United States since at least 1900.

These intense winds produced a record surge of 16.9 feet (5.2m) of water at the Burger King Headquarters and Deering Estate in Palmetto Bay. The central pressure was estimated at 922 millibar during landfall near the Homestead Air Force Base at 0905 UTC on August 24. The peak surge of 5.2 m gradually decreased to 2.9 m near the mouth of Miami River and to 1.5 m at the south side of the Biscayne Bay. Because of Andrew's compact size, the area of major storm surge was limited to the Biscayne Bay shoreline and missed the heavily populated downtown Miami and Miami Beach areas. Measured total precipitation during Hurricane Andrew was recorded to be only 2.94 inches at Miami International Airport, from August 20, 1992 through 25, 1992 (National Climate Data Center).

1.3 Site Condition

The project site is located along the southeast coastline of Florida fronted by a series of individual and barrier islands. Biscayne Bay, a lagoon-like water body stretching approximately 35 miles in length and up to 8 miles in width, is located landward of the island chain and fronts a majority of the project shoreline. Both the fronting barrier island and the project area are of low relief with an elevation range of 1 m National Geodetic Vertical Datum (NGVD) to 3 m NGVD. This low relief makes it susceptible to surge-induced inundation.

1.4 Overall Scope and Study Linkages

Climate change can have many manifestations, with different degrees of risk in terms of likelihood and consequence of impacts. For example, SLR can contribute to daily inundations of coastal facilities with each tidal cycle. In addition, porous bedrock in Florida results in a more direct connection of SLR and groundwater levels, with higher groundwater levels contributing to higher sewer infiltration and inflow. However, storm surge from tropical storms, while less likely, can have significant consequences in terms of flooding of critical facilities such as electrical systems and motors at pump stations and treatment plants.

Understanding climate risks entails two parallel activities:

1. Defining projected climate change for key climate variables. The projected changes are used to define a range of climate scenarios used in hydrologic and hydraulic modeling to understand risk to critical infrastructure assets.
2. Defining critical assets, which is typically tied to understanding the consequence of failure of a given asset, such as pump stations serving larger populations or critical infrastructure such as hurricane evacuation routes, or environmental assets such as wetlands. This also requires definition of critical thresholds for failure of these facilities, such as elevation of electrical systems, or ingress/egress access elevations.

Tasks entailed in Activity 1 include the assessment of extreme event and SLR, which are fed into coupled surge and flood modeling investigations. The resulting flood and water depth analyses are applied in the definition of critical assets and the design of facility hardening including economic analysis. These two activities can be inserted into an overall risk management analysis that defines the likelihood of asset failure and the consequence of failure. The overall conceptual framework is outlined in Figure 1-1. The tasks undertaken and the results presented in this report fall under the first category while the details of the associated subtask activities are presented in Section 3.

FIGURE 1-1
Conceptual Framework

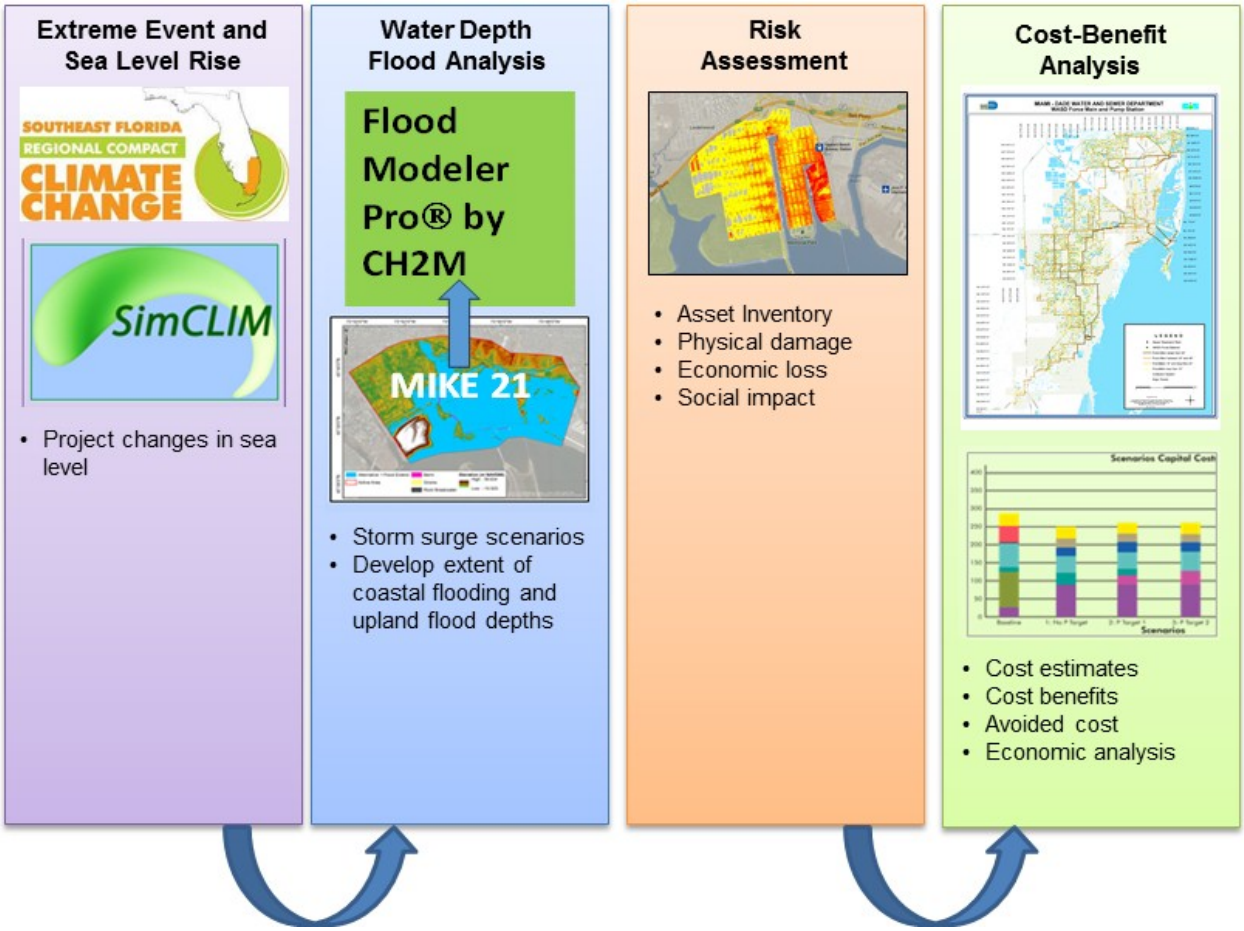

SECTION 2

Modeling Scope

2.1 Surge Modeling Subtasks and Flowchart

The overall modeling strategy entails coupling a two-dimensional (2D) depth-averaged regional hydrodynamic model (hereinafter referred to as the surge model) covering the water domain and a flood propagation/inundation model (hereinafter referred to as the flood model) covering the upland areas landward of the shoreline. This is a computationally efficient approach combining the spatially expansive surge model extending over the North Atlantic Ocean and the abutting coastal waters to take into account the storm genesis and development area, and the fast computing ability of the flood model that takes into account land topography and features in great detail.

The linkages between the two subtasks are presented in the Figure 2-1 flow chart. As indicated in Figure 2-1, the surge modeling and flood modeling subtasks are linked sequentially, with the former providing the boundary surge conditions to drive the latter. The details of the surge modeling subtasks and the associated activities are discussed in Section 3.

FIGURE 2-1
Flow Chart for Surge Modeling Tasks Linking Study Components

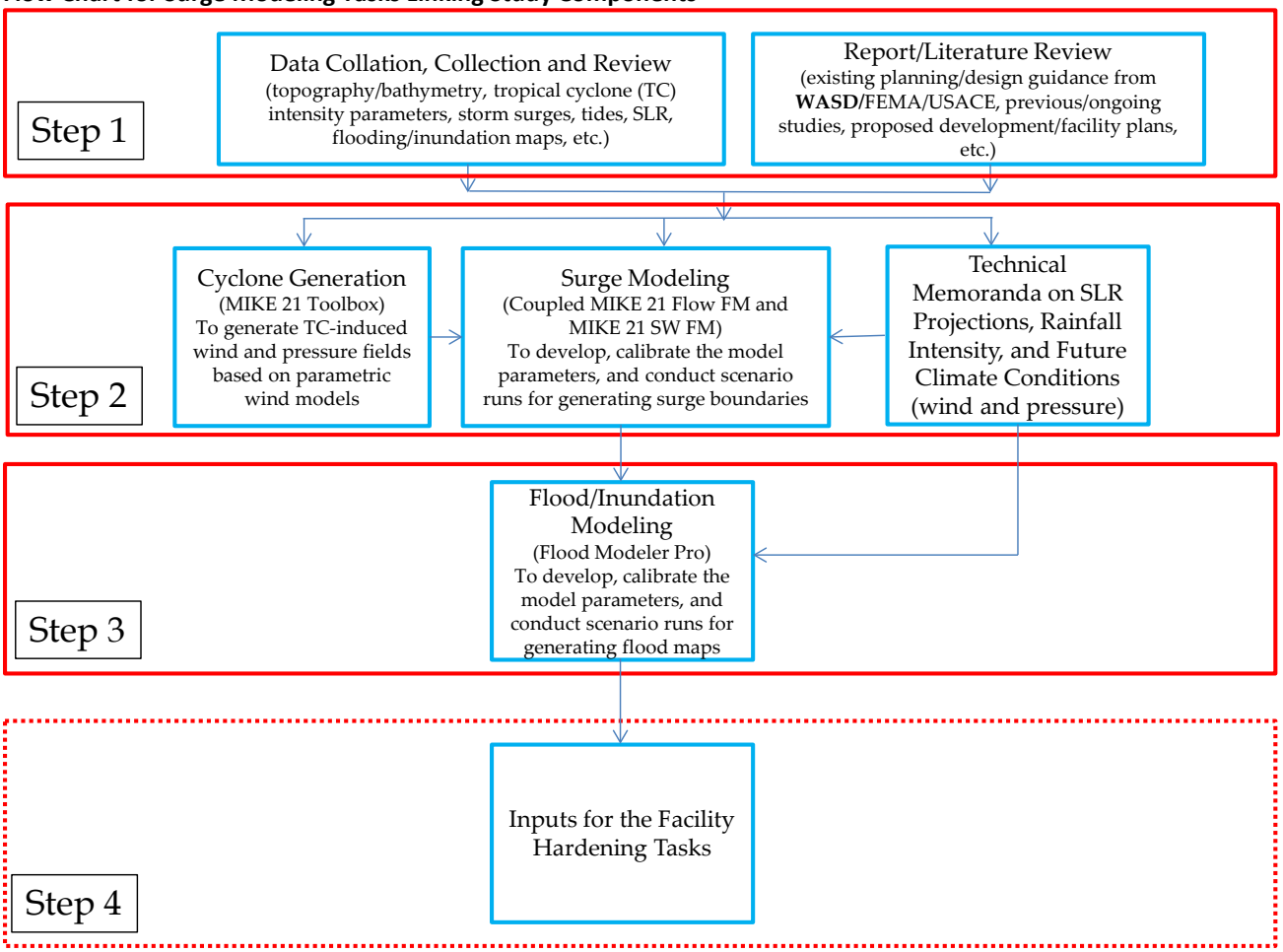

The surge modeling subtasks were completed using coupled flow wave modeling that intrinsically considers mutual feedback between the flow and the wave components developed using the MIKE 21 modeling platform (MIKE by DHI, 2014). The activities comprised:

Step 1:

- Data collation, collection and review covering bathymetry, tides, waves, winds, measured High Water Marks (HWM), surge information, hurricane data, published papers/reports on hurricane simulations and results on the meteorological and physical aspects, and available standards and guides on the planning aspects.

Step 2:

- Develop surge scenarios including the selection of the base historical hurricane and the storm events, SLR projections and future climate changes affecting the meteorological forcing.
- Develop hurricane induced wind and pressure fields using parametric wind models and comparison with published wind data. The wind and pressure fields are specified external inputs for the surge model.
- Develop storm surge model covering model domain and bathymetry, modelling platform and comparison with published surge maps.
- Extraction and preparation of storm surge elevations at transect locations along the project coastline for selected scenarios to drive the flood model.

Step 3 is discussed in Section 3.2.

SECTION 3

Modeling Methodology

3.1 Surge Modeling

3.1.1 Modeling Platform and Engine

Surge modeling was conducted by coupling the MIKE 21 Flow Flexible Mesh (FM) module (MIKE by DHI, 2014a) and MIKE 21 Spectral Wave (SW) FM module (MIKE by DHI, 2014b) available in the MIKE 21 suite of hydraulic software. Both modules are well known and the Owner's Representative has applied successfully the modules on numerous projects along the Atlantic seaboard as well as internationally.

MIKE 21 Flow FM utilizes FM and solves the 2D, depth-integrated, shallow water equations of continuity and momentum. The equations are spatially discretized using a cell-centered finite volume approach with triangular elements. Further details are provided in Appendix A.

MIKE 21 SW FM is a wind-wave model that describes the growth, propagation, and decay of short-period and short-crested waves in nearshore areas. The model takes into account the effects of refraction and shoaling due to varying depth, local wind generation, and energy dissipation from bottom friction and wave breaking. The model is a quasi-stationary, fully spectral parametric model, and the effect of the current is taken into account by deriving the basic equations in the model from the conservation equation for the spectral wave action density. The basic equations are solved using an Eulerian finite difference technique. Further details are provided in Appendix B.

3.1.2 Modeling Assumptions

Models are but an approximation to the physical reality and therefore the use of a numerical model inherently contains assumptions. The model assumptions as they pertain to surge modeling and the implications are presented below:

- Three-dimensional effects are small such that the use of a 2D, depth averaged model is adequate to account for the dominant flow and wave processes. This is deemed reasonable in relatively shallow water and with no large freshet discharge where stratification due to flow and salinity is insignificant. Furthermore, the focus here is on the surge phenomenon in terms of peak water surface elevation, which is less sensitive to stratification compared to flow and salinity changes.
- Non-erodible shoreline, that is, potential changes to storm surge propagation due to erosion and accretion such as bank/levee collapse and channel bed retro-gradation are not accounted for. This is considered reasonable as the project shorelines and channel boundaries are already hardened in the main.
- Effect of wave-overtopping contributing to mass discharge overland is deemed small as the project shoreline is not lined by levees.
- The SLR projection is applied as a uniform uplift of the open ocean boundary water levels. However, the change in the water level at the project site was checked so the quantum of SLR projection is recovered along the coast line at Biscayne Bay.

3.2 Flood Modeling

Flood inundation modeling was conducted for the drainage area that covers the critical assets within Miami-Dade County. Critical assets identified by the Owner's Representative included pump stations and wastewater treatment plants. The drainage area assessed as part of the rapid flood inundation assessment and critical assets in the drainage is shown in Figure 3-1.

FIGURE 3-1
Drainage Area

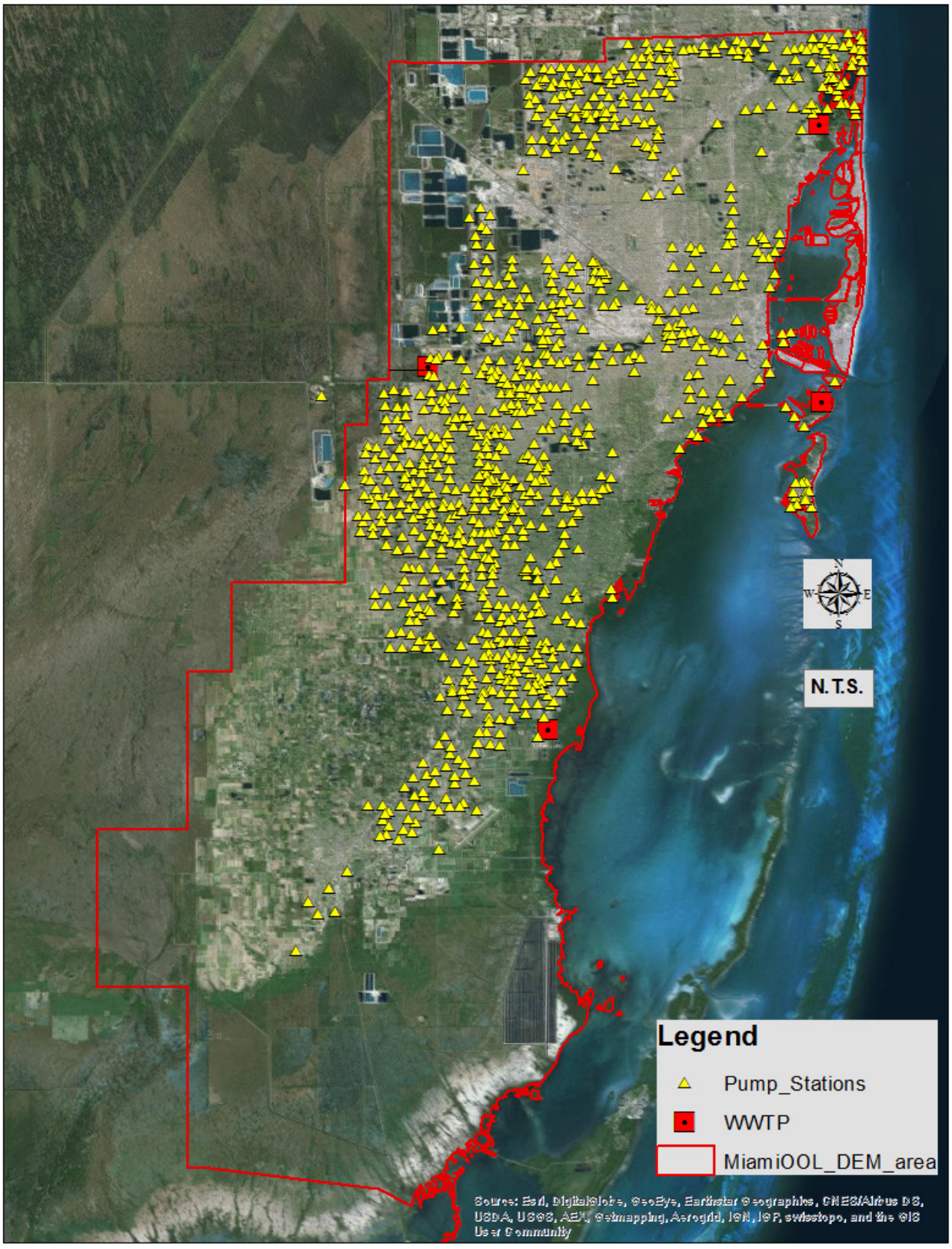

The Flood Modeller Pro software suite was used to simulate the flood inundation resulting from the storm surge coming on shore as well as from extreme rainfall conditions. The Flood Modeller 2D Alternating Direction Implicit (ADI) solver was used to simulate the surge inundation, while the 2D FAST solver was used to assess the inundation resulting from rainfall. The flood inundation modeling approach, which was first validated for use on the project through simulation of the inundation from Hurricane Andrew is illustrated on Figure 3-2.

FIGURE 3-2
Flood Inundation Modeling Approach

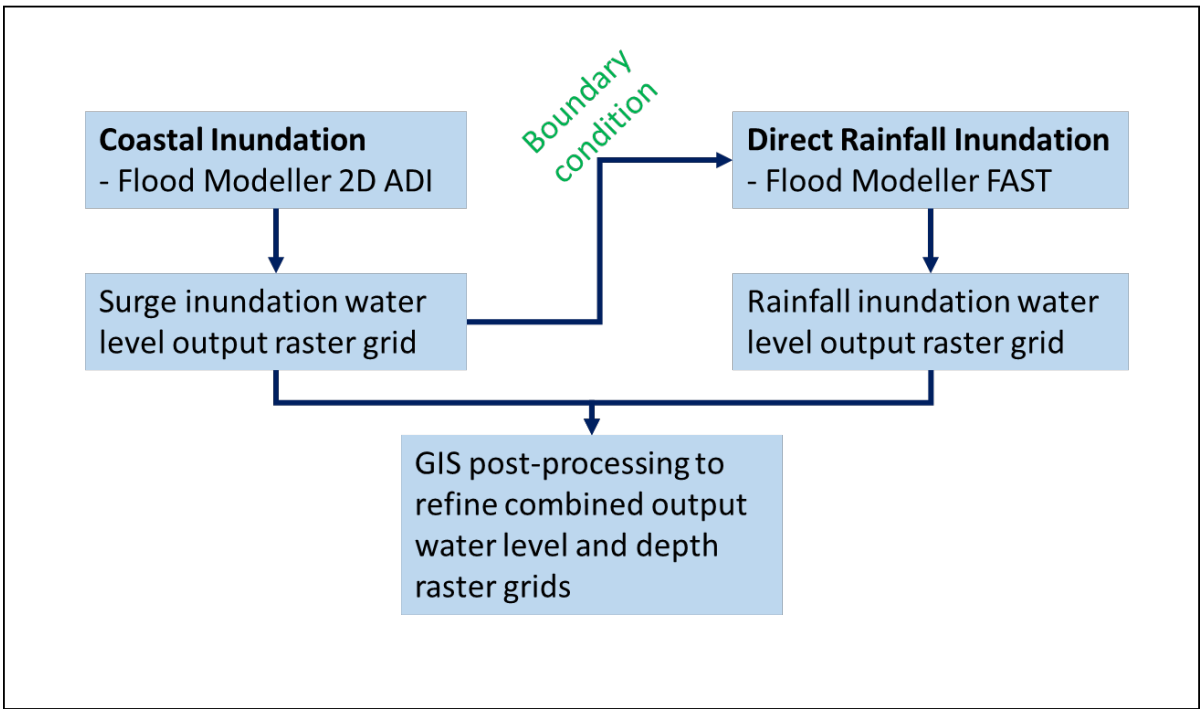

The output from these two solvers has been combined to produce flood depth grids for the 100-yr condition and the 100-yr plus SLR condition.

The following sections describe the modeling solvers, input data development, and boundary conditions in more detail.

3.2.1 Flood Modeller Pro 2D ADI Solver

The ADI Solver has been developed for fluvial, overland, estuarine, and coastal modelling problems where the flow is not rapidly changing. It is based on the long-established depth integrated velocities and solute transport numerical engine that was developed in the 1980s.

It is used throughout the world for surface water modelling, local and watershed scale assessments, flood mapping, embankment and asset failure, and other flood risk management studies.

The solver works by representing the model domain as a grid of square cells. Water levels are calculated at each cell center, and the two components of velocity at cell edges. This allows the model to use the velocity components to calculate flow across cell edges and between cells.

For this project, a broad scale model was developed to enable coastal flood inundation mapping to be developed for the entire WASD area of interest. The model setup is described in more detail in Section 4.2.

3.2.2 Flood Modeller Pro 2D FAST Solver

FAST is a computational engine that routes water over the floodplain using a simple set of rules based on how water levels respond to the topography described in the Digital Elevation Map (DEM). FAST enables a quick assessment of flooding using simplified hydraulic principles to generate results up to 1,000 times quicker when compared to other tools and methods available for flood inundation simulations (i.e., delivering results in minutes as opposed to hours or days). The software works by first pre-processing DEM data to identify depressions on the floodplain before routing water through these depressions. Water depths in the depressions are determined by volume of water flowing into that depression, level at which water can spill into neighboring depressions, and water level in neighboring depressions. FAST represents connectivity and volume filling effects on the floodplain, without having to represent detailed hydraulics.

It must be noted that no subsurface connectivity is explicitly represented in the FAST model and therefore, it must be recognized this tool should not be considered a substitute for fully hydrodynamic models needed for high accuracy (or high risk) tasks such as required for detailed engineering design or mapping products. However, because of the rapid setup time and fast simulation speed, these tools are used to leverage available data to assist watershed scale planning, feasibility study work, and the data collection planning process by identifying critical locations of assessment.

For this project, a FAST model was developed to enable direct rainfall induced surface water flood inundation mapping to be developed for the entire WASD area of interest, for combination with the coastal inundation mapping. The model setup is described in more detail in Section 4.2.

SECTION 4

Model Development

4.1 Surge Model

4.1.1 Model Mesh and Bathymetry

The surge model domain (Figure 4-1) covers the entire North Atlantic Ocean located east of 53 degrees west (including the contiguous Gulf of Mexico where the offshore boundary runs north-south from Newfoundland to the South America coast. The use of this large geographical extent is to minimize potential boundary effects and to emplace the entire development area of the TC therein. At the same time, it can be easily adapted to different hurricane tracks vial local bathymetry and mesh refinement in the project vicinity.

The model domain comprises varying resolutions of triangular mesh elements, ranging from 100 km near the open boundary, to 1.5 km offshore of Biscayne Bay and 300 m within the Bay to as fine as 30 m at certain locations of WASD's coastal facilities.

The DEM/bathymetry applied consists of a hierarchy of datasets arranged in decreasing priority of use as follows:

- LiDAR Miami-Dade 2007 (survey point spacing: 1 to 2 m)
- LiDAR Key West 2008 for the barrier islands (survey point spacing: 1 to 2 m)
- NOAA Electronic Navigation Chards (ENC) data in GIS/CAD formats (http://www.nauticalcharts.noaa.gov/csdl/ctp/encdirect_new.htm) (survey point spacing: 100 to 200 m)
- MIKE CMAP dataset (MIKE by DHI, 2012) (survey point spacing: 100 m to 200 m)
- Earth Topography 1 arc-minute, which is a 1 arc-minute global relief model of Earth's surface that integrates land topography and ocean bathymetry (http://www.ngdc.noaa.gov/mgg/global/global.html) (survey point spacing: 1,800 m)

FIGURE 4-1
Model Domain, Surge Model (the black line denotes the track of Hurricane Andrew of 1992)

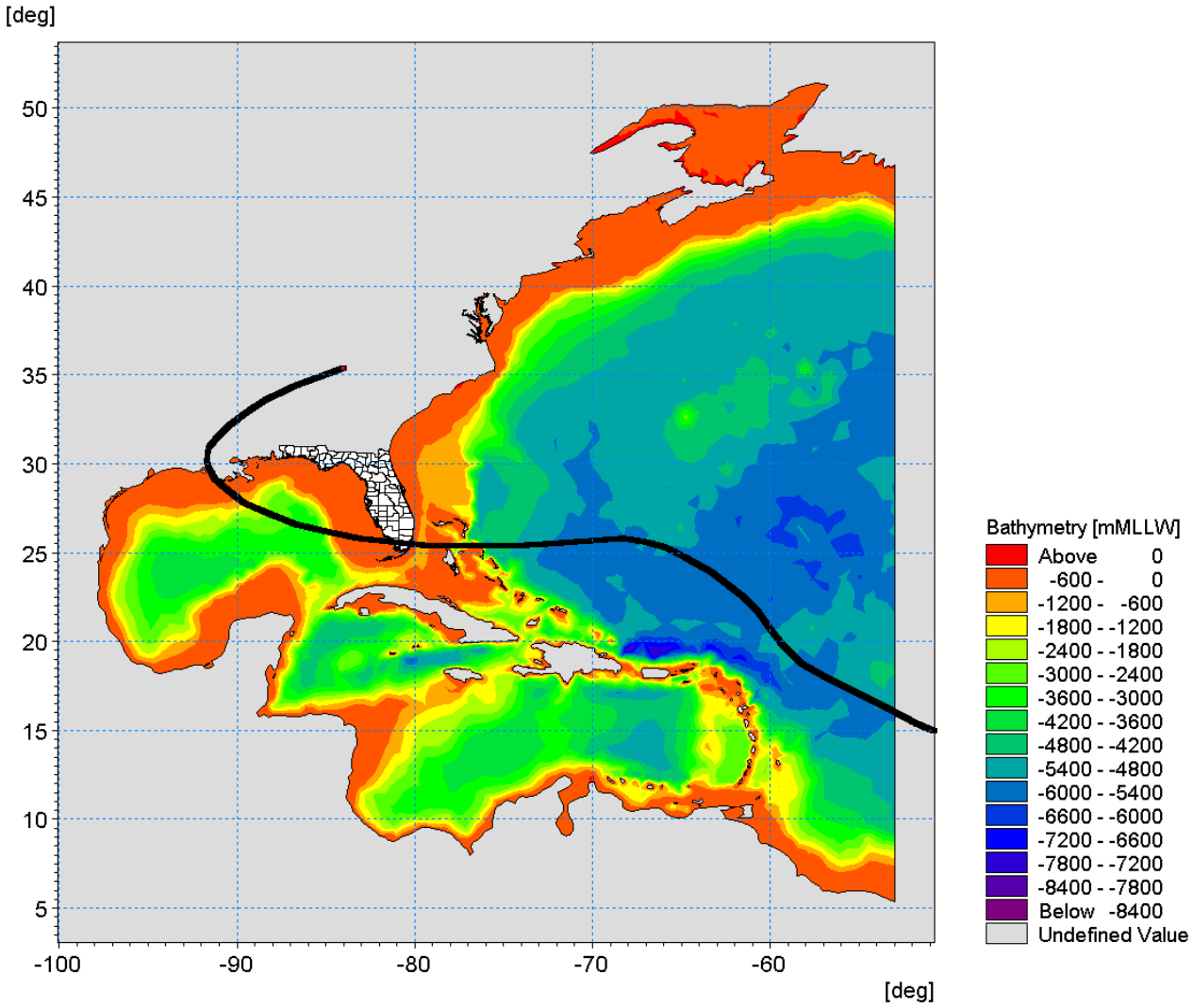

4.1.2 Comparison of Modeled and Measured Outputs

The surge model was applied to the simulation of Hurricane Andrew (1992), which was selected as the base hurricane as discussed in Section 5.1.3. The comparison of model outputs and measurement was made in terms of wind field and surge elevations.

Two parametric wind models contained in the Cyclone Generator of MIKE 21 Toolbox (MIKE by DHI, 2014c) were tested. They are the Holland model (Holland, 1980) and the model of Young and Sobey (1981). The inputs to the wind models comprised:

- Six-hourly time series of Hurricane parameters (longitude/latitude, maximum wind velocity, central/ambient pressure available from HURricane DATabase (HURDAT2) database of NHC
- The associated Radius to maximum wind calculated using the empirical equations of Vickery and Wadhera (2008) as a function of latitude and pressure deficit
- The associated Holland B parameter (for the Holland model) calculated using the empirical equations of Vickery and Wadhera (2008) as a function of latitude and pressure deficit.

Model parameters are summarized in Table 4-1.

TABLE 4-1
Summary of Wind Model Parameters

Model Parameter	Parameter Formulation/Value
Cyclone Type	Young and Sobey/Holland Single Vortex
Forward motion asymmetry	Harper, et al. (2001)
Inflow angle	Sobey, et al. (1977)
	$\delta_{fm} = 0.5$; $\theta_{max} = 115°$
Wind grid size	0.0135° (≅ 1.5km)
Time step	0.25hr

The resulting wind field based on the Holland Single Vortex formulation as shown in Figure 4-2 displays a peak wind speed of 69m/s during landfall that is similar to the reported peak of 75m/s (Landsea, et.al, 2004). The corresponding peak wind speed from the Young and Sobey (1977) model is lower. Therefore, the Holland Single Vortex was adopted for use in the scenario runs.

FIGURE 4-2
Model Wind field at the Time of landfall, Hurricane Andrew (1992) (the three yellow boxes denote the locations of the CDWWTP, SDWWTP, and NDWWTP)

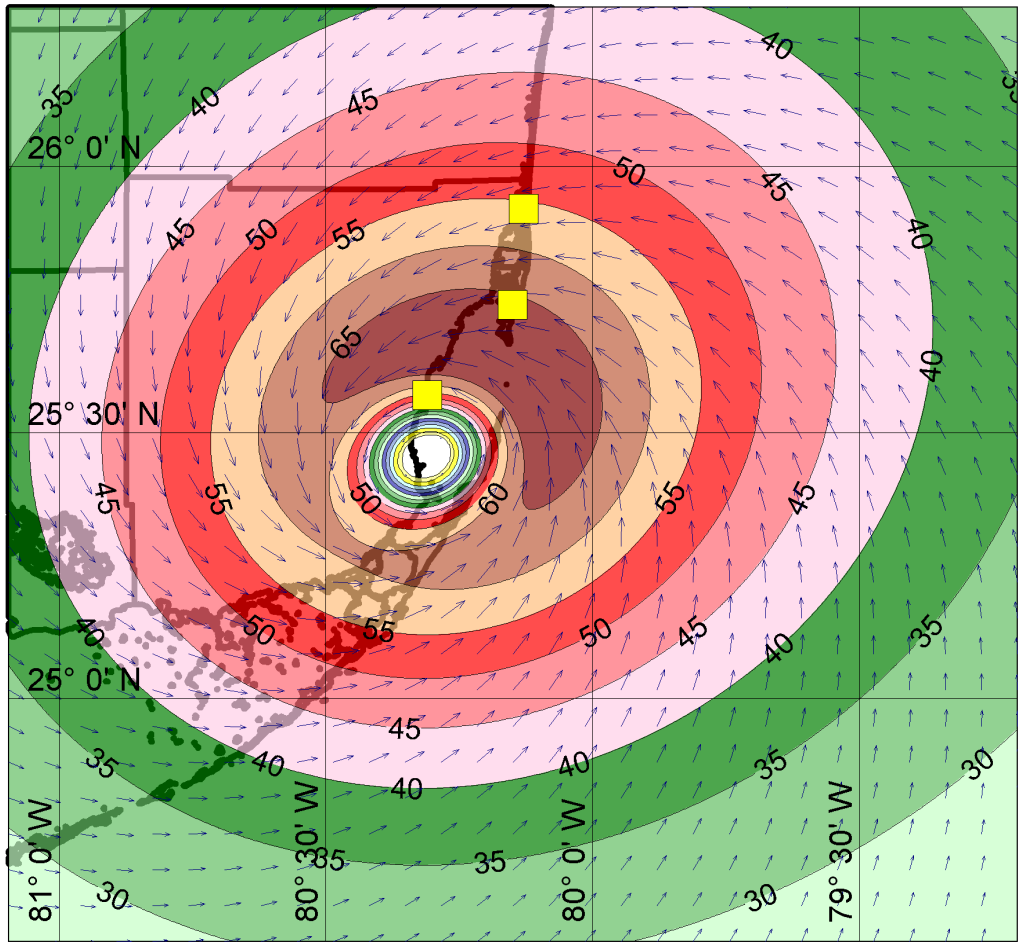

The wind/pressure field based on the Holland Single Vortex formulation was applied to the surge model as a surface forcing where predicted tide water level variation based on the Global Tide Model (GTM) (Anderson, 1995). GTM represented the major diurnal (K1, O1, P1, and Q1) and semidiurnal tidal constituents (M2, S2, N2, and K2) on a grid that has a grid size of 0.125°.

Varied model parameters include bottom roughness represented by Manning M units of $m^{1/3}/s$ and numerically equal to the inverse of the conventional Manning's n, and the wind stress/drag coefficient expressed using the formulation of Wu (1984) in the flow model. In the Wu (1984) model, the drag coefficient is implemented as a step function such that cd_1 is for wind speed below 7m/s and linearly varying to cd_2 up to a wind speed of 25m/s and thereafter remaining constant at that value.

The corresponding wave model parameters that were adjusted include bottom friction and wave breaking parameters. The best match of the modeled surge elevations to measured HWM is shown in Figure 4-3 while the corresponding model parameters are summarized in Tables 4-2 and 4-3 for the flow and wave models, respectively. Figure 4-3 indicates that the largest model surge elevation (4.9 m NGVD) occurs in a similar location to the measured (5.2 m NGVD). The same flow and wave model parameters were similarly in the scenario runs described next.

TABLE 4-2
Summary of Flow Model Parameters

Model Parameter	Parameter Formulation/Value
Manning M	$40m^{1/3}/s$
Eddy Viscosity	Smagorinsky coefficient = 0.28
Wind stress coefficient	Wu (1980
cd_1, Lower (wind speed <= 7m/s)	0.001255
cd_2 , Upper (wind speed >= 25m/s)	0.0026

TABLE 4-3
Summary of Wave Model Parameters

Model Parameter	Parameter Formulation/Value
Wave Equations	Fully spectral, instationary
Spectral discretization	16 (22.5° discretization) sectors
Wave breaking	α = 0.8 γ = 1.0
Bottom friction (Nikuradse roughness)	k_N = 0.04m
Air-sea interaction	Coupled, Charnock parameter = 0.01
White Capping	c_{dist} = 4.5; δ_{dist} = 0.5

FIGURE 4-3
Distribution of Modeled Peak Surge Elevation (m NGVD) Overlaid on Measured Surge Elevation Map (the red square boxes denote the track of historical Hurricane Andrew while the large red boxes, the locations of the three CDWWTP, SDWWTP, and NDWWTP)

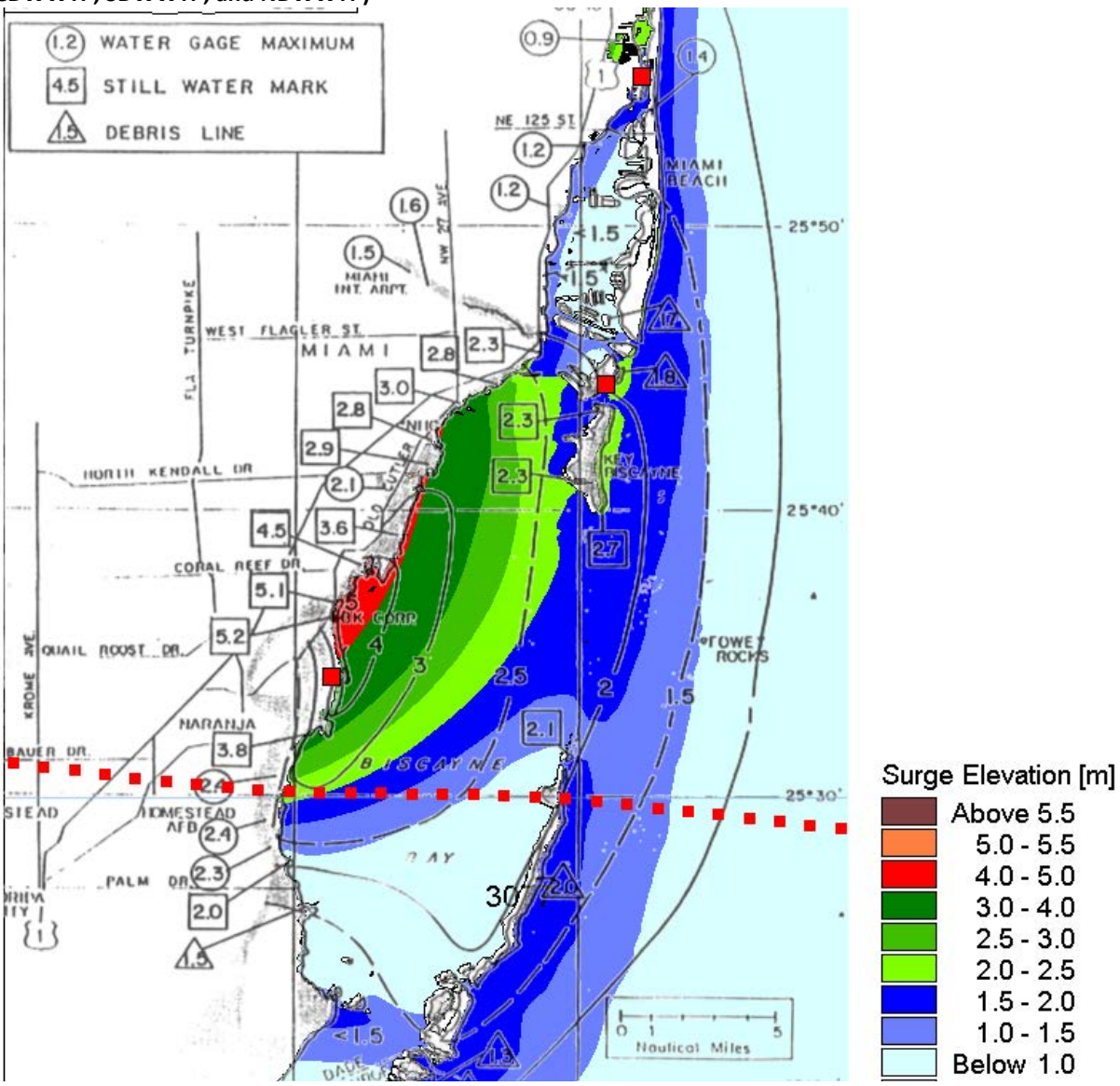

4.1.3 Scenario Selection

The approach to the selection of model scenarios is outlined below:

- Select a historical hurricane as the base hurricane set based on the worst observed wind/surge impacts that are considered extreme
- Select the baseline flood exceedance level to be used as reference
- Select the model scenarios to be run based on the available budget/schedule while also meeting the purpose of the facility hardening works.

Based on Section 2.2, Hurricane Andrew is undoubtedly the largest surge event to date. It is also an east-west moving storm system that generates higher nearshore surges compared to parallel bypassing (generally following a south-north heading) in the Biscayne Bay area due to the anti-clockwise rotation of the hurricane system relative to the shoreline orientation as illustrated in Figure 4-4. Due to the anti-clockwise rotation of tropical storms in the Northern Hemisphere, the first quadrant experiences the largest

wind and surge as the circumferential wind speed component is in line with the forward speed of the moving storm.

Since the FEMA's 1 percent probability flood level is widely used for flood management and providing the base flood elevation for structure design, this has been similarly adopted herein. FEMA's Flood Insurance Study (FIS) of 1993 but updated in 2009 provides the Stillwater elevations at the seaward end of the Biscayne Bay and ocean transects along the project shoreline. FEMA's Stillwater elevations correspond to the 100 yr return period surge elevation taking into account astronomical tides, meteorologically induced surge, and wave setup. They are different from the Base Flood Elevations (BFE) shown on FEMA's DFIRMs for the V zone in that BFEs include the additional consideration of wave crest elevation. The results of the coupled wave-surge modeling applied herein are consistent with the definition of FEMA's Stillwater elevations as reported in the FIS.

Hurricane Andrew is a compact hurricane and the associated surge elevations decrease spatially both up and down-coast spatially within the geographic spread of the three WWTPs. Therefore, Hurricane Andrew was able to induce large surge elevation at the SDWWTP which is located closer to the zone of high surge elevations centered at Palmetto Bay (Figure 2-1), but not at the CDWWTP or NDWWTP located further north when compared to the respective Stillwater elevations in the FIS.

Therefore, a track shift strategy was adopted by moving the historical track of Hurricane Andrew in uniform change of 0.05° to 0.1° latitude but maintaining a parallel track alignment throughout and also the same set of TC intensity parameters. The results shown in Figure 4-5 indicate that the peak surge elevation at the CDWWTP, SDWWTP, and WDWWTP are track dependent. Consequently, the tracks that are optimized to generate the largest surge elevation at the WWTPs are selected relative to the historical track where positive values denote shift northward) as:

- NDWWTP: +0.3° northward
- CDWWTP: +0.1° northward
- SDWWTP: -0.1° northward (or +0.1° southward)

In terms of surge elevation, the modeled track-shifted simulations based on the historical H. Andrew track and hurricane intensity generate location-specific peak surge elevations similar to a 50 to 100 yr return period surge event based on FEMA's Stillwater elevations at the same locations.

Because of the small relative difference in the FEMA's return period-based Stillwater elevations and the modeled surge values based on the three artificial tracks, it is deemed reasonable and practical to adopt a linear scaling approach to estimate the combined 100 yr and SLR-induced surge elevation based on the modeled track-shifted run results.

For the SLR projections, the target year has been selected as 2075. However, the SLR projections at the target year was based on WASD's instructions to follow the South Florida Climate Change Compact in 2015 (2015 unified SLR projection for southeast Florida), which is 1.23 m, compared to 0.91 m recommended by the Owner's Representative (2015). In addition, a lower projection of 0.93 m was applied in the surge modeling to assess whether or not linear scaling using the results of the 1.23 m SLR projection is reasonable.

FIGURE 4-4

Surge Generating Capacity as a Function of Track Heading (adapted from FEMA, 2014): Top: Land-falling tracks; Bottom: Parallel Bypassing Tracks

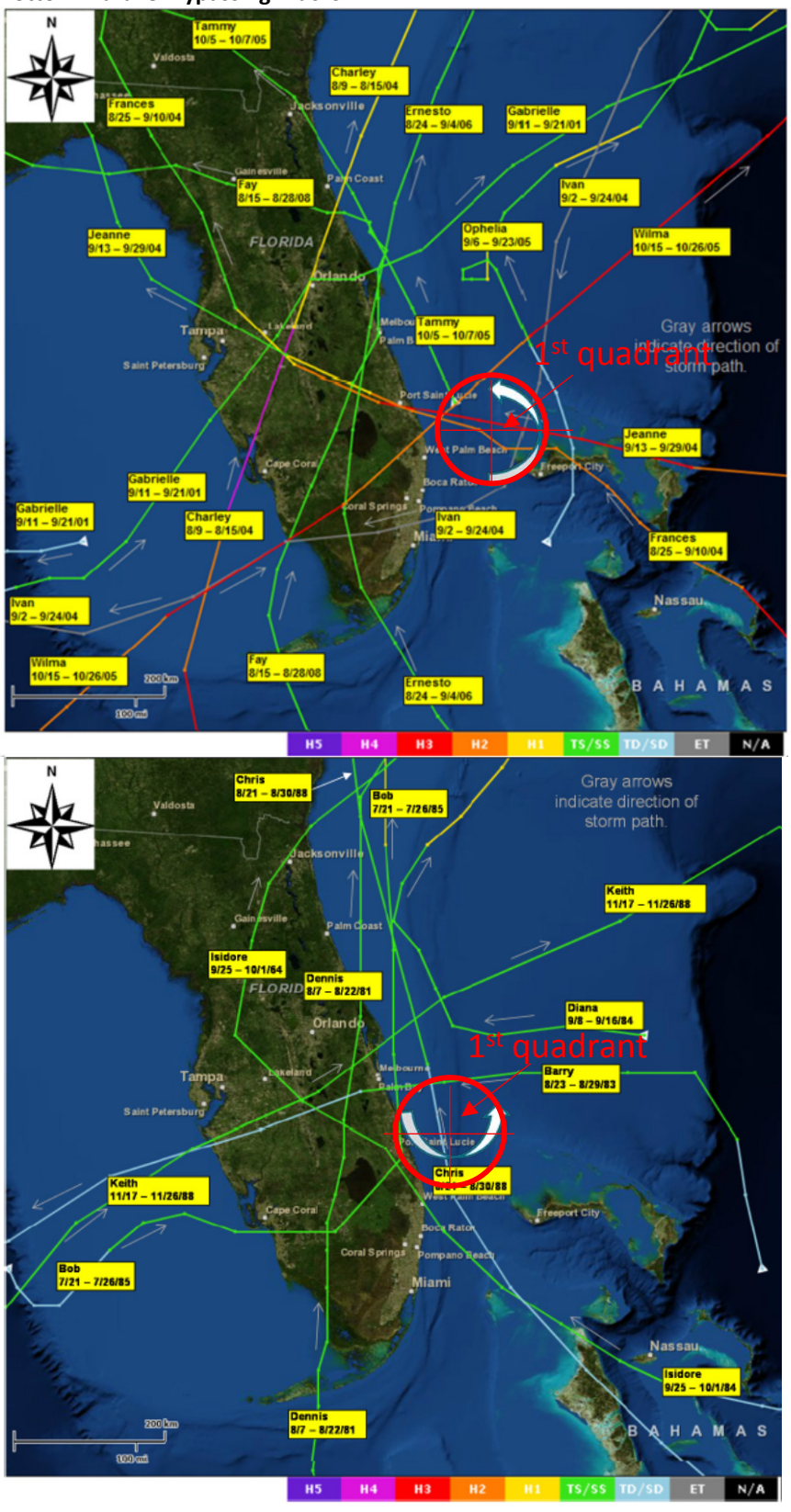

Comparison of TC-induced surge potentials by quadrants (top: land-falling tracks; bottom: parallel bypassing tracks)

FIGURE 4-5
Variation of Peak Surge Elevation by Track Shifts at the CDWWTP, SDWWTP, and WDWWTP

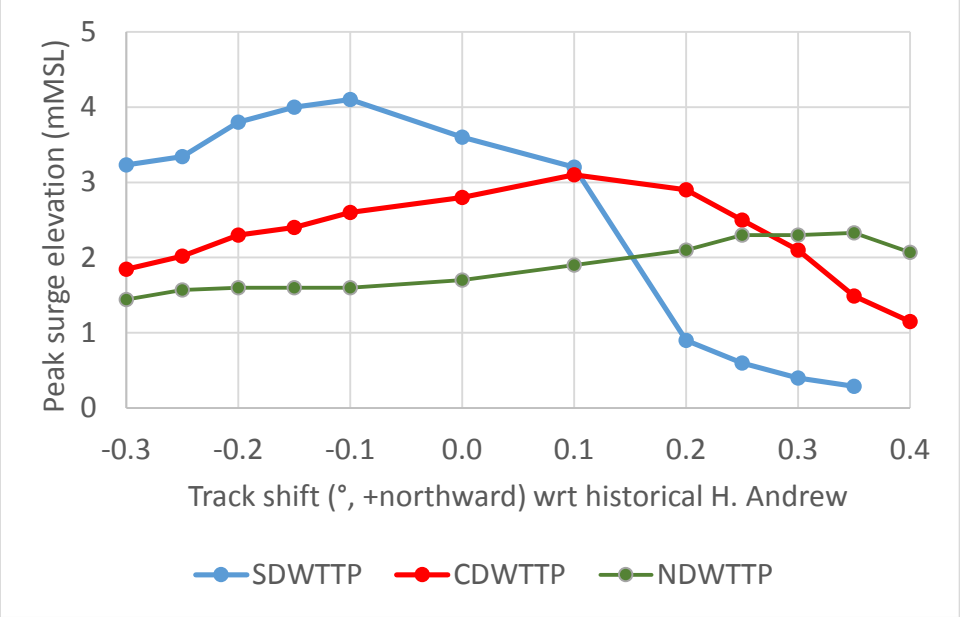

4.1.4 Input and Boundary Data

The three track-shifted run inputs employ the same setup as that already developed for the historical Hurricane Andrew, except that the latitude part of the track position was altered based on the optimized tracks discussed in Section 5.1.3. However, no corresponding changes to the latitude-dependent Radius to Maximum Wind and the Holland B parameter were made. Since the modeled results are pegged to FEMA's Stillwater elevations, this omission is not considered critical. For the with-SLR condition, additional future climate change in the maximum wind speed and pressure deficit, which were derived along the respective hurricane tracks were applied as adjusted inputs into the Cyclone Generator. However, since the maximum wind velocity were computed internally in the Holland Single Vortex formulation, only the change in the pressure deficit was explicitly applied.

For the boundary data, the original intention was to use the respective SLR projections at the offshore boundary located in the middle of the Atlantic Ocean (Figure 4-1). However, it was found that these values are spatially varying and are lower than the project SLR value of 1.23 m in the main. This may be because some of the earth processes (e.g., subsidence) that occur near continental landmass such as at the project site are either absent or do not occur to the same scale in the Atlantic Ocean. Since the surge model does not account for these non-hydraulic processes, there is a risk that the SLR value may not be recovered in the project vicinity if the projection-based values were applied at the offshore boundary. A preliminary run in the absence of hurricane but with the SLR applied as a uniform uplift of the tide-based water level boundary indicates that indeed the projected SLR value of 1.23 m was recovered in the project vicinity. The application of a uniform uplift equal to the adopted SLR projections was adopted in the scenario runs.

4.1.5 Interfacing with Flood Model

The results of the surge scenario runs were extracted at the seaward end of the FEMA transects as shown in Figure 4-6. The surge boundaries were provided in the form of time series commencing 3 days before the storm surge peak to half a day after the passage of the storm surge peak to permit the full development of the flood propagation inland overtime.

FIGURE 4-6
Locations of Transects for the Extraction of Surge Outputs (the blue squares denote the CDWWTP, SDWWTP, and WDWWTP)

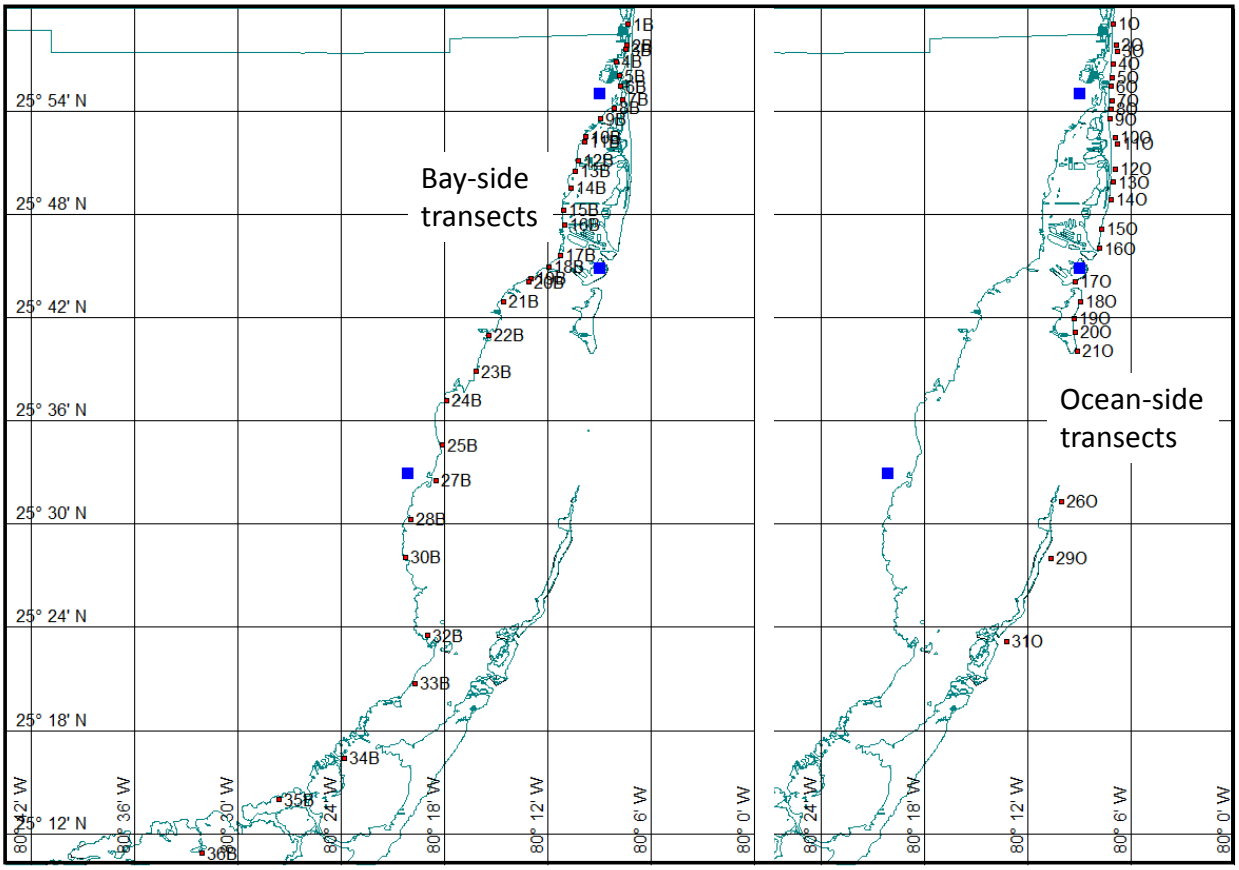

4.2 Inundation Model Setup

The Flood Modeller model input data shares much common data for the two different solvers, and the following has been used to develop the model.

4.2.1 Model Mesh

4.2.1.1 Digital Elevation Model (DEM)

This was developed from Florida Department of Emergency Management LiDAR from 2007. The data are available as a consistent data set at 5-foot resolution for the majority of the WASD area, but an additional strip of the same data set (only available at 10-foot resolution) was utilized from the Broward County area to the northern extent of the area of focus. These data sets were merged at a 20-foot resolution (using bilinear interpolation) to form a continuous DEM dataset for the entire area. More recent data from 2011 are available for Miami Beach and some of the barrier islands, but this data set was found to have some significant artefacts in the DEM surface that would have entailed significant beyond scope efforts to refine for use.

4.2.1.2 Coastal Inundation Model (2D ADI solver) Grid Resolution

The coastal inundation model using the Flood Modeller Pro 2D ADI solver was set at a 150-foot grid cell size to enable the coastal surge inundation zone to be simulated for the entire WASD area of interest. Greater

precision and resolution could be achieved in further work to refine the model by adjusting the grid cell, but at the cost of longer simulation times.

The model also makes use of the double precision calculation option to enable a more precise calculation of shallow depths in areas of the model.

4.2.1.3 Direct Rainfall (2D FAST Solver) Grid Resolution

The 2D FAST solver was set to a 50-foot grid cell resolution to enable the topographic surface to be represented by the model in more detail.

4.2.2 Canal Initial Conditions

4.2.2.1 Data Sources and Approach

The 2014 USGS Scientific Investigation report, 2014 *Hydrologic Conditions in Urban Miami-Dade County, Florida, and the Effect of Groundwater Pumpage and Increased Sea Level on Canal Leakage and Regional Groundwater Flow***,** provided by the County has information regarding the observed water levels at the structures on the canals in the study area. Following consultation with the County, the average of observed maximum levels at each structure were extracted from the report and used as initial conditions for the associated canals. This approach is considered conservative since canal gate operations may be adjusted to account for expected storm conditions, anecdotally it is understood that this cannot always be relied on to occur and so precautionary assumptions in this regard are considered prudent.

Appendix D provides the levels used at each stretch of the canal. Where information is not available, a reasonable level was assumed based on the available information from either the immediately downstream or upstream canal. Figure 4-7 shows the canals and structures in the study area.

4.2.2.2 Gate structure representation in topography

Elevation information associated to the gated structures (spillways and weirs), shown in Figure 4-7 was used to burn in to the DEM to represent a closed gate condition for a conservative modeling approach. The model will consider a ridge break in the topography while pre-processing the DEM along these structures (i.e., water would weir over the top of the gate breaklines if high enough). The gate opening information was provided by Miami-Dade County. The structures used with elevation information is provided in Appendix E.

4.2.3 Modeling Scenarios

Three modeling scenarios were developed for inland inundation modeling, as follows:

1. Hurricane Andrew (1992), based on measured coastal surge levels and measured rainfall
2. 100-year flood condition, based on FEMA 1 percent coastal flood elevation and estimated current 100-year precipitation
3. 100-year flood condition, based on FEMA 1 percent coastal flood elevation coupled with projected SLR in 2075 given by SE FL Climate Compact, and projected 2075 100-year precipitation.

Details on the assumed inputs and boundary conditions for each of these scenarios are presented.

FIGURE 4-7
Canal and Structures in the Study Area

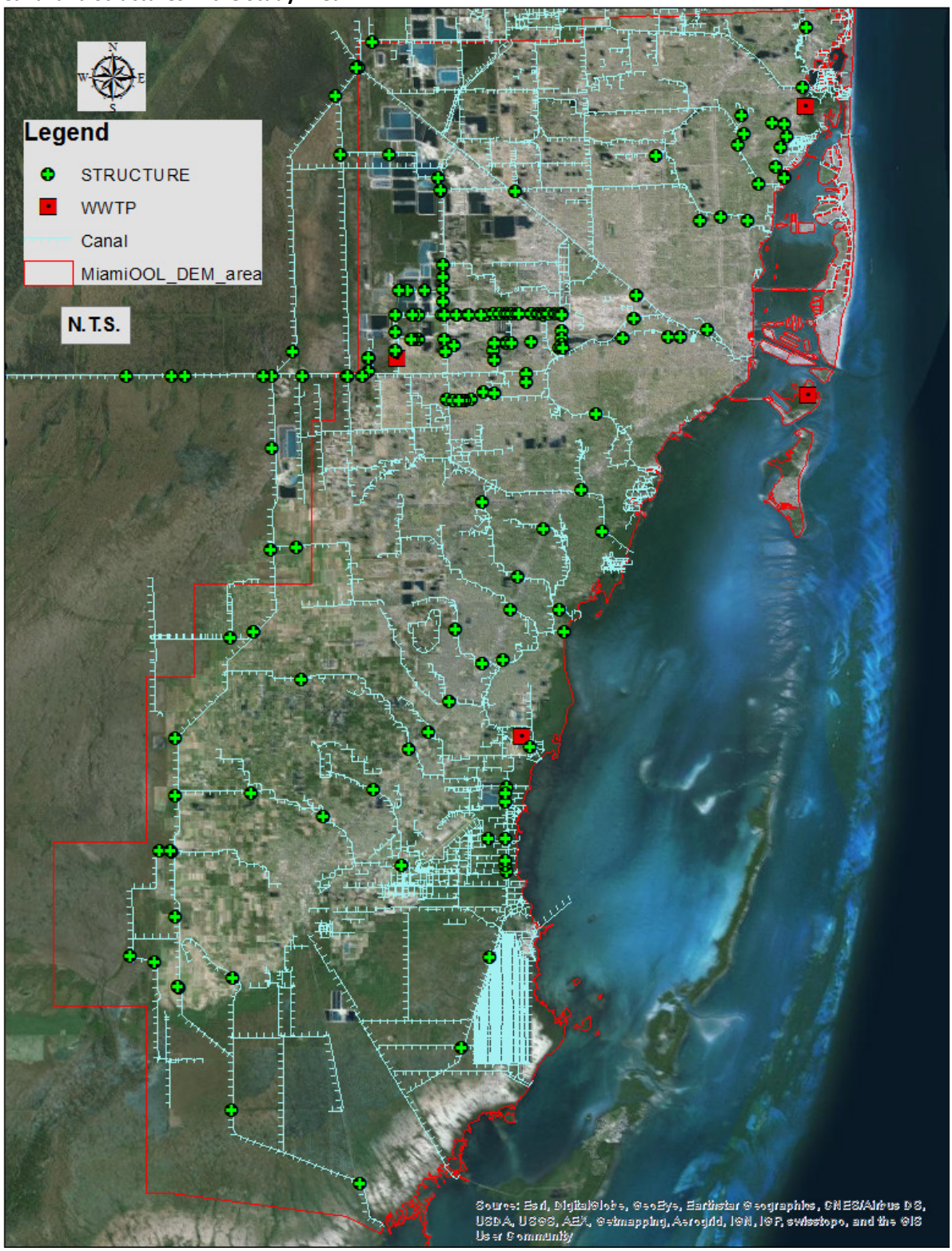

4.2.4 Input and Boundary Condition Data

4.2.4.1 Coastal Surge Boundary Conditions for 2D ADI Model

To drive the coastal inundation model (using the 2D ADI solver), coastal surge boundary condition input files were developed based on the water level time series extracted from the surge modeling described in Section 5. Locations of the extracted points were used to establish representative boundary line segments along the coast line in the study area. Each line segment was given a surge level time series based on the associated extraction point. Extraction points are shown in Figure 4-8.

Boundary conditions were developed for the following scenario models:

1. Hurricane Andrew (1992)
2. 100-year flood condition
3. 100-year with climate change and SLR condition

The coastal inundation model (2D ADI solver) output water level grid results were used as coastal boundary conditions for the direct rainfall inundation FAST model.

FIGURE 4-8
Surge Time Series Extraction Points

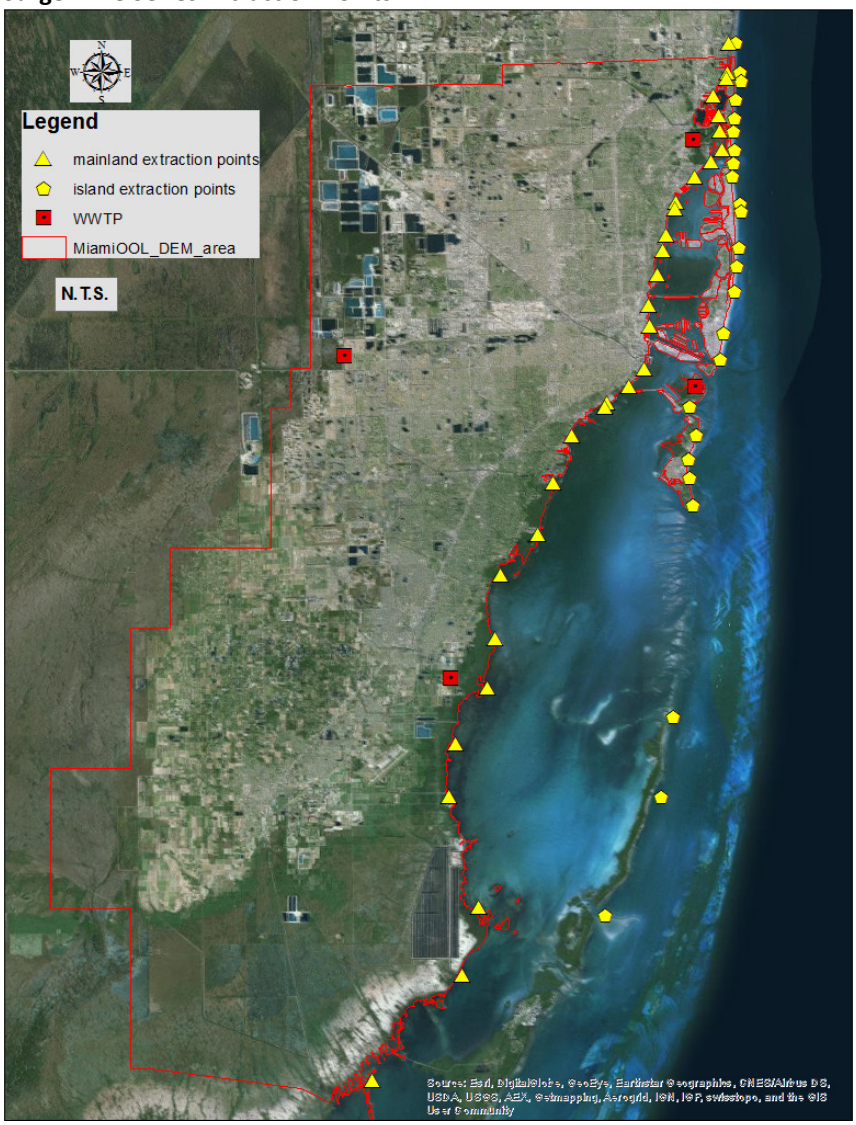

4.2.4.2 Rainfall Boundary Data

The following rainfall conditions were directly applied in the 2D FAST Solver model simulations, using the SFWMD 72-hour rainfall distribution, with the rainfall depths as follow):

- Hurricane Andrew coincident rainfall time series (2.9 inches)
- Historical 72-hour 1 in 100-year frequency storm hyetograph was developed (17.5 inches).
- 2075 projected 72-hour 1 in 100-year frequency rainfall hyetograph (21.0 inches).

The derivation and source of these data is provided in the rainfall projection report for this project *Rainfall Intensity, Duration, and Frequency Projections Based on Climate Change for Miami-Dade County*, (CH2M, May 2015).

4.2.5 Inundation Modeling Refinements for Consideration

To simulate flood inundation for an area the size of the WASD jurisdiction and present an overall picture of current and future potential flood risk requires compromise to achieve the appropriate level of detail and accuracy within project scope constraints.

The models presented here provide a broad scale understanding of flood inundation risk to the area, but further refinements could enhance the robustness of the models.

The resolution of the grids could be made more detailed to improve the representation of the flood flow mechanisms.

The representation of the canals could be enhanced to improve the model's performance in simulating the inland flood mechanisms.

Additional data, time, and effort would be required to make these enhancements and the benefit of increasing the detail and robustness of the mapping should be considered against these needs.

SECTION 5

Modeled Surge Boundary Condition

5.1 100-year Condition

The three track-shifted runs were first conducted and the modeled surge peaks extracted at the FEMA transects locations. The respective modeled surge peaks were pegged to the FEMA Stillwater elevations and the time series linearly scaled by the ratio of the FEMA Stillwater elevations to the modeled surge peaks. Therefore, the modeled surge peaks of the surge boundary conditions match the FEMA Stillwater elevations exactly as summarized in Appendix C. The variations of the surge peaks thus derived along the shoreline are shown in Figures 5-1 and 5-2 for the bay and ocean transect points, respectively.

FIGURE 5-1

Variation of Peak Surge Elevation along the Project Shoreline, Ocean Transects, 100-yr Return Period Event (the blue line denotes the 100-yr event while the red line, the 100yr + 1.23m SLR)

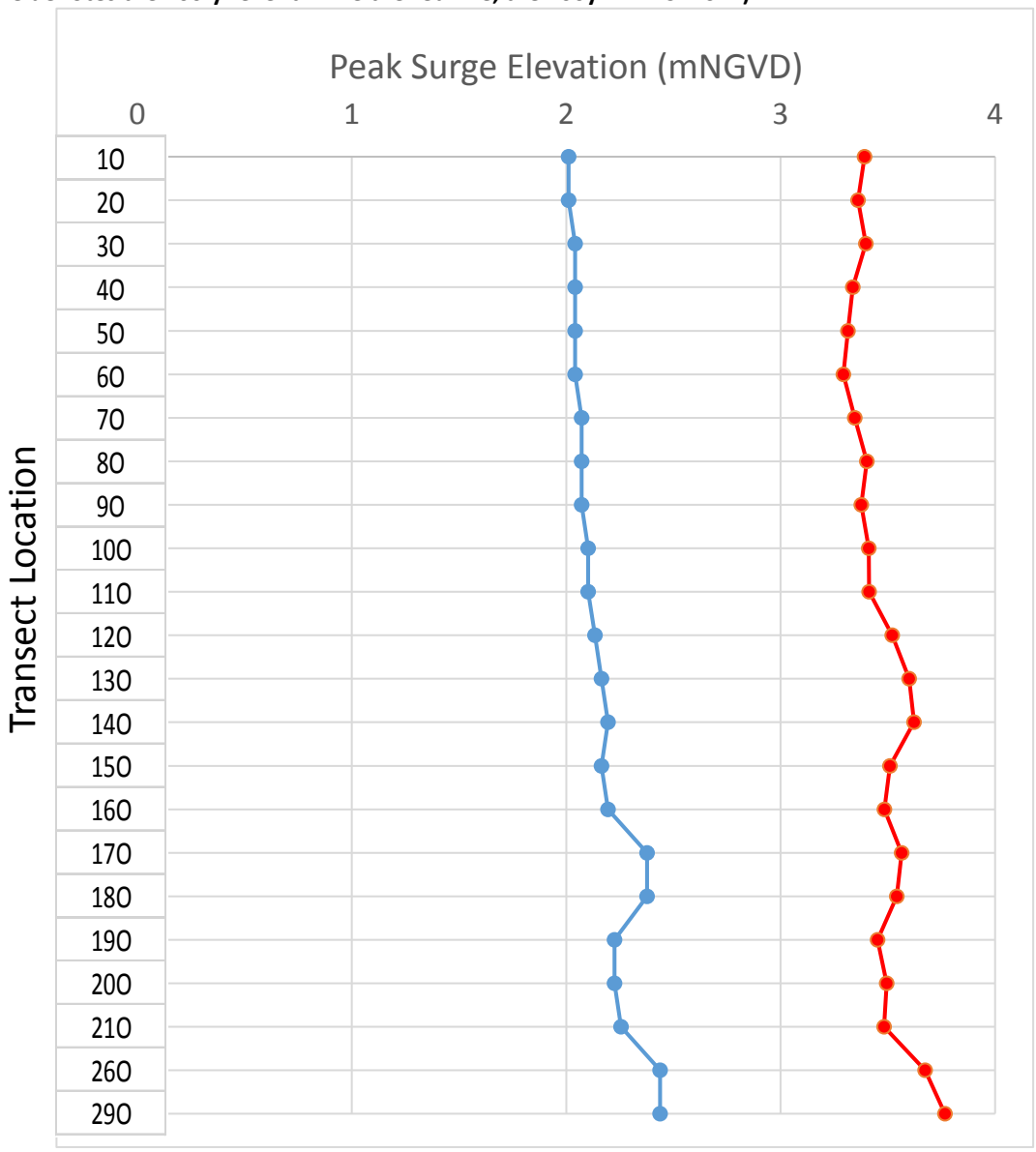

FIGURE 5-2
Variation of Peak Surge Elevation along the Project Shoreline, Ocean Transects, 100-yr Return Period Event (the blue line denotes the 100-yr event while the red line, the 100-yr + 1.23 m SLR)

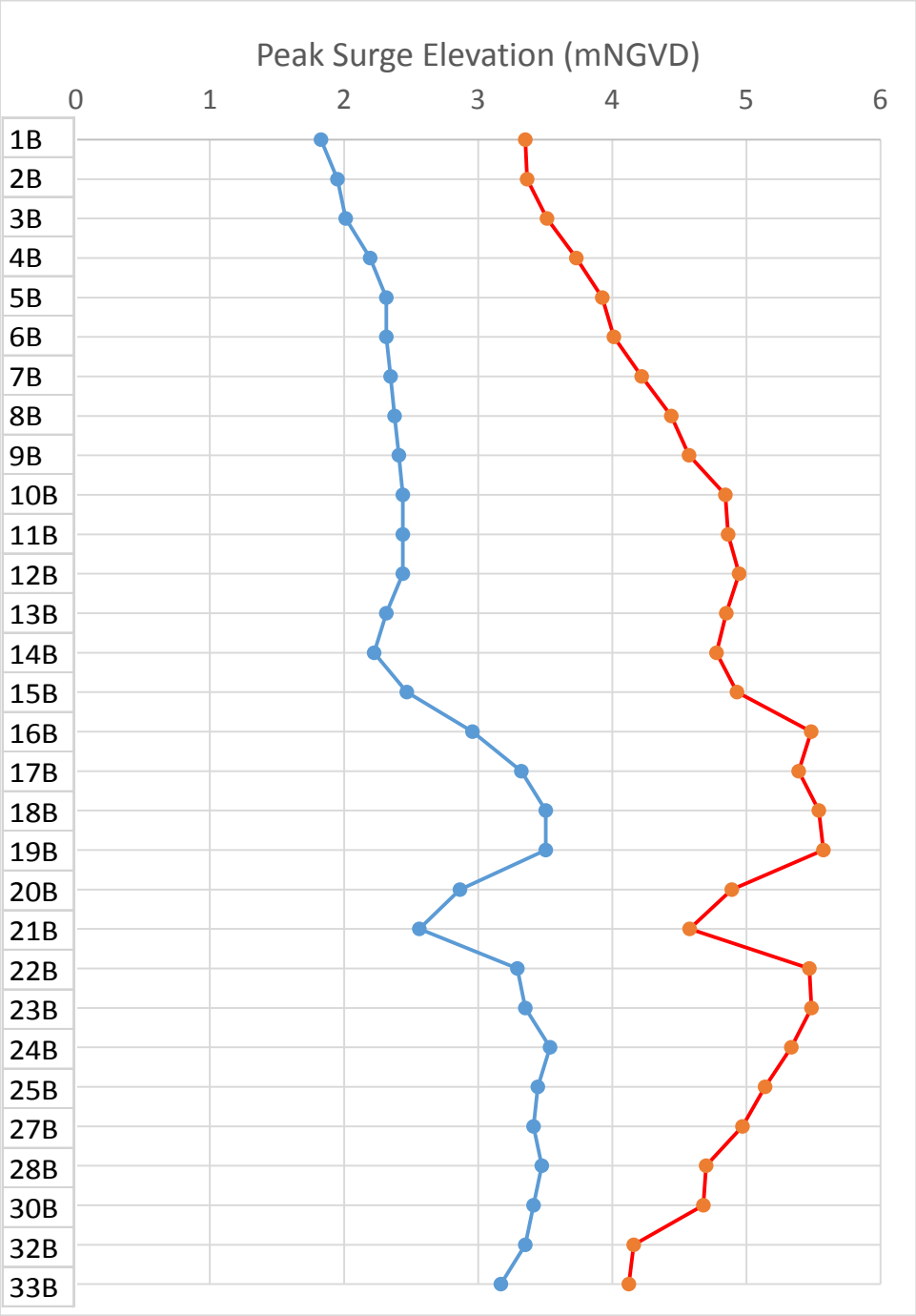

5.2 100-year Condition and 1.23 m Sea Level Rise Combined Condition

The three track-shifted runs were next conducted for the same setup as Section 6.1 except a uniform uplift of 1.23 m was applied at the offshore boundary. The resulting surge peaks were then similarly extracted along the FEMA transects and linearly scaled to the 100 yr plus SLR conditions by multiplying the results of Section 6.1 by the ratio of the modeled surge peaks of this section to the unadjusted modeled surged peaks of Section 6.1. The results are overlaid in Figures 6-1 and 6-2 for comparison. It is seen that for the ocean transect points, the increase in the peak surge elevation is only slightly above the SLR magnitude, which

could be explained by the increase in pressure deficit because of future climate change resulting in a faster wind field. Thus, this increase appears to be reasonable.

However, for the bay transects points, especially near to the center portion of the bay shoreline, the corresponding increase is higher than those at the ocean transect points. This disparity in surge amplification may suggest a resonance effect due to the increase in water surface elevation in the bay shaped water body. Another possible resonant mechanism could be the moving storm/pressure system as the contribution from the tide-SLR interaction appears to be small.

5.3 100-year Condition and 0.93 m Sea Level Rise Combined Condition

The last set of runs comprised changing the boundary uniform uplift in the water level from 1.23 m to 0.93 m and the resulting adjusted surge peaks along the FEMA transects derived in the same manner as Section 6.2.

5.4 Change Analysis of the Two Sea Level Rise Conditions

A comparison in the form of a scatter plot of the modeled surge elevations from Section 6.3 and those based on linearly scaling from the results of Section 6.2 is shown in Figure 5-3. Figure 5-3 shows that the linear scaling approach may be used as a first order estimate to derive the SLR impacts due to other SLR projections, but there is a broad trend toward a slight underestimation, more so for the ocean transects. The mean values of the ratio of the linear-scaled surge elevation/modeled surge elevation are 0.92 for the ocean transects and 0.97 for the bay transects, respectively.

FIGURE 5-3
Scatter Plot of Modeled Surge Elevations and Linearly Scaled Surge Elevations, 100-yr with SLR Conditions

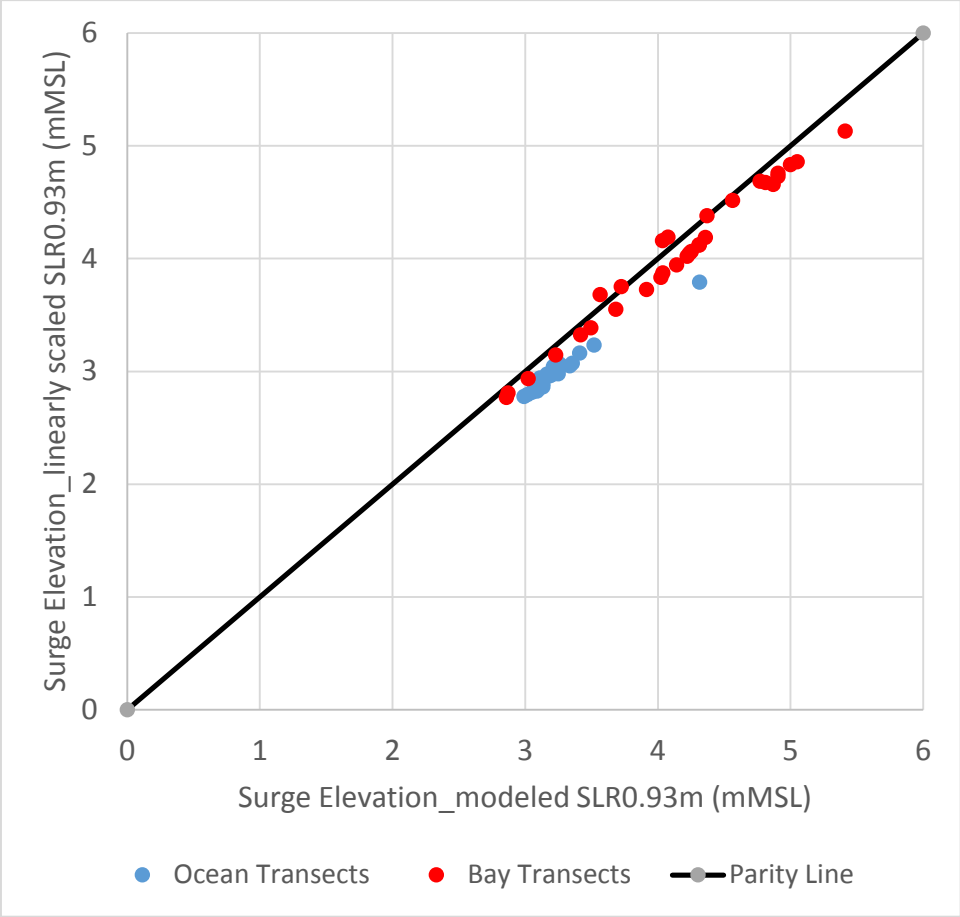

SECTION 6

Modeled Flood Extent and Depth Results

To assess the effectiveness of the inundation modeling approach, Hurricane Andrew conditions were simulated using the Flood Modeller setups described above.

6.1 Hurricane Andrew

The observed storm tide of Hurricane Andrew is shown in Figure 6-1. The combined results from the models and the flood inundation extents for Hurricane Andrew are shown in Figure 6-2. These results compare well with the debris line data presented by Sheng et al. (2015) during their recent presentation entitled *Coastal Inundation Risk for SE Florida: Incorporating Climate Change Impact on Hurricanes and Sea Level Rise*. Details provided in the storm surge and climate modeling presentation with Dr. Sheng on May 8, 2015, at the main government center in Fort Lauderdale (115 S Andrews Ave, Room 301, Fort Lauderdale, Florida 33301). The presentation file (BrowardMeeting05082015.pdf) was circulated to attendees.

6.2 Model Extents for 100-year Storm, and 100-Year Storm with Sea Level Rise

The 100-year inundation results are presented in Figure 6-3, while Figure 6-4 presents the results for the 100-year scenario with climate change and sea level rise condition.

The 100-year simulation results do show less flooding than the current FEMA Flood Zone maps for the area. The modeling methods are different however, and it is important to recognize that the mapping presented has been developed through simplified methods that do not explicitly model the detailed canal and drainage network in the area. Subsequent refinement of the models could address these limitations but would require a model that explicitly includes these hydraulic details.

The future 100-year inundation map shows broad and significant flooding throughout the WASD area.

For each simulation flood inundation depth grids, flood inundation water elevation grids, and flow direction shapefiles are available and used to estimate projected flooding depths at critical WASD facilities, as discussed in a separate report.

FIGURE 6-1
Observed Storm Tide of Hurricane Andrew

FIGURE 6-2
Hurricane Andrew Depth Grid

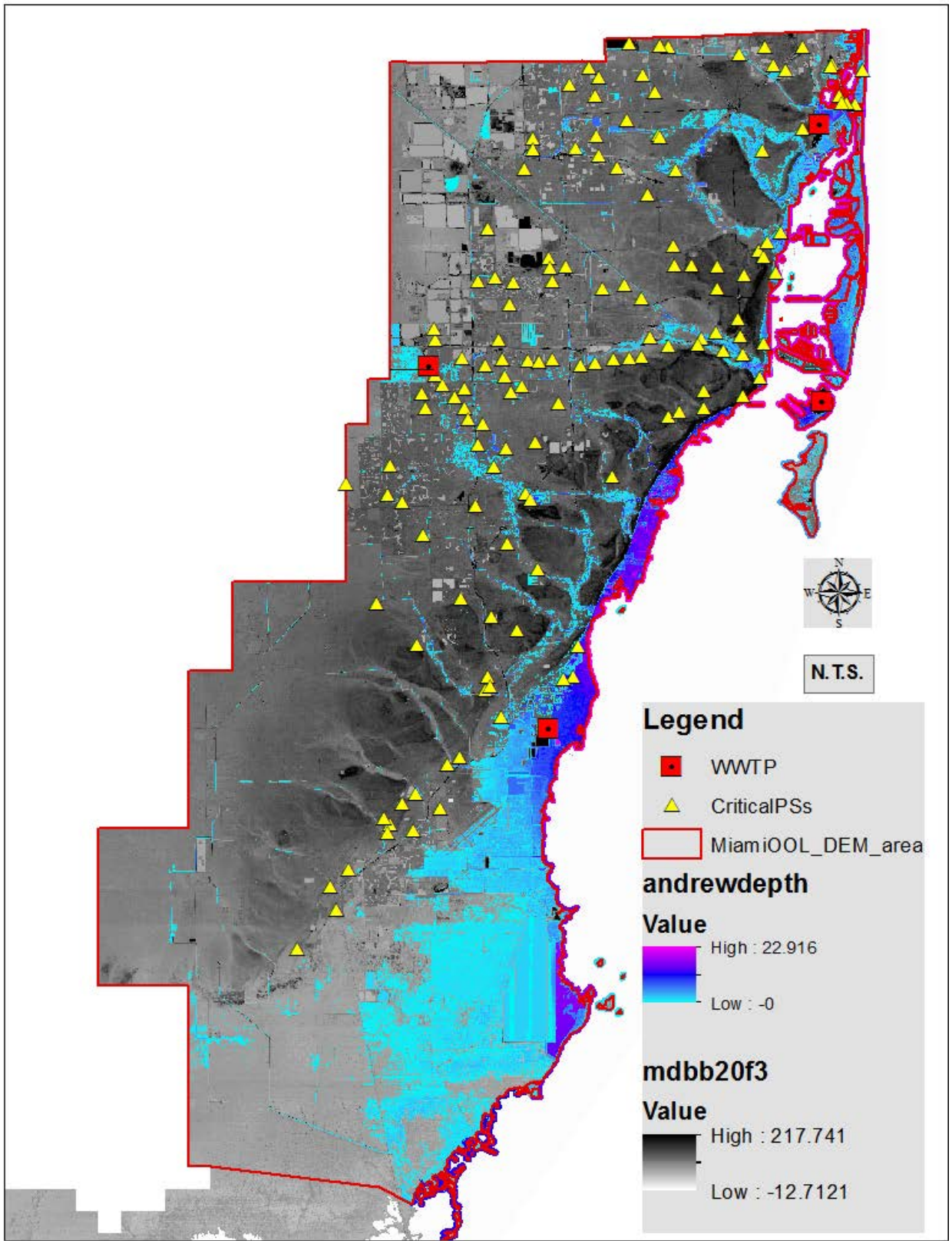

FIGURE 6-3
100-year Depth Grid

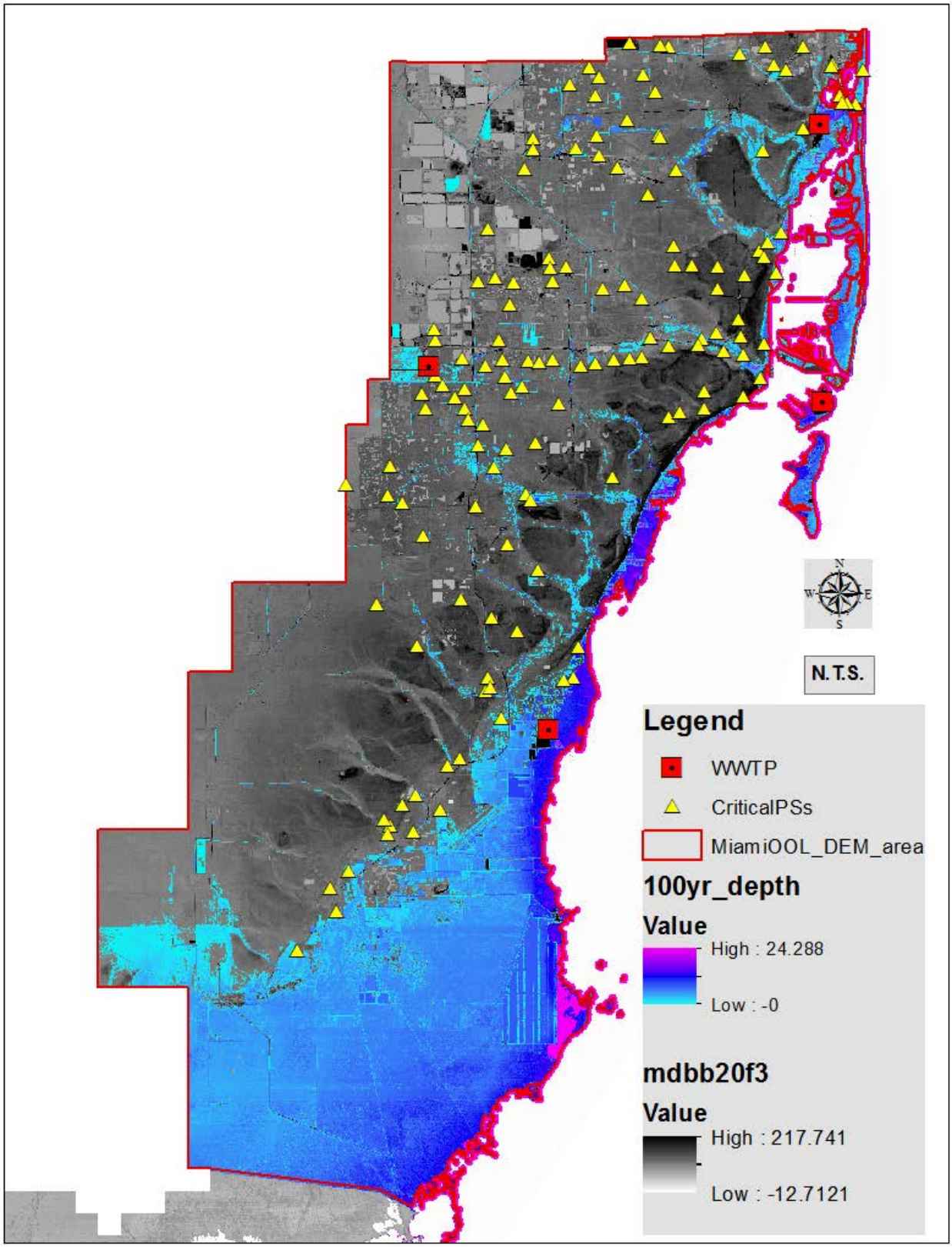

FIGURE 6-4
Future 100-year with Climate Change and Sea Level Rise Depth Grid

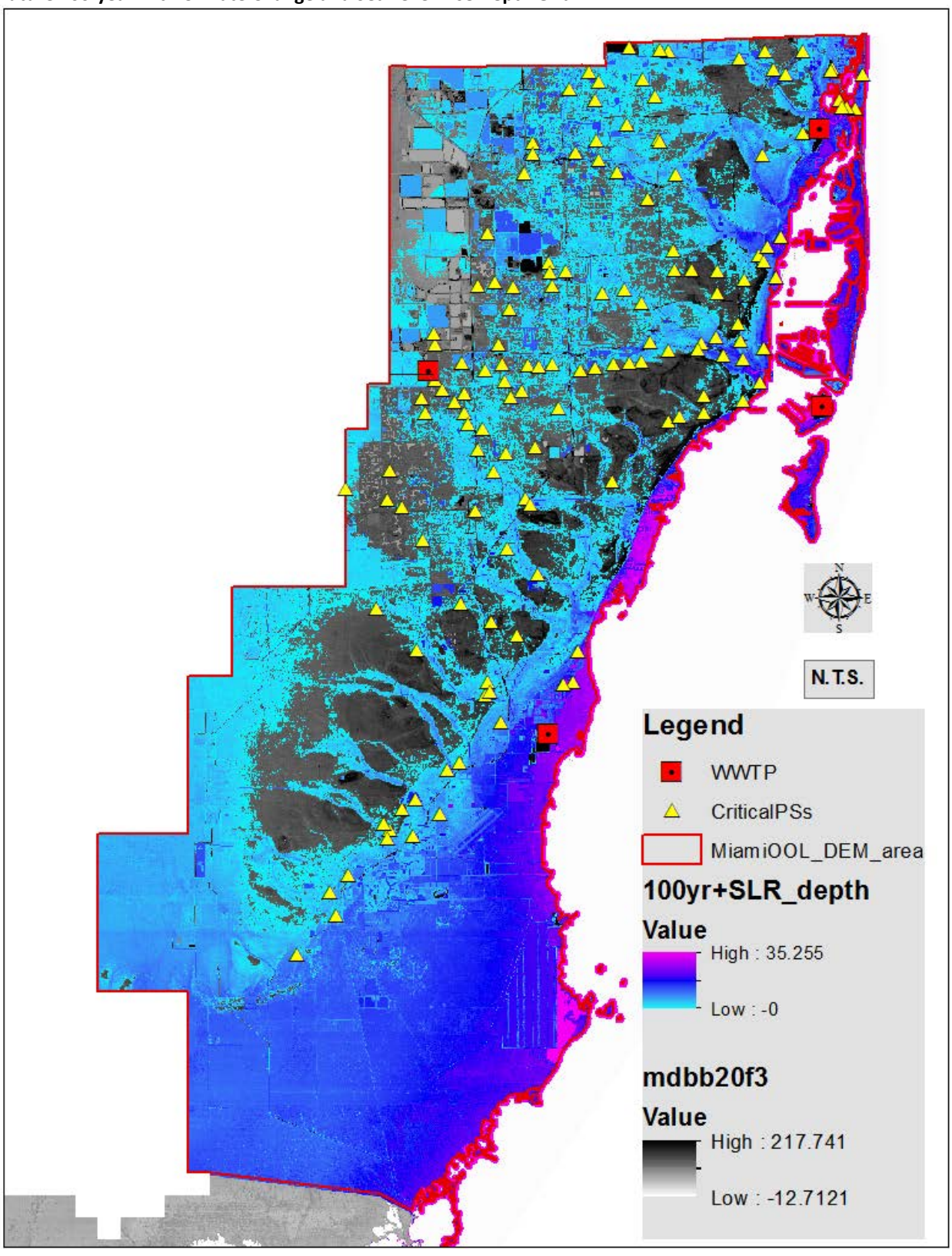

SECTION 7

Next Steps

The modeled outputs from the surge modeling component are consistent with FEMA's Stillwater elevations. However, these are not directly comparable to FEMA's BFEs that includes wave-height effects. While a first order estimate of future BFEs incorporating the effect of SLR can be made by assuming the same degree of wave height effects used in FEMA's BFEs, it is conceivable that a larger wave height effect may result in the future due to the larger water depths resulting from SLR. This increase in wave height effect in the future can be reasonably assessed by comparing the wave height results of the no- SLR and SLR scenario runs. By pegging the modeled no-SLR wave heights to the published FEMA's wave heights corresponding to FEMA's BFEs in FEMA's FIS, the increased wave heights for the SLR scenario can be estimated using linear scaling as was done for the 100yr plus SLR Stillwater elevations. The wave height attenuation overland can then be estimated using FEMA's WHAFIS (Wave Height Analysis for Flood Insurance Studies) to derive the BFEs corresponding to the future SLR condition.

As yet, the non-linear amplification in the peak water level under the SLR scenario has not been adequately investigated. By expanding the surge scenarios to include other SLR scenarios and hurricane track trajectories to complement the available result sets, the resulting comparison of amplification as a function of SLR magnitudes and hurricane track trajectories may illuminate the causative mechanisms.

The 100-year simulation results do show less flooding than the current FEMA Flood Zone maps for the area. The modeling methods are different however, and it is important to recognize that the mapping presented has been developed through simplified methods that do not explicitly model the detailed canal and drainage network in the area.

It is recommended that the inland flood inundation models be refined to address these limitations by explicitly including the following hydraulic details.

- A more detailed resolution of the hydraulic calculation grids to improve the representation of the flood flow mechanisms and increase the accuracy/precision of stage results.
- Enhancing the representation of the canals to improve the model's performance in simulating the inland flood mechanisms and the potential interconnected flood flow routes between canal subwatersheds.

SECTION 8

References

Andersen, O.B. 1995. *Global Ocean Tides from ERS-1 and TOPEX/POSEODON Altimetry*, Journal of Geophysical Research, Vol. 100 (C12), pp. 25,249-25,259.

CH2M HILL (CH2M). 2015. *Extreme Wind Speed and Sea Level Pressure Change Analysis for Miami-Dade County.* Ocean Outfall Legislation Program, Miami-Dade Country Water and Sewer Department, April.

CH2M HILL (CH2M). 2015. *Sea Level Rise Projections for Miami-Dade County*. Ocean Outfall Legislation Program, Miami-Dade Country Water and Sewer Department, April.

FEMA. 1995. Flood Insurance Study, Miami-Dade County, Florida and Incorporated Areas, January 20, 1993, revised July 17, 1995, 47p.

Harper and Holland, G. 1999. *An Updated Parametric Model of The Tropical Cyclone*, pp. 893–896.
Harper, B.A., Hardy, T.A., Mason, L.B., Bode, L., Young, I.R., Nielsen, P. (2001). Queensland climate change and community vulnerability to tropical cyclones, Ocean hazards assessment - Stage 1, report, Department of Natural Resources and Mines, Queensland, Brisbane, Australia, 368 p.

Holland, B.A. and G. 1980. *An Analytic Model of the Wind And Pressure Profiles in Hurricanes.* Monthly Weather review, volume 108, pp. 1212-1218.

Landsea, C.W., Franklin, J.J., McAdie, C.J., Beven II, J.L., Gross, J.M. 2004. *A Reanalysis of Hurricane Andrew's Intensity*, Bulletin of the American Meteorological Society, Nov 2004, pp. 1699-1712.

MIKE by DHI. 2012. MIKE CMAP bathymetry data set.

MIKE by DHI. 2014a. MIKE 21 Flow FM module, user manual.

MIKE by DHI. 2014b. MIKE 21 SW FM module, user manual.

MIKE by DHI. 2014c. MIKE 21 Toolbox, user manual.

National Oceanic and Atmospheric Administration (NOAA). 1993. H*urricane Andrew: South Florida and Louisiana, August 23-26*, 1002, Natural Disaster Survey Report, variously paginated.

National Oceanic and Atmospheric Administration (NOAA). 2013. *2013 National Hurricane Preparedness Week*, Miami-South Florida National Weather Service Forecast Office, 5p. (downloaded from **http://www.srh.noaa.gov/images/mfl/news/StormSurgeArticle.pdf**)

Shen, J. Zhang, K., Xiao, C. and Gong, W. 2006. *Improved Prediction of Storm Surge Inundation with a High-Resolution Unstructured Grid Model*. Journal of Coastal Research, Vol. 22/6, Nov 2006, pp. 1309-1319.

Sheng, Y and Paramygin, V.A. 2015. *Coastal Inundation Risk for SE Florida: Incorporating Climate Change Impact on Hurricanes and Sea Level Rise.*

Sobey, R.J., Harper, B.A., Stark, K.P. 1977. *Numerical Simulation of Tropical Cyclone Storm Surge*, Research Bulletin CS-14, Dept Civil and Systems Engineering, James Cook University.

Vickery, P.J. and Wadhera, D. 2008. *Statistical models of Holland pressure profile parameter and radius to maximum winds of hurricanes from flight-level pressure and H*Wind data*, Journal of Applied Meteorology and Climatology, American Meteorology Society, Vol. 47, Oct 2008, pp. 2497-2517.

Young, I.R. and Sobey, R.J. 1981. *The Numerical Prediction of Tropical Cyclone Wind-Waves*, James Cook University of North Queensland, Townville, Dept. of Civil & Systems Eng., Research Bulletin No. CS20.

Wu, J. 1980. *Wind Stress Coefficients over Sea Surface near Neutral Conditions*. A revisit, Journal of Physical Oceanography, Vol. 10, pp. 727-740.

Zhang, K., Li, Y, Liu, H., Xu, H & Shen, J. 2013. *Comparison of Three Methods for Estimating the Sea Level Rise Effect on Storm Surge Flooding*, Climatic Change, Springer, vol. 118(2), pp. 487-500.

Murray, M.H. (1994). *Storm-Tide Elevations Produced by Hurricane Andrew Along the Southern Florida Coasts*, August 24, 21992, USGS Open-File Report 94-116, 27 (downloaded from http://pubs.usgs.gov/of/1994/0116/report.pdf)

Appendix A
MIKE 21 & MIKE 3 Flow Model FM, Hydrodynamic Module Short Description

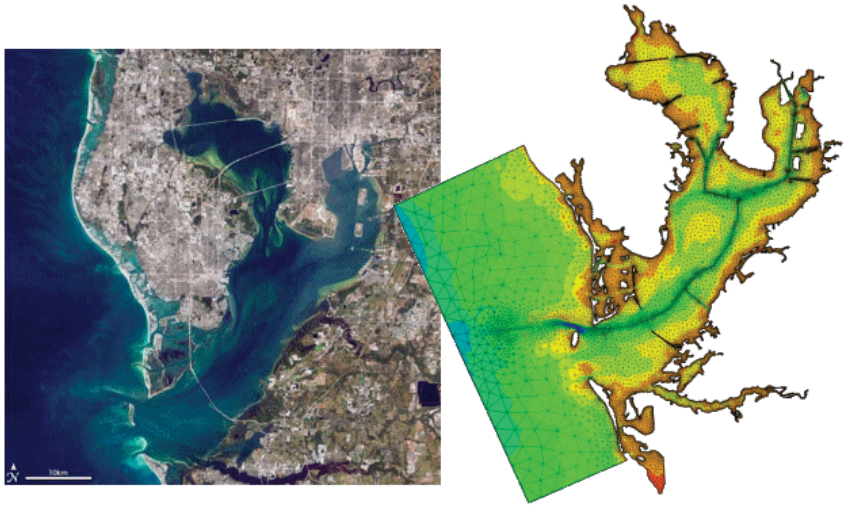

MIKE 21 & MIKE 3 Flow Model FM

Hydrodynamic Module

Short Description

Software for WATER ENVIRONMENTS

DHI headquarters
Agern Allé 5
DK-2970 Hørsholm
Denmark

+45 4516 9200 Telephone
+45 4516 9333 Support
+45 4516 9292 Telefax

mikebydhi@dhigroup.com
www.mikebydhi.com

MIKE213_HD_FM_Short_Description_.docx / AJS/EBR / 2013-09-19

MIKE 21 & MIKE 3 Flow Model FM

The Flow Model FM is a comprehensive modelling system for two- and three-dimensional water modelling developed by DHI. The 2D and 3D models carry the same names as the classic DHI model versions MIKE 21 & MIKE 3 with an 'FM' added referring to the type of model grid - Flexible Mesh.

The modelling system has been developed for complex applications within oceanographic, coastal and estuarine environments. However, being a general modelling system for 2D and 3D free-surface flows it may also be applied for studies of inland surface waters, e.g. overland flooding and lakes or reservoirs.

MIKE 21 & MIKE 3 Flow Model FM is a general hydrodynamic flow modelling system based on a finite volume method on an unstructured mesh

The Modules of the Flexible Mesh Series

DHI's Flexible Mesh (FM) series includes the following modules:

Flow Model FM modules

- Hydrodynamic Module, HD
- Transport Module, TR
- Ecology Module, ECO Lab
- Oil Spill Module, ELOS
- Sand Transport Module, ST
- Mud Transport Module, MT
- Particle Tracking Module, PT

Wave module

- Spectral Wave Module, SW

The FM Series meets the increasing demand for realistic representations of nature, both with regard to 'look alike' and to its capability to model coupled processes, e.g. coupling between currents, waves and sediments. Coupling of modules is managed in the Coupled Model FM.

All modules are supported by advanced user interfaces including efficient and sophisticated tools for mesh generation, data management, 2D/3D visualization, etc. In combination with comprehensive documentation and support, the FM series forms a unique professional software tool for consultancy services related to design, operation and maintenance tasks within the marine environment.

An unstructured grid provides an optimal degree of flexibility in the representation of complex geometries and enables smooth representations of boundaries. Small elements may be used in areas where more detail is desired, and larger elements used where less detail is needed, optimising information for a given amount of computational time.

The spatial discretisation of the governing equations is performed using a cell-centred finite volume method. In the horizontal plane an unstructured grid is used while a structured mesh is used in the vertical domain (3D).

This document provides a short description of the Hydrodynamic Module included in MIKE 21 & MIKE 3 Flow Model FM.

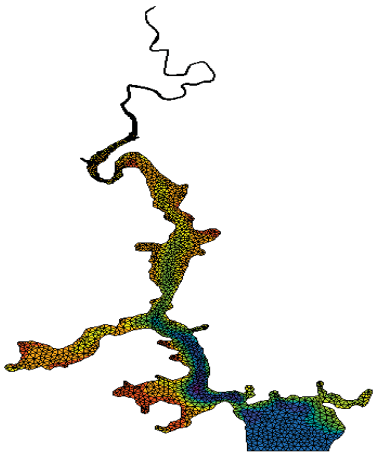

Example of computational mesh for Tamar Estuary, UK

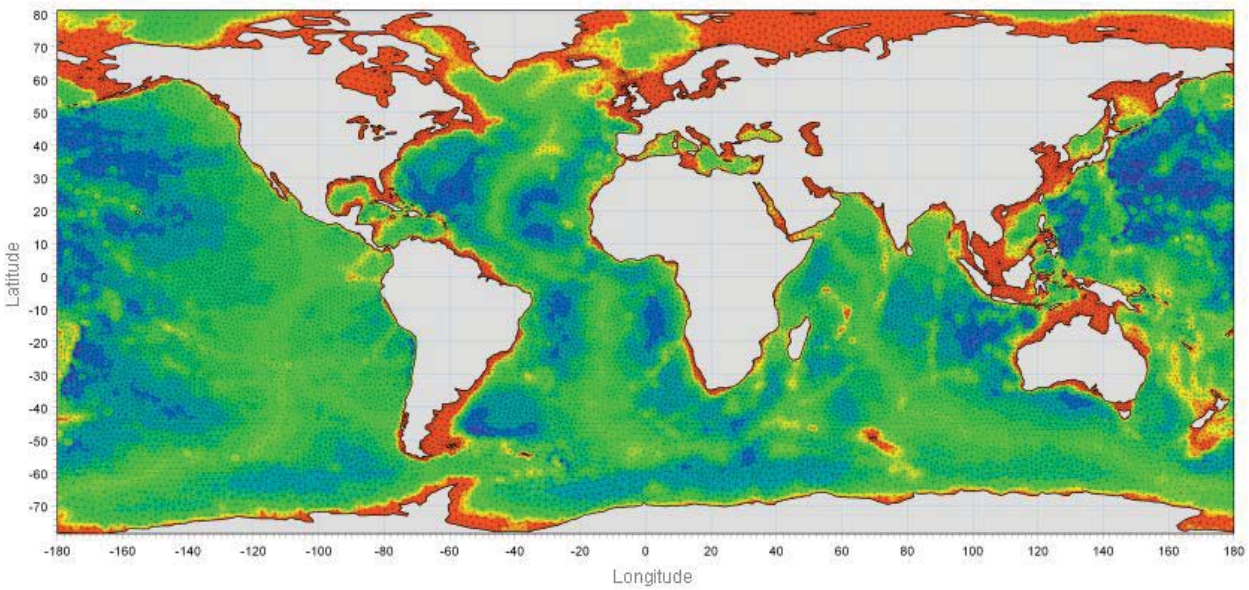

MIKE 21 & MIKE 3 FLOW MODEL FM supports both Cartesian and spherical coordinates. Spherical coordinates are usually applied for regional and global sea circulation applications. The chart shows the computational mesh and bathymetry for the planet Earth generated by the MIKE Zero Mesh Generator

MIKE 21 & MIKE 3 Flow Model FM - Hydrodynamic Module

The Hydrodynamic Module provides the basis for computations performed in many other modules, but can also be used alone. It simulates the water level variations and flows in response to a variety of forcing functions on flood plains, in lakes, estuaries and coastal areas.

Application Areas

The Hydrodynamic Module included in MIKE 21 & MIKE 3 Flow Model FM simulates unsteady flow taking into account density variations, bathymetry and external forcings.

The choice between 2D and 3D model depends on a number of factors. For example, in shallow waters, wind and tidal current are often sufficient to keep the water column well-mixed, i.e. homogeneous in salinity and temperature. In such cases a 2D model can be used. In water bodies with stratification, either by density or by species (ecology), a 3D model should be used. This is also the case for enclosed or semi-enclosed waters where wind-driven circulation occurs.

Typical application areas are

- Assessment of hydrographic conditions for design, construction and operation of structures and plants in stratified and non-stratified waters
- Environmental impact assessment studies
- Coastal and oceanographic circulation studies
- Optimization of port and coastal protection infrastructures
- Lake and reservoir hydrodynamics
- Cooling water, recirculation and desalination
- Coastal flooding and storm surge
- Inland flooding and overland flow modelling
- Forecast and warning systems

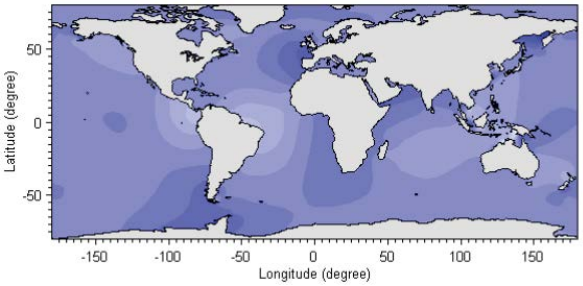

Example of a global tide application of MIKE 21 Flow Model FM. Results from such a model can be used as boundary conditions for regional scale forecast or hindcast models

The MIKE 21 & MIKE 3 Flow Model FM also support spherical coordinates, which makes both models particularly applicable for global and regional sea scale applications.

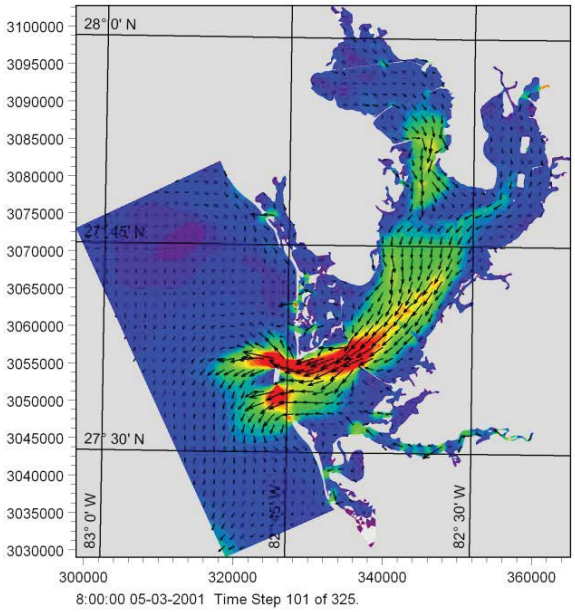

Example of a flow field in Tampa Bay, FL, simulated by MIKE 21 Flow Model FM

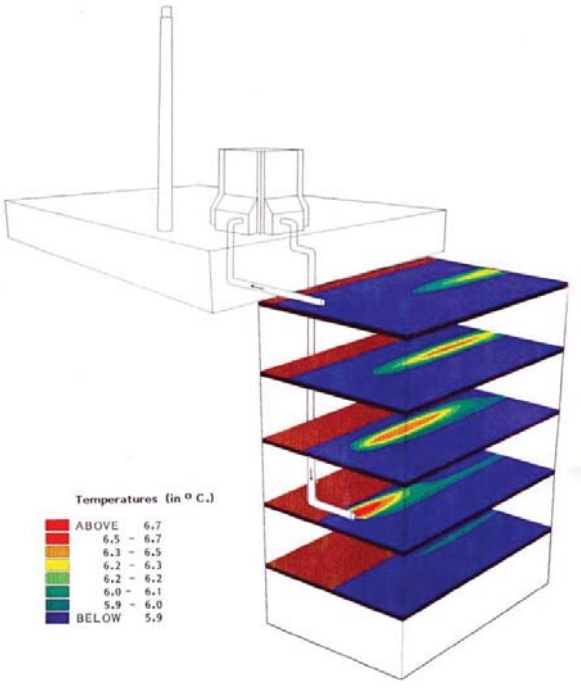

Study of thermal recirculation

Typical applications with the MIKE 21 & MIKE 3 Flow Model FM include cooling water recirculation and ecological impact assessment (eutrophication)

The Hydrodynamic Module is together with the Transport Module (TR) used to simulate the spreading and fate of dissolved and suspended substances. This module combination is applied in tracer simulations, flushing and simple water quality studies.

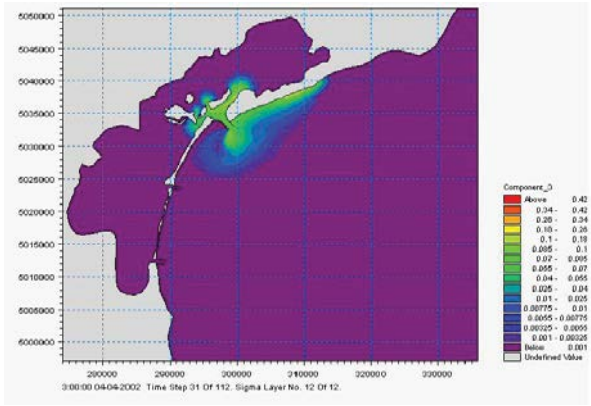

Tracer simulation of single component from outlet in the Adriatic, simulated by MIKE 21 Flow Model FM HD+TR

Prediction of ecosystem behaviour using the MIKE 21 & MIKE 3 Flow Model FM together with ECO Lab

The Hydrodynamic Module can be coupled to the Ecological Module (ECO Lab) to form the basis for environmental water quality studies comprising multiple components.

Furthermore, the Hydrodynamic Module can be coupled to sediment models for the calculation of sediment transport. The Sand Transport Module and Mud Transport Module can be applied to simulate transport of non-cohesive and cohesive sediments, respectively.

In the coastal zone the transport is mainly determined by wave conditions and associated wave-induced currents. The wave-induced currents are generated by the gradients in radiation stresses that occur in the surf zone. The Spectral Wave Module can be used to calculate the wave conditions and associated radiation stresses.

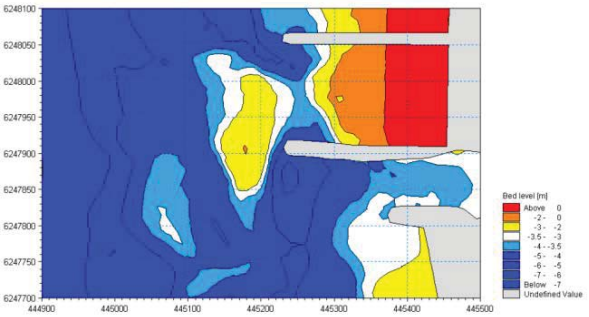

Coastal application (morphology) with coupled MIKE 21 HD, SW and ST, Torsminde harbour Denmark

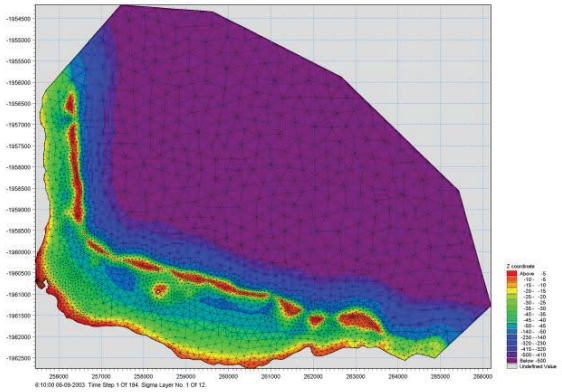

Model bathymetry of Taravao Bay, Tahiti

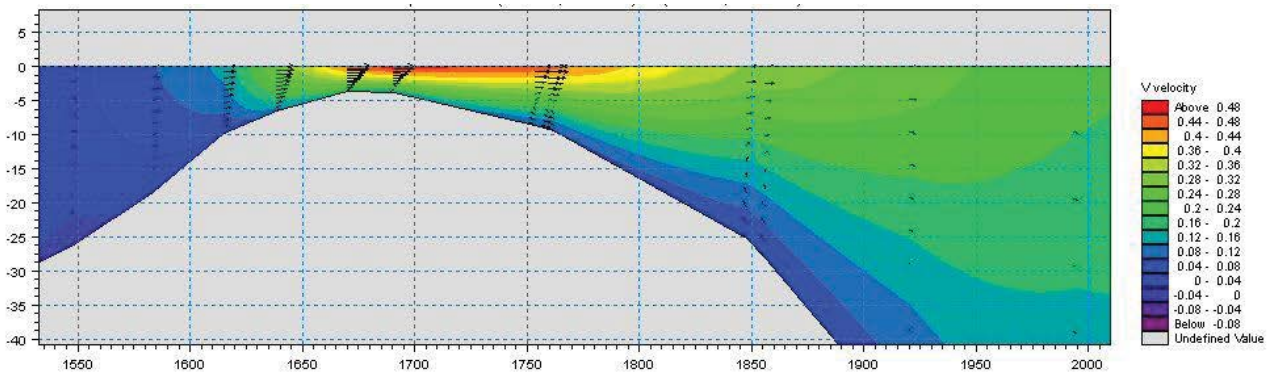

Example of Cross reef currents in Taravao Bay, Tahiti simulated with MIKE 3 Flow Model FM. The circulation and renewal of water inside the reef is dependent on the tides, the meteorological conditions and the cross reef currents, thus the circulation model includes the effects of wave induced cross reef currents

Computational Features

The main features and effects included in simulations with the MIKE 21 & MIKE 3 Flow Model FM – Hydrodynamic Module are the following:

- Flooding and drying
- Momentum dispersion
- Bottom shear stress
- Coriolis force
- Wind shear stress
- Barometric pressure gradients
- Ice coverage
- Tidal potential
- Precipitation/evaporation
- Wave radiation stresses
- Sources and sinks

Model Equations

The modelling system is based on the numerical solution of the two/three-dimensional incompressible Reynolds averaged Navier-Stokes equations subject to the assumptions of Boussinesq and of hydrostatic pressure. Thus, the model consists of continuity, momentum, temperature, salinity and density equations and it is closed by a turbulent closure scheme. The density does not depend on the pressure, but only on the temperature and the salinity.

For the 3D model, the free surface is taken into account using a sigma-coordinate transformation approach or using a combination of a sigma and z-level coordinate system.

Below the governing equations are presented using Cartesian coordinates.

The local continuity equation is written as

$$\frac{\partial u}{\partial x}+\frac{\partial v}{\partial y}+\frac{\partial w}{\partial z}=S$$

and the two horizontal momentum equations for the x- and y-component, respectively

$$\frac{\partial u}{\partial t}+\frac{\partial u^2}{\partial x}+\frac{\partial vu}{\partial y}+\frac{\partial wu}{\partial z}=fv-g\frac{\partial \eta}{\partial x}-$$
$$\frac{1}{\rho_0}\frac{\partial p_a}{\partial x}-\frac{g}{\rho_0}\int_z^\eta \frac{\partial \rho}{\partial x}dz+F_u+\frac{\partial}{\partial z}\left(\nu_t\frac{\partial u}{\partial z}\right)+u_sS$$

$$\frac{\partial v}{\partial t}+\frac{\partial v^2}{\partial y}+\frac{\partial uv}{\partial x}+\frac{\partial wv}{\partial z}=-fu-g\frac{\partial \eta}{\partial y}-$$
$$\frac{1}{\rho_0}\frac{\partial p_a}{\partial y}-\frac{g}{\rho_0}\int_z^\eta \frac{\partial \rho}{\partial y}dz+F_v+\frac{\partial}{\partial z}\left(\nu_t\frac{\partial v}{\partial z}\right)+v_sS$$

Temperature and salinity

In the Hydrodynamic Module, calculations of the transports of temperature, *T*, and salinity, *s* follow the general transport-diffusion equations as

$$\frac{\partial T}{\partial t}+\frac{\partial uT}{\partial x}+\frac{\partial vT}{\partial y}+\frac{\partial wT}{\partial z}=F_T+\frac{\partial}{\partial z}\left(D_v\frac{\partial T}{\partial z}\right)+\hat{H}+T_sS$$

$$\frac{\partial s}{\partial t}+\frac{\partial us}{\partial x}+\frac{\partial vs}{\partial y}+\frac{\partial ws}{\partial z}=F_s+\frac{\partial}{\partial z}\left(D_v\frac{\partial s}{\partial z}\right)+s_sS$$

Unstructured mesh technique gives the maximum degree of flexibility, for example: 1) Control of node distribution allows for optimal usage of nodes 2) Adoption of mesh resolution to the relevant physical scales 3) Depth-adaptive and boundary-fitted mesh. Below is shown an example from Ho Bay Denmark with the approach channel to the Port of Esbjerg

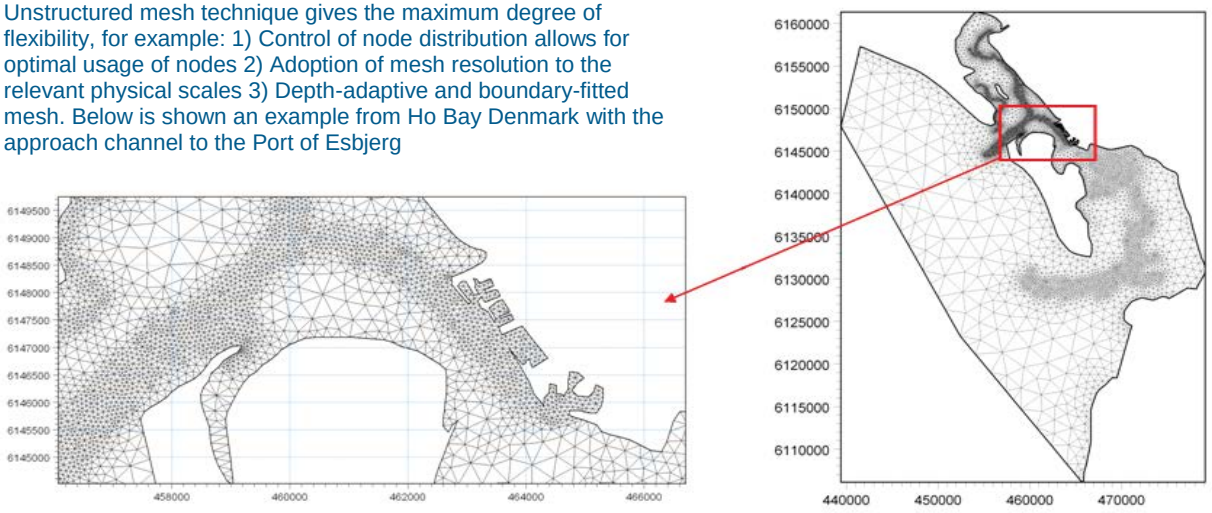

The horizontal diffusion terms are defined by

$$(F_T, F_s) = \left[\frac{\partial}{\partial x}\left(D_h \frac{\partial}{\partial x} \right) + \frac{\partial}{\partial y}\left(D_h \frac{\partial}{\partial y} \right) \right](T, s)$$

The equations for two-dimensional flow are obtained by integration of the equations over depth.

Heat exchange with the atmosphere is also included.

Symbol list	
t	time
x, y, z	Cartesian coordinates
u, v, w	flow velocity components
T, s	temperature and salinity
D_v	vertical turbulent (eddy) diffusion coefficient
$\hat{H}$	source term due to heat exchange with atmosphere
S	magnitude of discharge due to point sources
T_s, s_s	temperature and salinity of source
F_T, F_s, F_c	horizontal diffusion terms
D_h	horizontal diffusion coefficient
h	depth

Solution Technique

The spatial discretisation of the primitive equations is performed using a cell-centred finite volume method. The spatial domain is discretised by subdivision of the continuum into non-overlapping elements/cells.

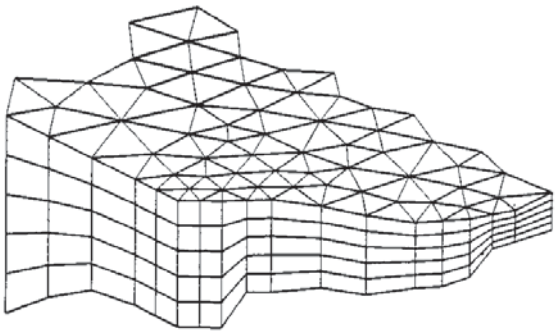

Principle of 3D mesh

In the horizontal plane an unstructured mesh is used while a structured mesh is used in the vertical domain of the 3D model. In the 2D model the elements can be triangles or quadrilateral elements. In the 3D model the elements can be prisms or bricks whose horizontal faces are triangles and quadrilateral elements, respectively.

Model Input

Input data can be divided into the following groups:

- Domain and time parameters:
  - computational mesh (the coordinate type is defined in the computational mesh file) and bathymetry
  - simulation length and overall time step
- Calibration factors
  - bed resistance
  - momentum dispersion coefficients
  - wind friction factors
- Initial conditions
  - water surface level
  - velocity components
- Boundary conditions
  - closed
  - water level
  - discharge
- Other driving forces
  - wind speed and direction
  - tide
  - source/sink discharge
  - wave radiation stresses

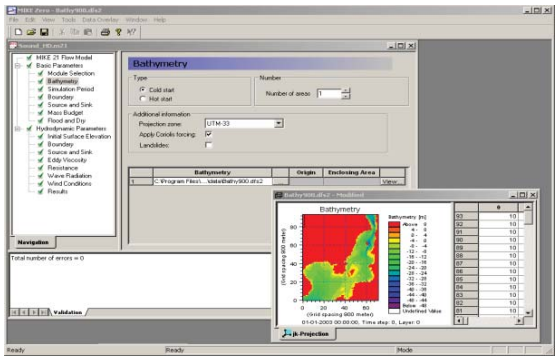

View button on all the GUIs in MIKE 21 & MIKE 3 FM HD for graphical view of input and output files

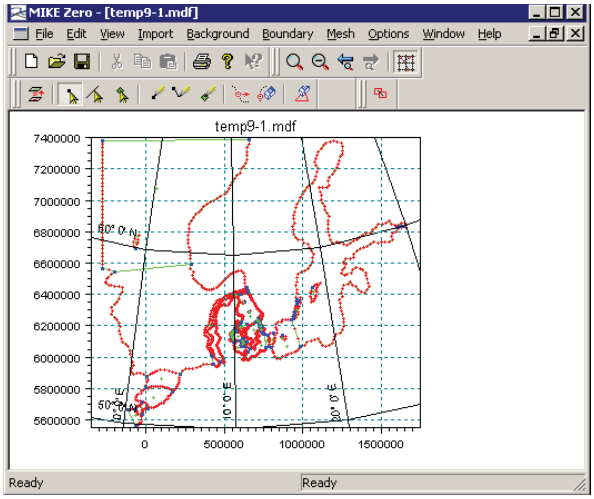

The Mesh Generator is an efficient MIKE Zero tool for the generation and handling of unstructured meshes, including the definition and editing of boundaries

Providing MIKE 21 & MIKE 3 Flow Model FM with a suitable mesh is essential for obtaining reliable results from the models. Setting up the mesh includes the appropriate selection of the area to be modelled, adequate resolution of the bathymetry, flow, wind and wave fields under consideration and definition of codes for defining boundaries.

2D visualization of a computational mesh (Odense Estuary)

Bathymetric values for the mesh generation can e.g. be obtained from the MIKE by DHI product MIKE C-Map. MIKE C-Map is an efficient tool for extracting depth data and predicted tidal elevation from the world-wide Electronic Chart Database CM-93 Edition 3.0 from Jeppesen Norway.

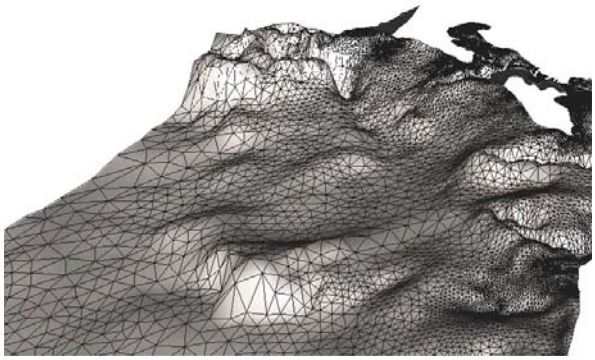

3D visualization of a computational mesh

If wind data is not available from an atmospheric meteorological model, the wind fields (e.g. cyclones) can be determined by using the wind-generating programs available in MIKE 21 Toolbox.

Global winds (pressure & wind data) can be downloaded for immediate use in your simulation. The sources of data are from GFS courtesy of NCEP, NOAA. By specifying the location, orientation and grid dimensions, the data is returned to you in the correct format as a spatial varying grid series or a time series. The link is:

www.mikebydhi.com/Download/DocumentsAndTools/Tools/AvailableData.aspx

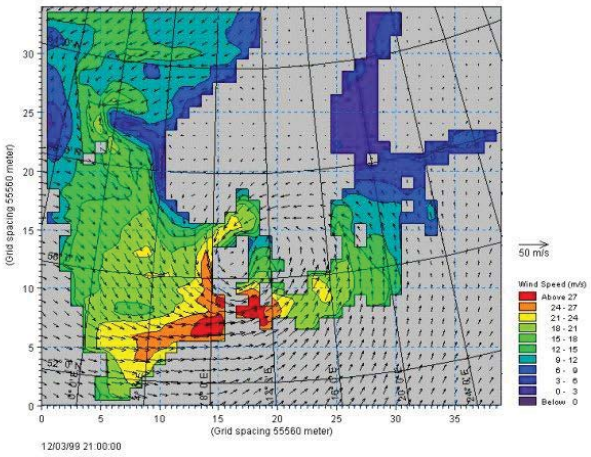

The chart shows a hindcast wind field in the North Sea and Baltic Sea as wind speed and wind direction

Model Output

Computed output results at each mesh element and for each time step consist of:

- Basic variables
  - water depth and surface elevation
  - flux densities in main directions
  - velocities in main directions
  - densities, temperatures and salinities
- Additional variables
  - Current speed and direction
  - Wind velocities
  - Air pressure
  - Drag coefficient
  - Precipitation/evaporation
  - Courant/CFL number
  - Eddy viscosity
  - Element area/volume

The output results can be saved in defined points, lines and areas. In the case of 3D calculations the results are saved in a selection of layers.

Output from MIKE 21 & MIKE 3 Flow Model FM is typically post-processed using the Data Viewer available in the common MIKE Zero shell. The Data Viewer is a tool for analysis and visualization of unstructured data, e.g. to view meshes, spectra, bathymetries, results files of different format with graphical extraction of time series and line series from plan view and import of graphical overlays.

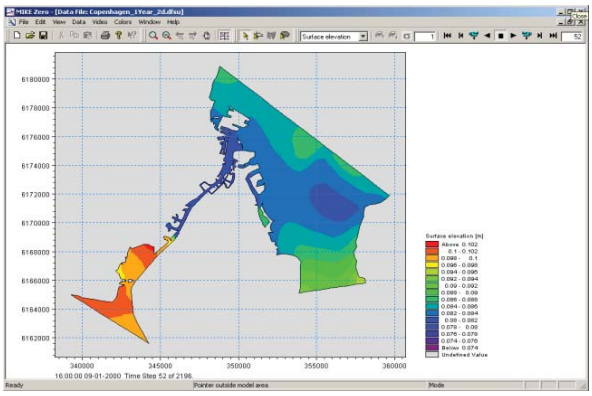

The Data Viewer in MIKE Zero – an efficient tool for analysis and visualization of unstructured data including processing of animations. Above screen dump shows surface elevations from a model setup covering Port of Copenhagen

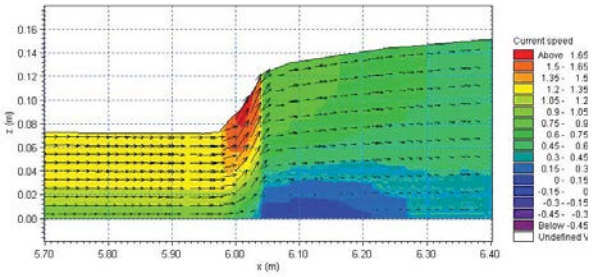

Vector and contour plot of current speed at a vertical profile defined along a line in Data Viewer in MIKE Zero

Validation

Prior to the first release of MIKE 21 & MIKE 3 Flow Model FM the model has successfully been applied to a number of rather basic idealized situations for which the results can be compared with analytical solutions or information from the literature.

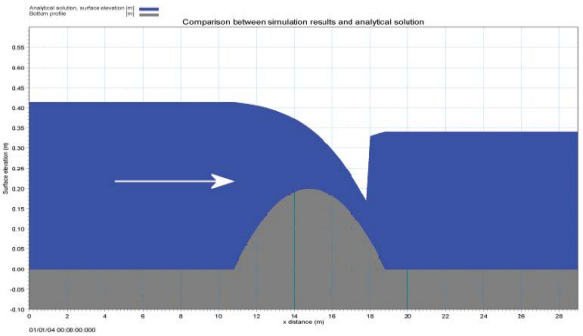

The domain is a channel with a parabola-shaped bump in the middle. The upstream (western) boundary is a constant flux and the downstream (eastern) boundary is a constant elevation. Below: the total depths for the stationary hydraulic jump at convergence. Red line: 2D setup, green line: 3D setup, black line: analytical solution

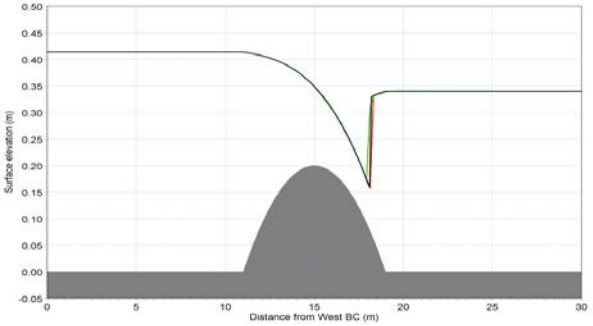

A dam-break flow in an L-shaped channel (a, b, c):

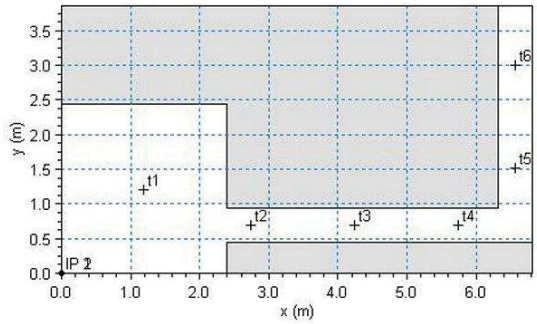

a) Outline of model setup showing the location of gauging points

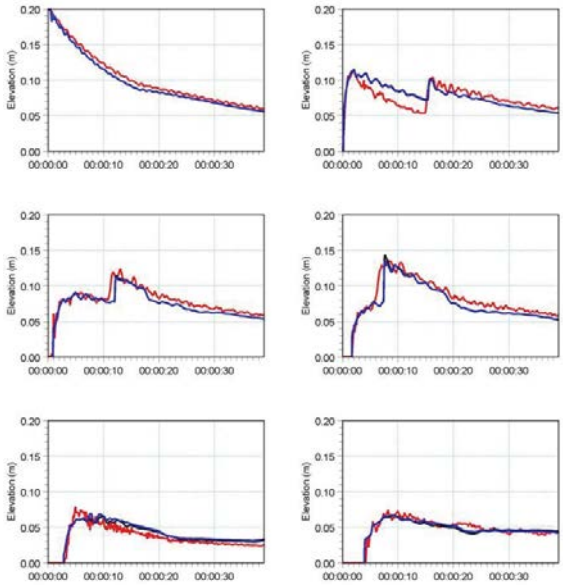

b) Comparison between simulated and measured water levels at the six gauge locations.
(Blue) coarse mesh (black) fine mesh and (red) measurements

The model has also been applied and tested in numerous natural geophysical conditions; ocean scale, inner shelves, estuaries, lakes and overland, which are more realistic and complicated than academic and laboratory tests.

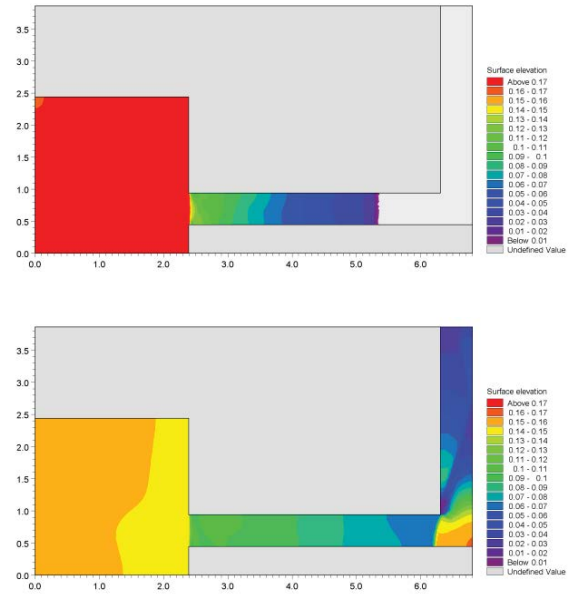

c) Contour plots of the surface elevation at T = 1.6 s (top) and T = 4.8 s (bottom)

Example from Ho Bay, a tidal estuary (barrier island coast) in South-West Denmark with access channel to the Port of Esbjerg. Below: Comparison between measured and simulated water levels

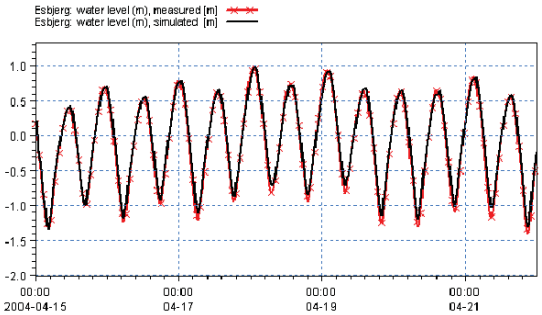

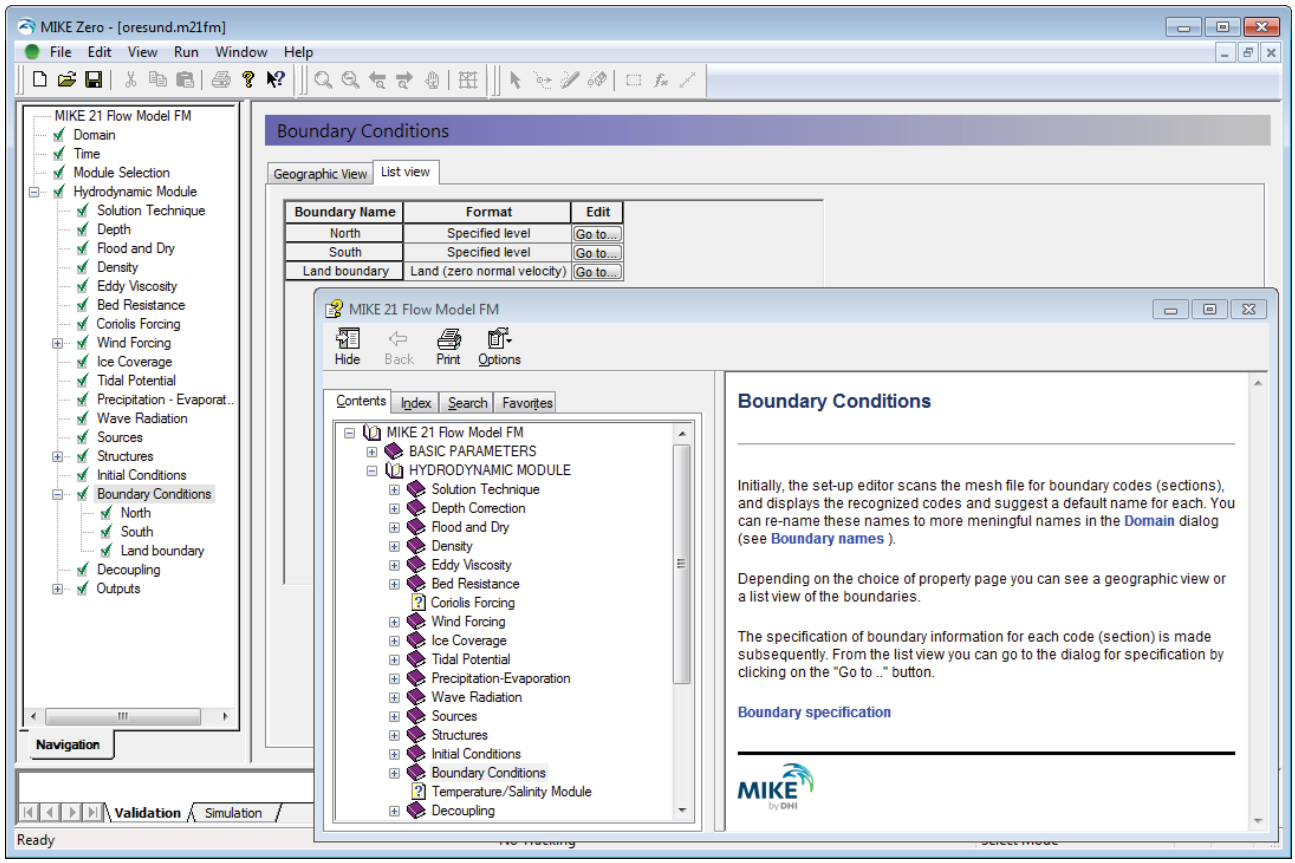

The user interface of the MIKE 21 and MIKE 3 Flow Model FM (Hydrodynamic Module), including an example of the extensive Online Help system

Graphical User Interface

The MIKE 21 & MIKE 3 Flow Model FM Hydrodynamic Module is operated through a fully Windows integrated graphical user interface (GUI). Support is provided at each stage by an Online Help system.

The common MIKE Zero shell provides entries for common data file editors, plotting facilities and utilities such as the Mesh Generator and Data Viewer.

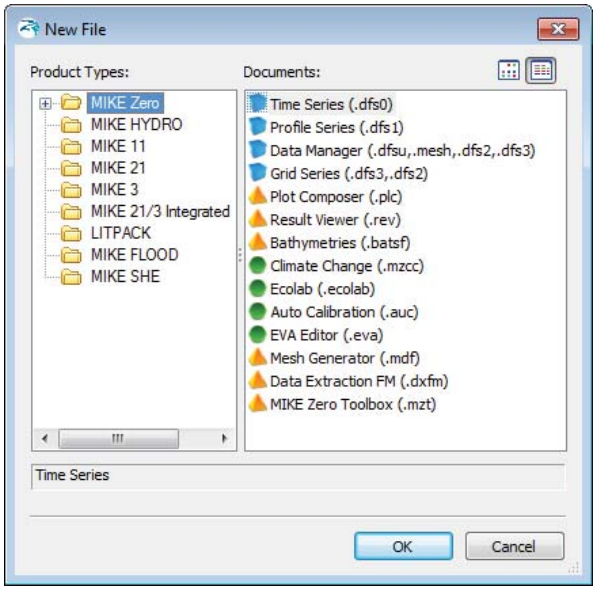

Overview of the common MIKE Zero utilities

Parallelisation

The computational engines of the MIKE 21/3 FM series are available in versions that have been parallelised using both shared memory (OpenMP) as well as distributed memory architecture (MPI). The result is much faster simulations on systems with many cores.

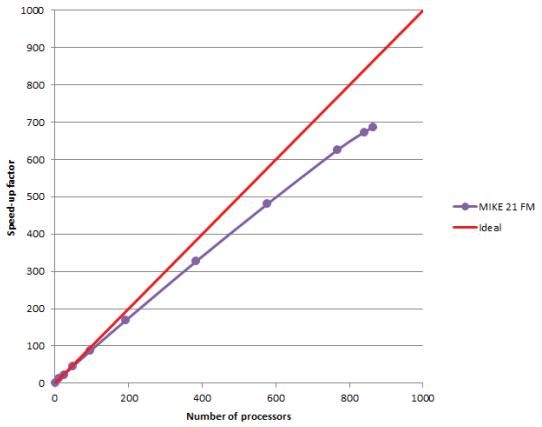

MIKE 21 FM speed-up using a HPC Cluster for Release 2012 with distributed memory architecture (purple)

Hardware and Operating System Requirements

Release 2012 version of the MIKE 21 and MIKE 3 Flow Model FM Hydrodynamic Module supports Microsoft Windows XP Professional Edition (32 and 64 bit), Microsoft Windows Vista Business (32 and 64 bit) and Microsoft Windows 7 Enterprise (32 and 64 bit). Release 2014 version will only support Microsoft Windows 7 Professional SP1 (32 and 64 bit) and Microsoft Windows 8 Professional (64 bit). Microsoft Internet Explorer 6.0 (or higher) is required for network license management as well as for accessing the Online Help.

The recommended minimum hardware requirements for executing MIKE 21 & MIKE 3 Flow Model FM Hydrodynamic Module are:

Processor:	3 GHz PC (or higher)
Memory (RAM):	4 GB (or higher)
Hard disk:	160 GB (or higher)
Monitor:	SVGA, resolution 1024x768
Graphic card:	64 MB RAM (or higher), 32 bit true colour
Media:	DVD drive compatible with dual layer DVDs

Support

News about new features, applications, papers, updates, patches, etc. are available here:

www.mikebydhi.com/Download/DocumentsAndTools.aspx

For further information on MIKE 21 & MIKE 3 Flow Model FM software, please contact your local DHI office or the Software Support Centre:

MIKE by DHI
DHI
Agern Allé 5
DK-2970 Hørsholm
Denmark

Tel: +45 4516 9333
Fax: +45 4516 9292

www.mikebydhi.com
mikebydhi@dhigroup.com

Documentation

The MIKE 21 & MIKE 3 Flow Model FM modules are provided with comprehensive user guides, online help, scientific documentation, application examples and step-by-step training examples.

References

Petersen, N.H., Rasch, P. “Modelling of the Asian Tsunami off the Coast of Northern Sumatra”, presented at the 3rd Asia-Pacific DHI Software Conference in Kuala Lumpur, Malaysia, 21-22 February, 2005

French, B. and Kerper, D. Salinity Control as a Mitigation Strategy for Habitat Improvement of Impacted Estuaries. 7th Annual EPA Wetlands Workshop, NJ, USA 2004.

DHI Note, “Flood Plain Modelling using unstructured Finite Volume Technique” January 2004 – download from

www.mikebydhi.com/Download/DocumentsAndTools/PapersAndDocs/Hydrodynamics.aspx

Appendix B
MIKE 21 Wave Modelling MIKE 21 SW – Spectral Waves FM Short Description

MIKE 21 Wave Modelling

MIKE 21 SW – Spectral Waves FM

Short Description

DHI headquarters
Agern Allé 5
DK-2970 Hørsholm
Denmark

+45 4516 9200 Telephone
+45 4516 9333 Support
+45 4516 9292 Telefax

mikebydhi@dhigroup.com
www.mikebydhi.com

MIKE21_SW_FM_Short_Description_.docx / HKH /EBR/ 2013-09-19

MIKE 21 SW - SPECTRAL WAVE MODEL FM

MIKE 21 SW is a state-of-the-art third generation spectral wind-wave model developed by DHI. The model simulates the growth, decay and transformation of wind-generated waves and swells in offshore and coastal areas.

MIKE 21 SW includes two different formulations:

- Fully spectral formulation
- Directional decoupled parametric formulation

The fully spectral formulation is based on the wave action conservation equation, as described in e.g. Komen et al (1994) and Young (1999). The directional decoupled parametric formulation is based on a parameterisation of the wave action conservation equation. The parameterisation is made in the frequency domain by introducing the zeroth and first moment of the wave action spectrum. The basic conservation equations are formulated in either Cartesian co-ordinates for small-scale applications and polar spherical co-ordinates for large-scale applications.

The fully spectral model includes the following physical phenomena:

- Wave growth by action of wind
- Non-linear wave-wave interaction
- Dissipation due to white-capping
- Dissipation due to bottom friction
- Dissipation due to depth-induced wave breaking
- Refraction and shoaling due to depth variations
- Wave-current interaction
- Effect of time-varying water depth
- Effect of ice coverage on the wave field

The discretisation of the governing equation in geographical and spectral space is performed using cell-centred finite volume method. In the geographical domain, an unstructured mesh technique is used. The time integration is performed using a fractional step approach where a multi-sequence explicit method is applied for the propagation of wave action.

MIKE 21 SW is a state-of-the-art numerical modelling tool for prediction and analysis of wave climates in offshore and coastal areas. © BIOFOTO/Klaus K. Bentzen

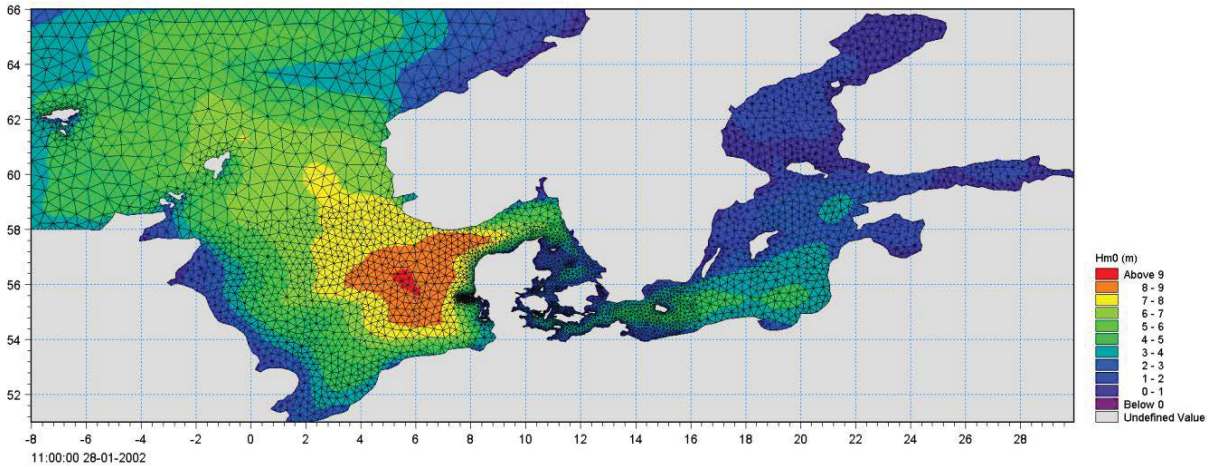

A MIKE 21 SW forecast application in the North Sea and Baltic Sea. The chart shows a wave field (from the NSBS model) illustrated by the significant wave height in top of the computational mesh. See also www.waterforecast.com

Computational Features

The main computational features of MIKE 21 SW - Spectral Wave Model FM are as follows:

- Fully spectral and directionally decoupled parametric formulations
- Source functions based on state-of-the-art 3rd generation formulations
- Instationary and quasi-stationary solutions
- Optimal degree of flexibility in describing bathymetry and ambient flow conditions using depth-adaptive and boundary-fitted unstructured mesh
- Coupling with hydrodynamic flow model for modelling of wave-current interaction and time-varying water depth
- Flooding and drying in connection with time-varying water depths
- Cell-centred finite volume technique
- Fractional step time-integration with an multi-sequence explicit method for the propagation
- Extensive range of model output parameters (wave, swell, air-sea interaction parameters, radiation stress tensor, spectra, etc.)

Application Areas

MIKE 21 SW is used for the assessment of wave climates in offshore and coastal areas - in hindcast and forecast mode.

A major application area is the design of offshore, coastal and port structures where accurate assessment of wave loads is of utmost importance to the safe and economic design of these structures.

Illustrations of typical application areas of DHI's MIKE 21 SW – Spectral Wave Model FM

Measured data are often not available during periods long enough to allow for the establishment of sufficiently accurate estimates of extreme sea states.

In this case, the measured data can then be supplemented with hindcast data through the simulation of wave conditions during historical storms using MIKE 21 SW.

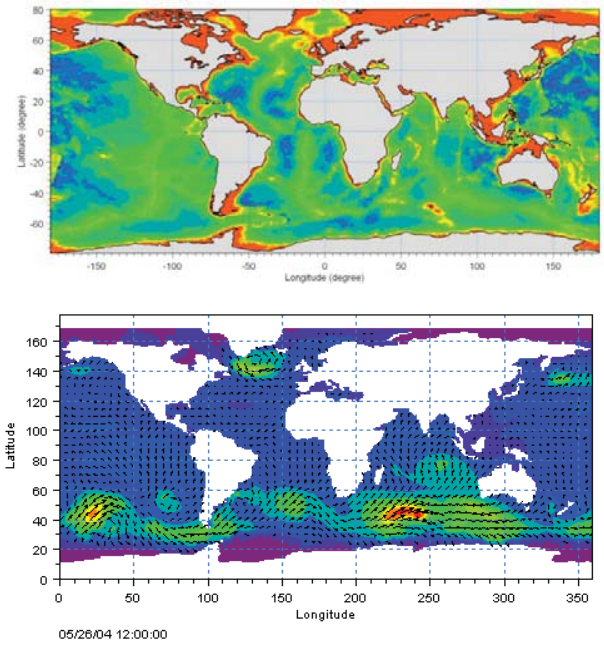

Example of a global application of MIKE 21 SW. The upper panel shows the bathymetry. Results from such a model (cf. lower panel) can be used as boundary conditions for regional scale forecast or hindcast models. See http://www.waterforecast.com for more details on regional and global modelling

MIKE 21 SW is particularly applicable for simultaneous wave prediction and analysis on regional scale and local scale. Coarse spatial and temporal resolution is used for the regional part of the mesh and a high-resolution boundary and depth-adaptive mesh is describing the shallow water environment at the coastline.

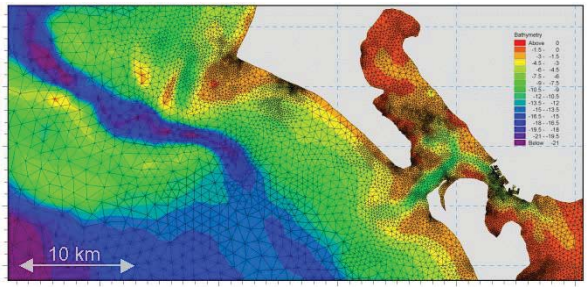

Example of a computational mesh used for transformation of offshore wave statistics using the directionally decoupled parametric formulation

MIKE 21 SW is also used for the calculation of the sediment transport, which for a large part is determined by wave conditions and associated wave-induced currents. The wave-induced current is generated by the gradients in radiation stresses that occur in the surf zone.

MIKE 21 SW can be used to calculate the wave conditions and associated radiation stresses. The long-shore currents and sediment transport are then calculated using the flow and sediment transport models available in the MIKE 21 package. For such type of applications, the directional decoupled parametric formulation of MIKE 21 SW is an excellent compromise between the computational effort and accuracy.

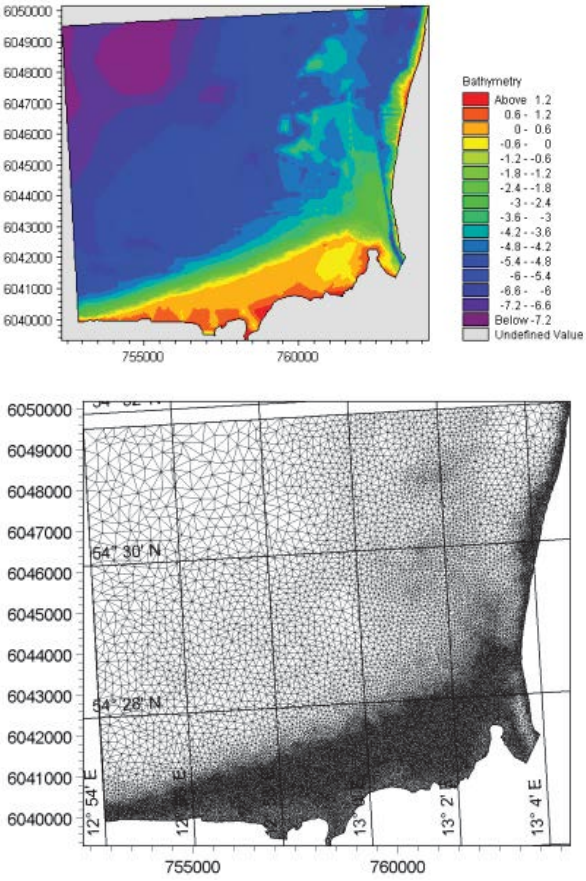

Bathymetry (upper) and computational mesh (lower) used in a MIKE 21 SW application on wave induced currents in Gellen Bay, Germany

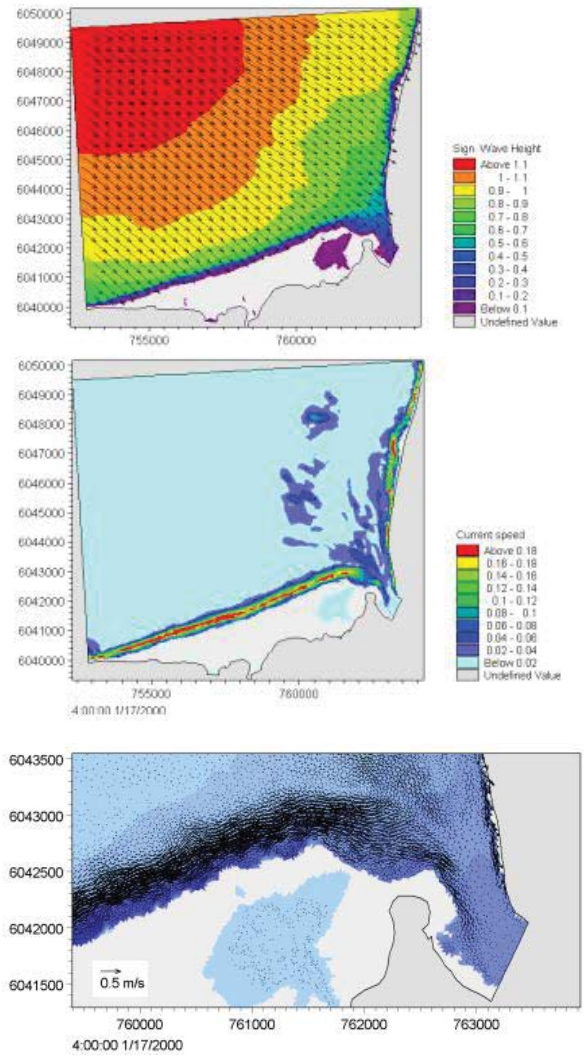

Map of significant wave height (upper), current field (middle) and vector field (lower). The flow field is simulated by DHI's MIKE 21 Flow Model FM, which is dynamically coupled to MIKE 21 SW

Model Equations

In MIKE 21 SW, the wind waves are represented by the wave action density spectrum $N(\sigma,\theta)$. The independent phase parameters have been chosen as the relative (intrinsic) angular frequency, $\sigma = 2\pi f$ and the direction of wave propagation, θ. The relation between the relative angular frequency and the absolute angular frequency, ω, is given by the linear dispersion relationship

$$\sigma = \sqrt{gk\tanh(kd)} = \omega - \bar{k}\cdot\bar{U}$$

where g is the acceleration of gravity, d is the water depth and $\bar{U}$ is the current velocity vector and $\bar{k}$ is the wave number vector with magnitude k and direction θ. The action density, $N(\sigma,\theta)$, is related to the energy density $E(\sigma,\theta)$ by

$$N = \frac{E}{\sigma}$$

Fully Spectral Formulation

The governing equation in MIKE 21 SW is the wave action balance equation formulated in either Cartesian or spherical co-ordinates. In horizontal Cartesian co-ordinates, the conservation equation for wave action reads

$$\frac{\partial N}{\partial t} + \nabla\cdot(\bar{v}N) = \frac{S}{\sigma}$$

where $N(\bar{x},\sigma,\theta,t)$ is the action density, t is the time, $\bar{x} = (x,y)$ is the Cartesian co-ordinates, $\bar{v} = (c_x, c_y, c_\sigma, c_\theta)$ is the propagation velocity of a wave group in the four-dimensional phase space $\bar{x}$, σ and θ. S is the source term for energy balance equation. ∇ is the four-dimensional differential operator in the $\bar{x}$, σ, θ-space. The characteristic propagation speeds are given by the linear kinematic relationships

$$(c_x, c_y) = \frac{d\bar{x}}{dt} = \bar{c}_g + \bar{U} = \frac{1}{2}\left(1 + \frac{2kd}{\sinh(2kd)}\right)\frac{\sigma}{k} + \bar{U}$$

$$c_\sigma = \frac{d\sigma}{dt} = \frac{\partial\sigma}{\partial d}\left[\frac{\partial d}{\partial t} + \bar{U}\cdot\nabla_{\bar{x}} d\right] - c_g\bar{k}\cdot\frac{\partial\bar{U}}{\partial s}$$

$$c_\theta = \frac{d\theta}{dt} = -\frac{1}{k}\left[\frac{\partial\sigma}{\partial d}\frac{\partial d}{\partial m} + \bar{k}\cdot\frac{\partial\bar{U}}{\partial m}\right]$$

Here, s is the space co-ordinate in wave direction θ and m is a co-ordinate perpendicular to s. $\nabla_{\bar{x}}$ is the two-dimensional differential operator in the $\bar{x}$-space.

Source Functions

The source function term, S, on the right hand side of the wave action conservation equation is given by

$$S = S_{in} + S_{nl} + S_{ds} + S_{bot} + S_{surf}$$

Here S_{in} represents the momentum transfer of wind energy to wave generation, S_{nl} the energy transfer due non-linear wave-wave interaction, S_{ds} the dissipation of wave energy due to white-capping (deep water wave breaking), S_{bot} the dissipation due to bottom friction and S_{surf} the dissipation of wave energy due to depth-induced breaking.

The default source functions S_{in}, S_{nl} and S_{ds} in MIKE 21 SW are similar to the source functions implemented in the WAM Cycle 4 model, see Komen et al (1994).

The wind input is based on Janssen's (1989, 1991) quasi-linear theory of wind-wave generation, where the momentum transfer from the wind to the sea not only depends on the wind stress, but also the sea state itself. The non-linear energy transfer (through the resonant four-wave interaction) is approximated by the DIA approach, Hasselmann et al (1985). The source function describing the dissipation due to white-capping is based on the theory of Hasselmann (1974) and Janssen (1989). The bottom friction dissipation is modelled using the approach by Johnson and Kofoed-Hansen (2000), which depends on the wave and sediment properties. The source function describing the bottom-induced wave breaking is based on the well-proven approach of Battjes and Janssen (1978) and Eldeberky and Battjes (1996).

A detailed description of the various source functions is available in Komen et al (1994) and Sørensen et al (2003), which also includes the references listed above.

Directional Decoupled Parametric Formulation

The directionally decoupled parametric formulation is based on a parameterisation of the wave action conservation equation. Following Holthuijsen et al (1989), the parameterisation is made in the frequency domain by introducing the zeroth and first moment of the wave action spectrum as dependent variables.

A similar formulation is used in the MIKE 21 NSW Near-shore Spectral Wind-Wave Model, which is one of the most popular models for wave transformation in coastal and shallow water environment. However, with MIKE 21 SW it is not necessary to set up a number of different orientated bathymetries to cover varying wind and wave directions.

The parameterisation leads to the following coupled equations

$$\frac{\partial(m_0)}{\partial t}+\frac{\partial(c_x m_0)}{\partial x}+\frac{\partial(c_y m_0)}{\partial y}+\frac{\partial(c_\theta m_0)}{\partial \theta}=T_0$$

$$\frac{\partial(m_1)}{\partial t}+\frac{\partial(c_x m_1)}{\partial x}+\frac{\partial(c_y m_1)}{\partial y}+\frac{\partial(c_\theta m_1)}{\partial \theta}=T_1$$

where $m_0(x, y, \theta)$ and $m_1(x, y, \theta)$ are the zeroth and first moment of the action spectrum $N(x, y, \sigma, \theta)$, respectively. $T_0(x, y, \theta)$ and $T_1(x, y, \theta)$ are source functions based on the action spectrum. The moments $m_n(x, y, \theta)$ are defined as

$$m_n(x,y,\theta)=\int_0^\infty \omega^n N(x,y,\omega,\theta)d\omega$$

The source functions T_0 and T_1 take into account the effect of local wind generation (stationary solution mode only) and energy dissipation due to bottom friction and wave breaking. The effects of wave-current interaction are also included. The source functions for the local wind generation are derived from empirical growth relations, see Johnson (1998) for details.

Numerical Methods

The frequency spectrum (fully spectral model only) is split into a prognostic part for frequencies lower than a cut-off frequency σ_{max} and an analytical diagnostic tail for the high-frequency part of the spectrum

$$E(\sigma,\theta)=E(\sigma_{\max},\theta)\left(\frac{\sigma}{\sigma_{\max}}\right)^{-m}$$

where m is a constant (= 5) as proposed by Komen et al (1994).

The directional decoupled parametric formulation in MIKE 21 SW is used extensively for calculation of the wave transformation from deep-water to the shoreline and for wind-wave generation in local areas

Space Discretisation

The discretisation in geographical and spectral space is performed using cell-centred finite volume method. In the geographical domain an unstructured mesh is used. The spatial domain is discretised by subdivision of the continuum into non-overlapping elements. Triangle and quadrilateral shaped polygons are presently supported in MIKE 21 SW. The action density, $N(\sigma,\theta)$ is represented as a piecewise constant over the elements and stored at the geometric centres.

In frequency space either an equidistant or a log-arithmic discretisation is used. In the directional space, an equidistant discretisation is used for both types of models. The action density is represented as piecewise constant over the discrete intervals, $\Delta\sigma$ and $\Delta\theta$, in the frequency and directional space.

Integrating the wave action conservation over an area A_i, the frequency interval $\Delta\sigma_l$ and the directional interval $\Delta\theta_m$ gives

$$\frac{\partial}{\partial t}\int_{\Delta\theta_m}\int_{\Delta\sigma_l}\int_{A_i} N d\Omega d\sigma d\theta - \int_{\Delta\theta_m}\int_{\Delta\sigma_l}\int_{A_i}\frac{S}{\sigma}d\Omega d\sigma d\theta$$
$$= \int_{\Delta\theta_m}\int_{\Delta\sigma_l}\int_{A_i}\nabla\cdot(\bar{v}N)d\Omega d\sigma d\theta$$

where Ω is the integration variable defined on A_i. Using the divergence theorem and introducing the convective flux $\bar{F} = \bar{v}N$, we obtain

$$\frac{\partial N_{i,l,m}}{\partial t} = -\frac{1}{A_i}\left[\sum_{p=1}^{NE}(F_n)_{p,l,m}\Delta l_p\right]$$
$$-\frac{1}{\Delta\sigma_l}\left[(F_\sigma)_{i,l+1/2,m} - (F_\sigma)_{i,l-1/2,m}\right]$$
$$-\frac{1}{\Delta\theta_m}\left[(F_\theta)_{i,l,m+1/2} - (F_\theta)_{i,l,m-1/2}\right] + \frac{S_{i,l,m}}{\sigma_l}$$

where NE is the total number of edges in the cell, $(F_n)_{p,l,m} = (F_x n_x + F_y n_y)_{p,l,m}$ is the normal flux trough the edge p in geographical space with length Δl_p. $(F_\sigma)_{i,l+1/2,m}$ and $(F_\theta)_{i,l,m+1/2}$ is the flux through the face in the frequency and directional space, respectively.

The convective flux is derived using a first-order upwinding scheme. In that

$$F_n = c_n\left(\frac{1}{2}(N_i + N_j) - \frac{1}{2}\frac{c}{|c|}(N_i - N_j)\right)$$

where c_n is the propagation speed normal to the element cell face.

Time Integration

The integration in time is based on a fractional step approach. Firstly, a propagation step is performed calculating an approximate solution N^* at the new time level (n+1) by solving the homogenous wave action conservation equation, i.e. without the source terms. Secondly, a source terms step is performed calculating the new solution N^{n+1} from the estimated solution taking into account only the effect of the source terms.

The propagation step is carried out by an explicit Euler scheme

$$N^*_{i,l,m} = N^n_{i,l,m} + \Delta t\left(\frac{\partial N_{i,l,m}}{\partial t}\right)^n$$

To overcome the severe stability restriction, a multi-sequence integration scheme is employed. The maximum allowed time step is increased by employing a sequence of integration steps locally, where the number of steps may vary from point to point.

A source term step is performed using an implicit method (see Komen et al, 1994)

$$N^{n+1}_{i,l,m} = N^*_{i,l,m} + \Delta t\left[\frac{(1-\alpha)S^*_{i,l,m} + \alpha S^{n+1}_{i,l,m}}{\sigma_l}\right]$$

where α is a weighting coefficient that determines the type of finite difference method. Using a Taylor series to approximate S^{n+1} and assuming the off-diagonal terms in $\partial S/\partial E = \gamma$ are negligible, this equation can be simplified as

$$N^{n+1}_{i,l,m} = N^n_{i,l,m} + \frac{(S^*_{i,l,m}/\sigma_l)\Delta t}{(1-\alpha\gamma\Delta t)}$$

For growing waves ($\gamma > 0$) an explicit forward difference is used ($\alpha = 0$), while for decaying waves ($\gamma < 0$) an implicit backward difference ($\alpha = 1$) is applied.

MIKE 21 SW is also applied for wave forecasts in ship route planning and improved service for conventional and fast ferry operators

Model Input

The necessary input data can be divided into following groups:

- Domain and time parameters:
  - computational mesh
  - co-ordinate type (Cartesian or spherical)
  - simulation length and overall time step
- Equations, discretisation and solution technique
  - formulation type
  - frequency and directional discretisation
  - number of time step groups
  - number of source time steps
- Forcing parameters
  - water level data
  - current data
  - wind data
  - ice data
- Source function parameters
  - non-linear energy transfer
  - wave breaking (shallow water)
  - bottom friction
  - white capping
- Initial conditions
  - zero-spectrum (cold-start)
  - empirical data
  - data file
- Boundary conditions
  - closed boundaries
  - open boundaries (data format and type)

Providing MIKE 21 SW with a suitable mesh is essential for obtaining reliable results from the model. Setting up the mesh includes the appropriate selection of the area to be modelled, adequate resolution of the bathymetry, flow, wind and wave fields under consideration and definition of codes for essential and land boundaries.

Furthermore, the resolution in the geographical space must also be selected with respect to stability considerations.

As the wind is the main driving force in MIKE 21 SW, accurate hindcast or forecast wind fields are of utmost importance for the wave prediction.

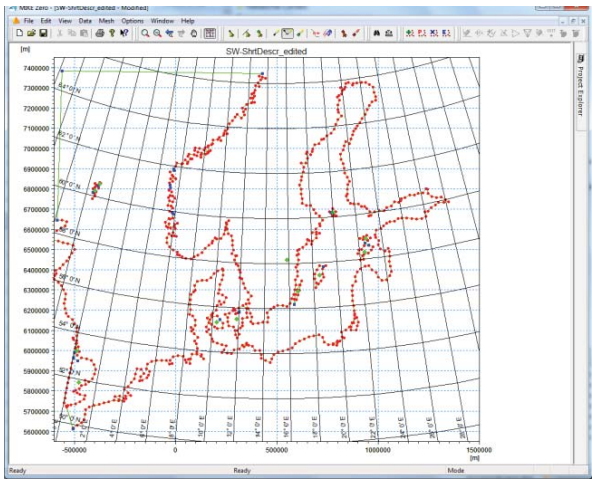

The Mesh Generator is an efficient MIKE Zero tool for the generation and handling of unstructured meshes, including the definition and editing of boundaries

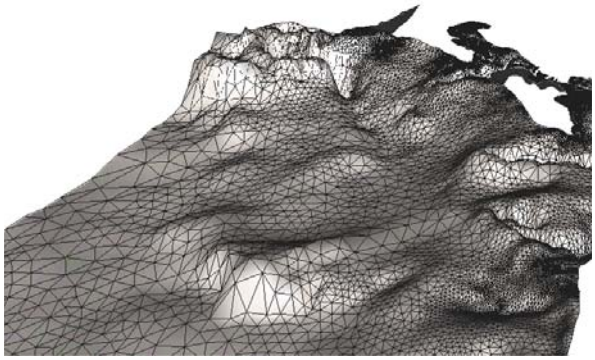

3D visualisation of a computational mesh

If wind data is not available from an atmospheric meteorological model, the wind fields (e.g. cyclones) can be determined by using the wind-generating programs available in MIKE 21 Toolbox.

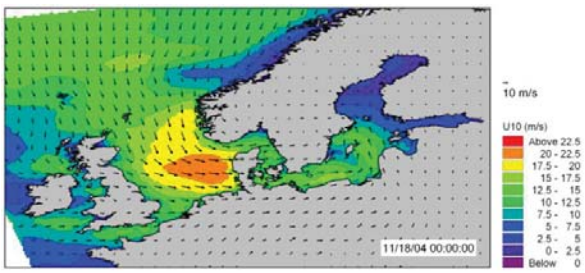

The chart shows an example of a wind field covering the North Sea and Baltic Sea as wind speed and wind direction. This is used as input to MIKE 21 SW in forecast and hindcast mode

Model Output

At each mesh point and for each time step four types of output can be obtained from MIKE 21 SW:

- Integral wave parameters divided into wind sea and swell such as
  - significant wave height, H_{m0}
  - peak wave period, T_p
  - averaged wave period, T_{01}
  - zero-crossing wave period, T_{02}
  - wave energy period, T_{-10}
  - peak wave direction, θ_p
  - mean wave direction, θ_m
  - directional standard deviation, σ
  - wave height with dir., $H_{m0}\cos\theta_m$, $H_{m0}\sin\theta_m$
  - radiation stress tensor, S_{xx}, S_{xy} and S_{yy}

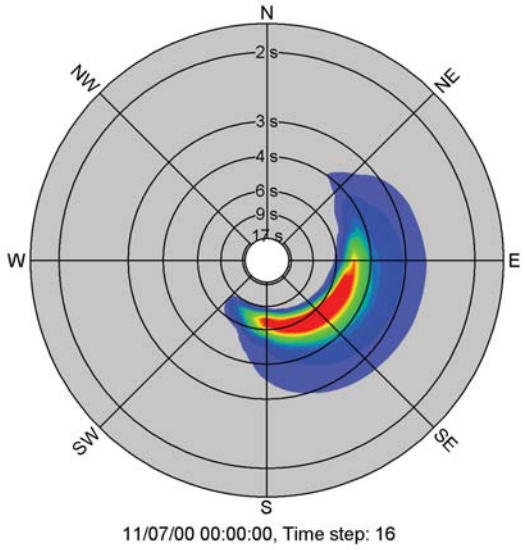

Example of model output (directional-frequency wave spectrum) processed using the Polar Plot control in the MIKE Zero Plot Composer

The distinction between wind-sea and swell can be calculated using either a constant threshold frequency or a dynamic threshold frequency with an upper frequency limit.

- Input parameters
  - water level, h
  - current velocity, $\overline{U}$
  - wind speed, U_{10}
  - wind direction, θ_w
- Model parameters
  - bottom friction coefficient, C_f
  - breaking parameter, γ
  - Courant number, Cr
  - time step factor, α
  - characteristic edge length, Δl
  - area of element, a
  - wind friction speed, u_*
  - roughness length, z_0
  - drag coefficient, C_D
  - Charnock parameter, z_{ch}
- Directional-frequency wave spectra at selected grid points and or areas as well as direction spectra and frequency spectra

Output from MIKE 21 SW is typically post-processed using the Data Viewer available in the common MIKE Zero shell. The Data Viewer is a tool for analysis and visualisation of unstructured data, e.g. to view meshes, spectra, bathymetries, results files of different format with graphical extraction of time series and line series from plan view and import of graphical overlays.

Various other editors and plot controls in the MIKE Zero Composer (e.g. Time Series Plot, Polar Plot, etc.) can be used for analysis and visualisation.

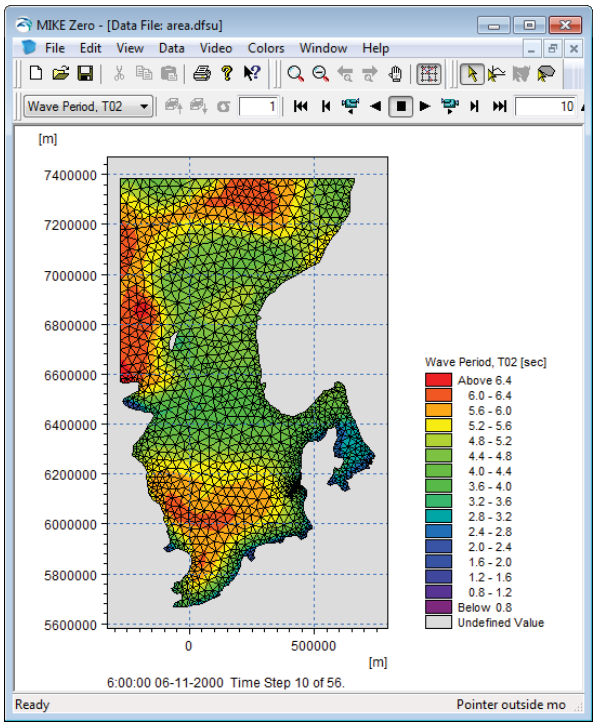

The Data Viewer in MIKE Zero – an efficient tool for analysis and visualisation of unstructured data including processing of animations

Validation

The model has successfully been applied to a number of rather basic idealised situations for which the results can be compared with analytical solutions or information from the literature. The basic tests covered fundamental processes such as wave propagation, depth-induced and current-induced shoaling and refraction, wind-wave generation and dissipation.

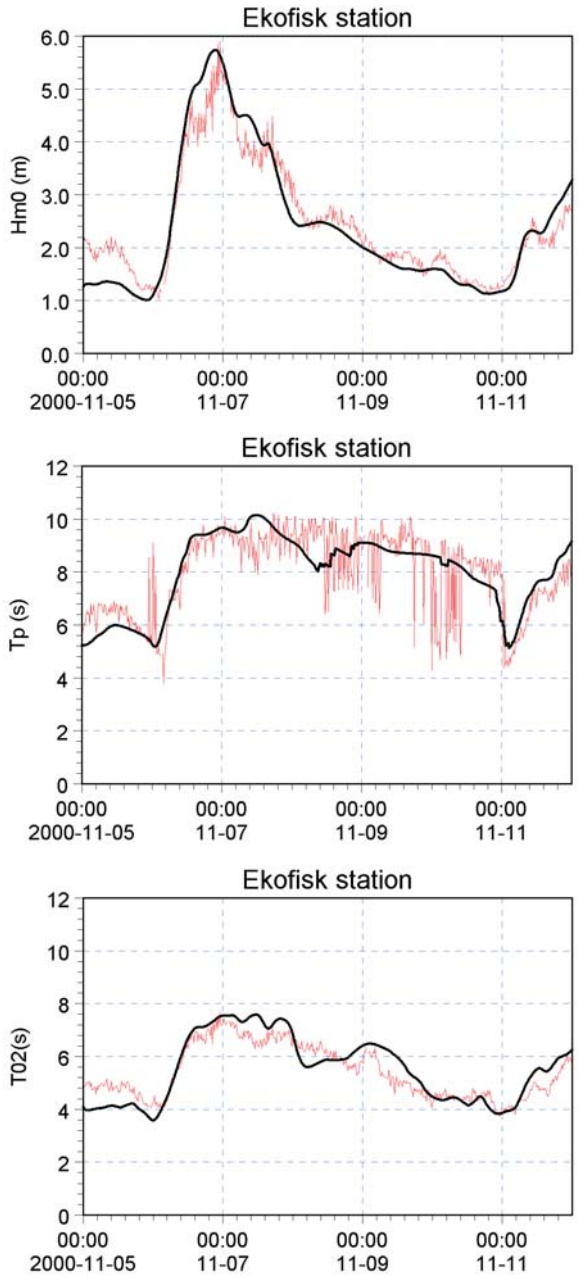

Comparison between measured and simulated significant wave height, peak wave period and mean wave period at the Ekofisk offshore platform (water depth 70 m) in the North Sea). (——) calculations and (——) measurements

A major application area of MIKE 21 SW is in connection with design and maintenance of offshore structures

The model has also been tested in natural geophysical conditions (e.g. in the North Sea, the Danish West Coast and the Baltic Sea), which are more realistic and complicated than the academic test and laboratory tests mentioned above.

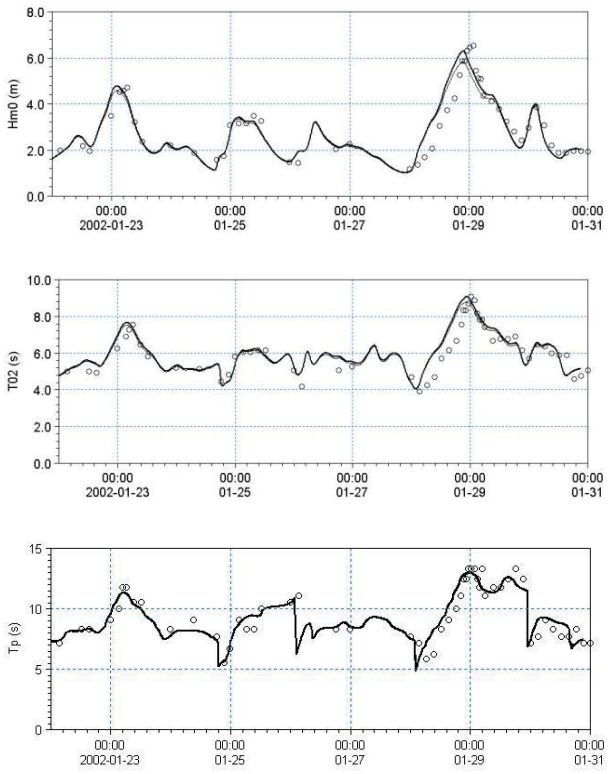

Comparison between measured and simulated significant wave height, peak wave period and mean wave period at Fjaltring located at the Danish west coast (water depth 17.5 m).(——) calculations and (o) measurements

The Fjaltring directional wave rider buoy is located offshore relative to the depicted arrow

MIKE 21 SW is used for prediction of the wave conditions at the complex Horns Rev (reef) in the southeastern part of the North Sea. At this site, a 168 MW offshore wind farm with 80 turbines has been established in water depths between 6.5 and 13.5 m.

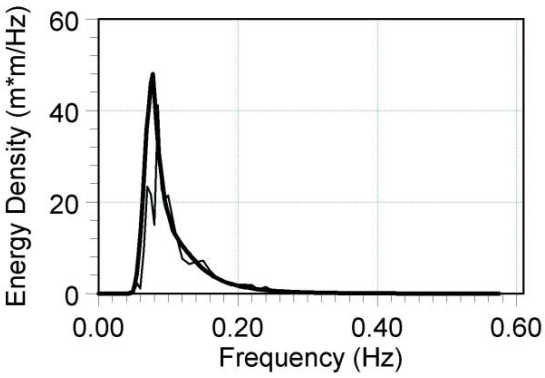

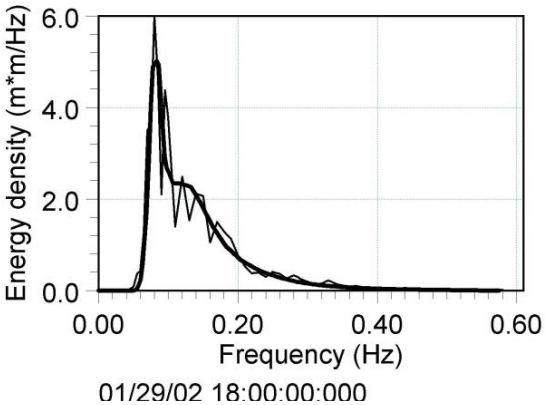

Comparison of frequency spectra at Fjaltring. (——) calculations and (——)measurements

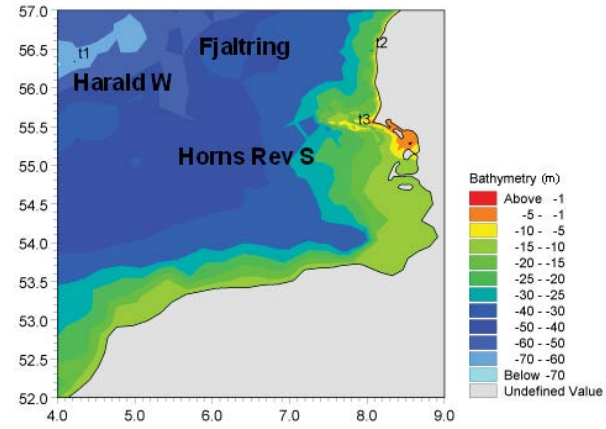

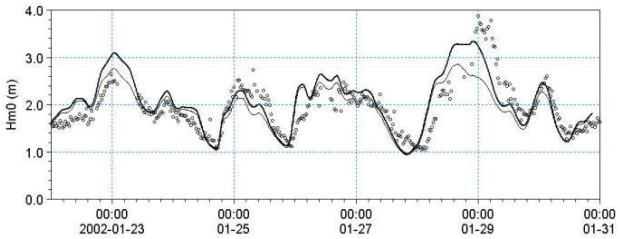

The upper panels show the Horns Rev offshore wind farm and MIKE C-map chart. 'The middle panel shows a close-up of the mesh near the Horns Rev S wave rider buoy (t3, 10 m water depth. The lower panel shows a comparison between measured and simulated significant wave height at Horns Rev S, (——) calculations including tide and surge and (—-) calculations excluding including tide and surge, (o) measurements

The predicted nearshore wave climate along the island of Hiddensee and the coastline of Zingst located in the micro-tidal Gellen Bay, Germany have been compared to field measurements (Sørensen et al, 2004) provided by the MORWIN project. From the illustrations it can be seen that the wave conditions are well reproduced both offshore and in more shallow water near the shore. The RMS values (on significant wave height) are less than 0.25m at all five stations.

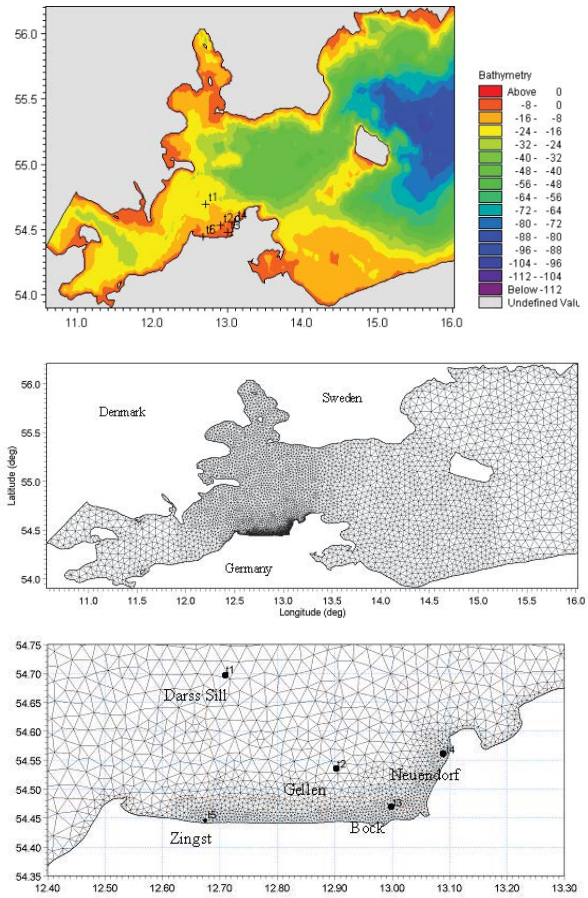

A MIKE 21 SW hindcast application in the Baltic Sea. The upper chart shows the bathymetry and the middle and lower charts show the computational mesh. The lower chart indicates the location of the measurement stations

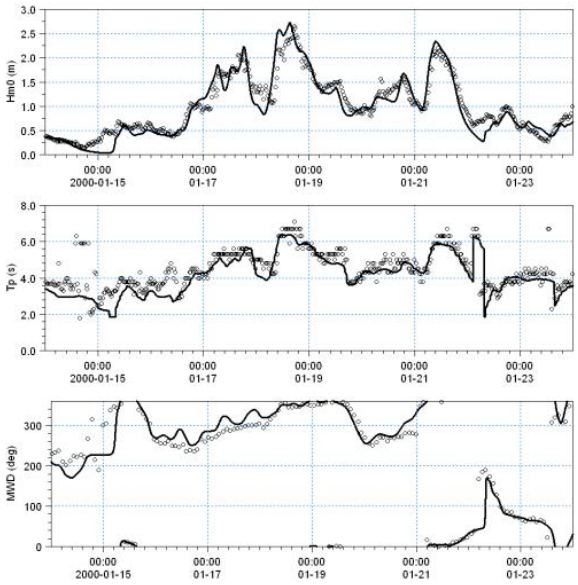

Time series of significant wave height, H_{m0}, peak wave period, T_p , and mean wave direction, MWD, at Darss sill (Offshore, depth 20.5 m). (——) Calculation and (o) measurements. The RMS value on H_{m0} is approximately 0.2 m

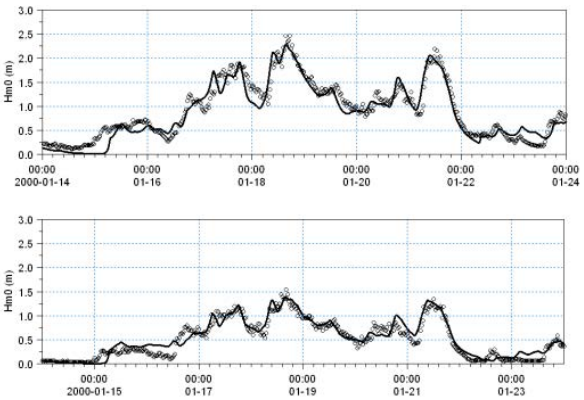

Time series of significant wave height, H_{m0}, at Gellen (upper, depth 8.3m) and Bock (lower, depth 5.5 m). (——) Calculation and (o) measurements. The RMS value on H_{m0} is approximately 0.15 m

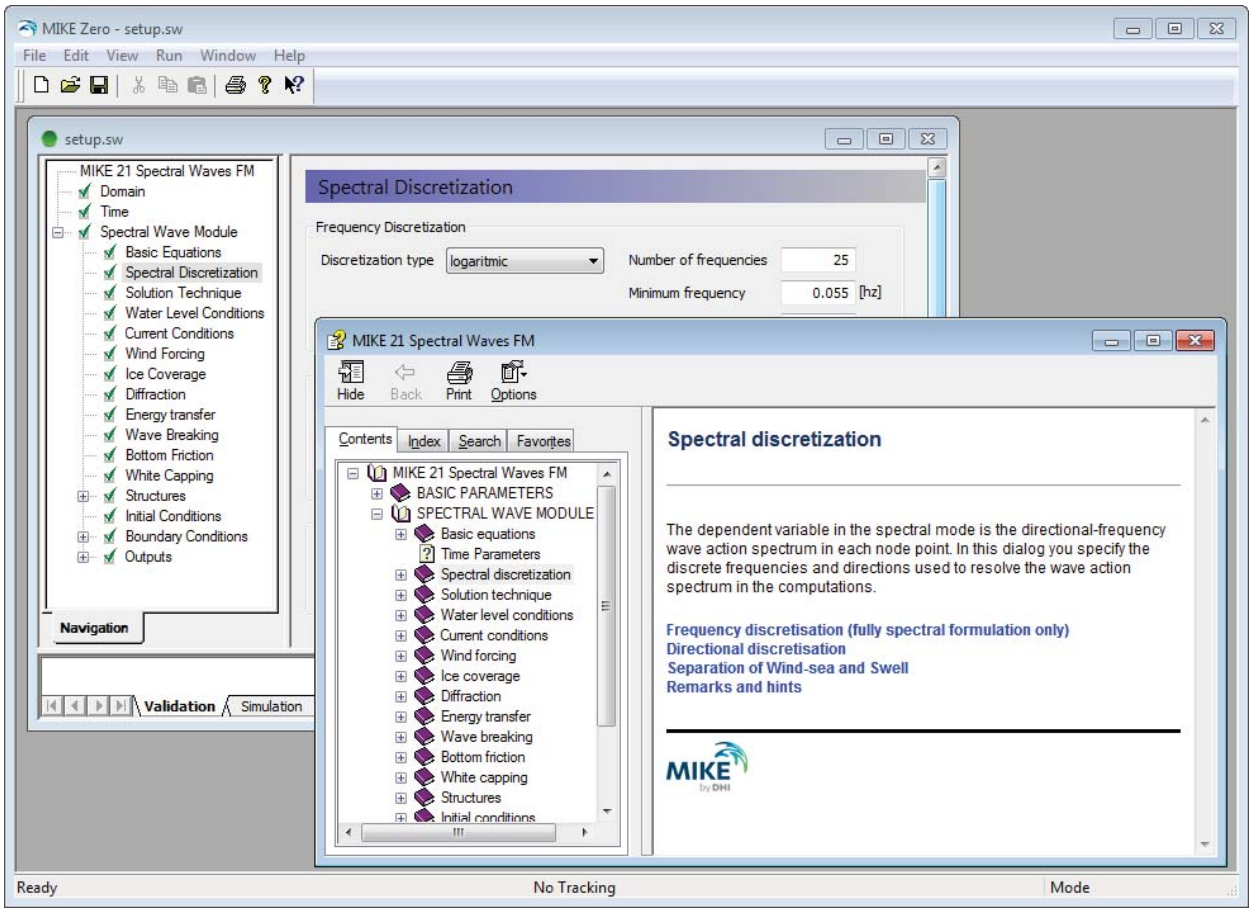

Graphical user interface of MIKE 21 SW, including an example of the Online Help System

Graphical User Interface

MKE 21 SW is operated through a fully Windows integrated Graphical User Interface (GUI). Support is provided at each stage by an Online Help System.

The common MIKE Zero shell provides entries for common data file editors, plotting facilities and a toolbox for/utilities as the Mesh Generator and Data Viewer.

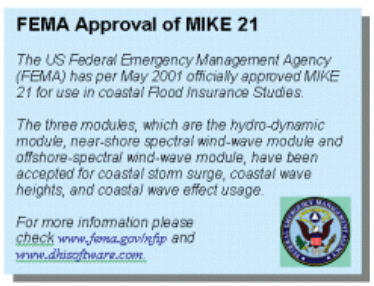

FEMA approval of the MIKE 21 package

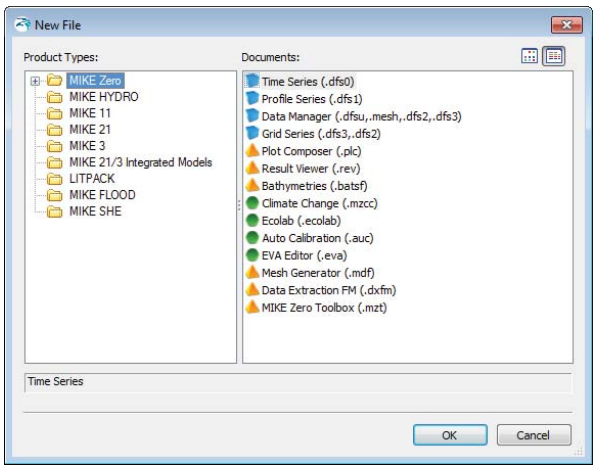

Overview of the common MIKE Zero utilities

Parallelisation

The computational engines of the MIKE 21/3 FM series are available in versions that have been parallelised using both shared memory (OpenMP) as well as distributed memory architecture (MPI). The result is much faster simulations on systems with many cores.

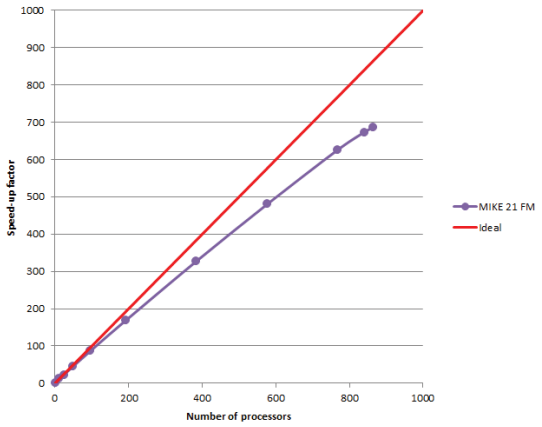

MIKE 21 FM speed-up using a HPC Cluster for Release 2012 with distributed memory architecture (purple)

Hardware and Operating System Requirements

Release 2012 version of the MIKE 21 SW Module supports Microsoft Windows XP Professional Edition (32 and 64 bit), Microsoft Windows Vista Business (32 and 64 bit) and Microsoft Windows 7 Enterprise (32 and 64 bit). Release 2014 version will only support Microsoft Windows 7 Professional SP1 (32 and 64 bit) and Microsoft Windows 8 Professional (64 bit). Microsoft Internet Explorer 6.0 (or higher) is required for network license management as well as for accessing the Online Help.

The recommended minimum hardware requirements for executing MIKE 21 SW are:

Processor:	3 GHz PC (or higher)
Memory (RAM):	4 GB (or higher)
Hard disk:	160 GB (or higher)
Monitor:	SVGA, resolution 1024x768
Graphic card:	64 MB RAM (or higher), 32 bit true colour
Media:	DVD drive compatible with dual layer DVDs

Support

News about new features, applications, papers, updates, patches, etc. are available here:

www.mikebydhi.com/Download/DocumentsAndTools.aspx

For further information on MIKE 21 SW, please contact your local DHI office or the Software Support Centre:

MIKE by DHI
DHI
Agern Allé 5
DK-2970 Hørsholm
Denmark

Tel: +45 4516 9333
Fax: +45 4516 9292

www.mikebydhi.com
mikebydhi@dhigroup.com

Documentation

The MIKE 21 & MIKE 3 modules are provided with comprehensive user guides, online help, scientific documentation, application examples and step-by-step training examples.

References

Sørensen, O. R., Kofoed-Hansen, H., Rugbjerg, M. and Sørensen, L.S., 2004: A Third Generation Spectral Wave Model Using an Unstructured Finite Volume Technique. In Proceedings of the 29th International Conference of Coastal Engineering, 19-24 September 2004, Lisbon, Portugal.

Johnson, H.K., and Kofoed-Hansen, H., (2000). Influence of bottom friction on sea surface roughness and its impact on shallow water wind wave modelling. *J. Phys. Oceanog.,* **30,** 1743-1756.

Johnson, H.K., Vested, H.J., Hersbach, H. Højstrup, J. and Larsen, S.E., (1999). On the coupling between wind and waves in the WAM model. *J. Atmos. Oceanic Technol.,* **16,** 1780-1790.

Johnson, H.K. (1998). On modeling wind-waves in shallow and fetch limited areas using the method of Holthuijsen, Booij and Herbers. *J. Coastal Research,* **14**, 3, 917-932.

Young, I.R., (1999). Wind generated ocean waves, in Elsevier Ocean Engineering Book Series, Volume 2, Eds. R. Bhattacharyya and M.E. McCormick, Elsevier.

Komen, G.J., Cavaleri, L., Doneland, M., Hasselmann, K., Hasselmann S. and Janssen, P.A.E.M., (1994). Dynamics and modelling of ocean waves. Cambridge University Press, UK, 560 pp.

Holthuijsen, L.H, Booij, N. and Herbers, T.H.C. (1989). A prediction model for stationary, short-crested waves in shallow water with ambient currents, *Coastal Engr*., **13**, 23-54.

References on Applications

Kofoed-Hansen, H., Johnson, H.K., Højstrup, J. and Lange, B., (1998). Wind-wave modelling in waters with restricted fetches. In: Proc of 5th International Workshop on Wave Hindcasting and Forecasting, 27-30 January 1998, Melbourne, FL, USA, pp. 113-127.

Kofoed-Hansen, H, Johnson, H.K., Astrup, P. and Larsen, J., (2001). Prediction of waves and sea surface roughness in restricted coastal waters. In: Proc of 27th International Conference of Coastal Engineering, pp.1169-1182.

Al-Mashouk, M.A., Kerper, D.R. and Jacobsen, V., (1998). Red Sea Hindcast study: Development of a sea state design database for the Red Sea.. *J Saudi Aramco Technology*, **1**, 10 pp.

Rugbjerg, M., Nielsen, K., Christensen, J.H. and Jacobsen, V., (2001). Wave energy in the Danish part of the North Sea. In: Proc of 4th European Wave Energy Conference, 8 pp.

Appendix C
Summary of FEMA's Stillwater Elevations and BFEs

Transect	Stillwater Elevation (ft)		Base Flood Elevation (ft)		Wave height (ft)	
	In the Atlantic Ocean	In Biscayne Bay	In the Atlantic Ocean	In Biscayne Bay	In the Atlantic Ocean	In Biscayne Bay
1	6.6	6	10.2	6	4	*0.0*
2	6.6	6.4	10.2	7.4	4	*1.0*
3	6.7	6.6	10.2	7.4	4	*0.8*
4	6.7	7.2	10.4	9	4	**1.8**
5	6.7	7.6	10.4	9.4	4	**1.8**
6	6.7	7.6	10.4	8.7	4	*1.1*
7	6.8	7.7	10.5	9.5	4	**1.8**
8	6.8	7.8	10.5	10.1	4	**2.3**
9	6.8	7.9	10.5	10.3	4	**2.4**
10	6.9	8	10.7	10.9	4	**2.9**
11	6.9	8	10.7	10.9	4	**2.9**
12	7	8	10.8	10.1	4	**2.1**
13	7.1	7.6	11	9.5	4	**1.9**
14	7.2	7.3	11.1	10	4	**2.7**
15	7.1	8.1	11	10.7	4	**2.6**
16	7.2	9.7	11.1	13.2	4	**3.5**
17	7.8	10.9	12.1	14.6	4	**3.7**
18	7.8	11.5	12.1	14.6	4	**3.1**
19	7.3	11.5	11.3	16.1	4	**4.6**
20	7.3	9.4	11.3	9.9	4	*0.5*
21	7.4	8.4	11.4	9.5	4	*1.1*
22	n/a	10.8	n/a	16.7	n/a	**5.9**
23	n/a	11	n/a	17	n/a	**6.0**
24	n/a	11.6	n/a	17.9	n/a	**6.3**
25	n/a	11.3	n/a	17.5	n/a	**6.2**
26	8	n/a	12.4	n/	4	n/a
27	n/a	11.2	n/a	17.5	n/a	**6.3**
28	n/a	11.4	n/a	17.6	n/a	**6.2**
29	8	n/a	12.4		4	n/a
30	n/a	11.2	n/a	17.3	n/a	**6.1**
31	8.7	n/a	13.4		5	n/a
32	11	n/a	16.1		5	n/a
33	n/a	10.4	n/a	14.5	n/a	**4.1**
34	n/a	9.7	n/a	14	n/a	**4.3**
35	n/a	11.6	n/a	17.9	n/a	**6.3**
36	n/a	11.6	n/a	17.5	n/a	**5.9**

The modeled peak surge elevations of the surge boundaries applied herein are the same as the values under “Stillwater Elevation” at the same transect locations. All elevations are referenced to NGVD29. (Source: Flood Insurance Study, Miami-Dade County, FEMA, 1995)

Appendix D
Canal Stages extracted from USGS Scientific Study Report 2015

NAME	Stage ft Navd88
(E-1)	1.00
(G)	3.00
(H)	3.00
(I)	3.00
(K)	3.00
(L)	3.00
(M)	3.00
(N)	3.00
(O)	3.00
(W-1)	1.00
(W-2)	1.00
(W-3)	1.00
25 ST CANAL AT FEC	1.50
87 AVE DITCH	0.80
ADEMAR PARK DITCH	0.50
AEROJET CANAL	2.50
AIRPORT TO OPA LOCKA CANAL	1.50
ARCH CREEK	0.50
ARROY TRANQUILO WATERWAY	0.50
ARROYO PACIFICO	0.50
ARROYO SERENO	0.50
ATLANTIC WATERWAY	0.25
ATLAS TERMINAL CANAL	0.25
B. GARDENS DITCH	0.50
BAKER'S HAULOVER CUT	0.50
BAL HARBOUR YACHT BASIN	0.50
BAY HARBOR WATERWAY	0.50
BEL-AIRE CANAL	1.00
BEL-AIRE CANAL	3.00
BEL-AIRE CANAL	4.00
BELAIRE SECTION CANAL	2.00
BELLA VISTA BAY	0.25
BIGMAN CANAL	0.75

NAME	Stage ft Navd88
BIRD DRIVE CANAL	3.00
BIRD DRIVE EXTENSION CANAL	3.00
BISCAYNE CANAL	0.50
BISCAYNE CANAL	2.00
BISCAYNE POINT CANAL	0.50
BISCAYNE POINT DITCH	0.50
BISCAYNE RIVER DITCH	0.50
BISCAYNE WATERWAY	0.50
BISCAYNE YACHT AND COUNTRY CLUB	0.25
BLACK CREEK	0.80
BLACK CREEK	1.00
BLACK CREEK	4.00
BROAD CANAL	1.80
BROWARD COUNTY	2.00
BURLINGTON CANAL	2.00
C-1 EXT @ SW 150 ST	4.00
C-100 A SPUR (6)	3.00
C-100 SPUR EXTENSION (BIGMAN)	0.75
C-100A CANAL	2.00
C-100A EXTENSION CANAL	0.75
C-100A SPUR (4)	0.75
C-100A SPUR (5)	2.50
C-100B	2.00
C-102 EXTENSION CANAL	3.00
C-102	0.50
C-102N EXTENSION CANAL	3.00
C-103	0.75
C-103	0.75
C-110	1.50
C-111 BASIN SOUTH	0.50
C-111	1.50
C-111F	1.50
C-113 EXTENSION	3.00
C-113	3.00

NAME	Stage ft Navd88
C-2 CULVERT SW 93 AVE GOLF	0.75
C-357	4.00
C-4 PUMP STATION	3.00
C-6 SPUR @ NW 106 ST	1.50
C-6 TO LAKE AT NW 25 ST	0.50
C-9	1.00
C-9	2.00
C111 EXT NORTH	2.00
CALDER CANAL	1.00
CARD SOUND BASIN	0.50
CARD SOUND BASIN	1.50
CARD SOUND ROAD CANAL	0.50
CARD SOUND ROAD CANAL	1.50
CARD SOUND ROAD DITCH	1.50
CAROL CITY CANAL (A-2)	2.00
CAROL CITY CANAL (A-2B)	2.00
CAROL CITY CANAL (A-3)	2.00
CAROL CITY CANAL (A-4)	2.00
CAROL CITY CANAL (A-7)	2.00
CAROL CITY CANAL (A-8)	2.00
CAROL CITY CANAL (A-9)	2.00
CAROL CITY CANAL (A)	2.00
CAROL CITY CANAL (B-1)	2.00
CAROL CITY CANAL (B)	2.00
CAROL CITY CANAL A-2A	2.00
CAROL CITY CANAL	2.00
COCOPLUM DITCH 2	0.50
COCOPLUM DITCH 3	0.50
COLLINS CANAL	0.50
COMFORT CANAL	0.40
COMFORT CANAL	0.50
COMFORT CANAL	1.50
COMFORT SR836 @ NW 42 AVE	1.50
COOLING CANAL	0.50

NAME	Stage ft Navd88
COOLING CANAL	0.75
COOLING CANALS DISCHARGE	0.50
CORAL BAY WATERWAY	0.50
CORAL GABLES CANAL	0.50
CORAL GABLES CANAL	1.50
CORAL GABLES CANAL	3.00
CORAL GABLES WATERWAY	0.50
CORAL HAVEN LAGOON	3.00
CORAL PARK CANAL	3.00
CORAL WAY CANAL	3.00
CORAL WAY DITCH ENCLOSED	3.00
CORAL WAY SLAB COVERED TRENCH	3.00
CORONADO HARBOR 2ND ADDN WATERWAY	0.50
CUTLER WETLANDS C-1 FLOWWAY	0.50
CUTLER CREEK	0.75
CUTLER DRAIN	2.00
CUTLER DRAIN	2.50
CUTLER DRAIN	0.75
CUTLER DRAIN	3.00
CUTLER DRAIN	4.00
CUTLER RIDGE CANAL	1.00
CUTLER WETLANDS C-1 FLOWWAY	0.50
CUTLER WETLANDS C-1 FLOWWAY	0.80
DADE BROWARD LEVEE	3.50
DAVIS HARBOR WATERWAY	0.50
DRESSELS DAIRY CANAL	1.50
DRESSELS DAIRY CANAL	3.00
EAST ANDOVER CANAL	1.00
EASTERN SHORES 2ND ADD WATERWAY	0.25
EASTERN SHORES WATERWAY	0.25
ENCHANTED LAKE DITCH 1	0.25
ENCHANTED LAKE DITCH 2	0.25
ENCHANTED LAKE DITCH 3	0.25
ENCHANTED LAKE DITCH 4	0.25

NAME	Stage ft Navd88
ENCHANTED LAKE DITCH 5	0.25
ENCHANTED LAKE DITCH 6	0.25
EXISTING SLOUGH	3.00
F. E. C. CANAL	1.50
FDOT DITCH AT SW 227-288 TER	0.80
FEC BORROW DITCH CANAL	1.50
FEC BORROW DITCH	1.50
FINGER LAKES NW 92 AVE	3.00
FIU DITCH	0.25
FLORIDA CITY CANAL	0.50
FLORIDA CITY CANAL	0.75
FLORIDA CITY CANAL	1.50
FLORIDA TURNPIKE	2.00
FLOW RIGHTS ONLY	3.00
GABLES ESTATES WATERWAY	0.50
GOLDEN BEACH WATERWAY	0.25
GOLDEN GLADES CANAL	2.00
GOLDEN GLADES DITCH	2.00
GOULDS CANAL	0.75
GOULDS CANAL	1.50
GOULDS CHANNEL	0.50
GRAHAM'S DAIRY i-75 INTERCH.	2.00
GRAHAMS DAIRY CANAL	1.50
GRAHAMS DAIRY CANAL	2.00
GRAHAMS DAIRY CANAL	3.50
GRAHAMS DAIRY DITCH	2.00
GRATIGNY CANAL	1.50
GRATIGNY ENCLOSURE	1.50
GREYNOLDS PARK	0.25
HARDING TOWNSITE PARK DITCH	0.50
HAWTHORNE AVE CANAL	0.50
HEFTLER HOMES	3.00
HERBERT HOOVER/HOMESTEAD BAYFRONT MARINA	0.50

NAME	Stage ft Navd88
HIGH HOPE NURSERY DITCH	0.75
HIGHLAND OAKS CANAL 20 ft easement	0.25
HIGHLAND OAKS CANAL	0.25
HOMESTEAD AIR BASE CANAL	0.75
HOMESTEAD AIR BASE DITCH	0.75
HOMESTEAD AIR BASE	0.75
HOMESTEAD BAYFRONT PARK	0.50
INDIAN CREEK LAKE	0.50
INDIAN CREEK	0.50
INTRACOASTAL WATERWAY	0.25
INTRACOSTAL WATERWAY	0.25
JOCKEY CLUB CANAL	0.50
JOHN T PEACOCK ESTATES DITCH 1	0.50
JOHN T PEACOCK ESTATES DITCH 2	0.50
KENDALE SPUR CANAL	0.75
KENDALE SPUR CANAL	3.00
KENDALE SPUR CULVERT	3.00
KENDALL LAKES WEST	3.00
KENDALL SPUR (1)	0.75
KENDALL WEST GOLF	3.00
KEYSTONE ARMS DITCH	0.50
KEYSTONE ISLAND WATERWAY	0.50
KINGS POINT CANAL	0.25
L-31	0.60
L-31	0.75
L-31E CANAL	0.50
L-31E	0.50
L-31E	0.75
L-31N	3.50
L-31N	4.00
L-31W CANAL	2.50
L-31W CANAL	4.50
LAGO MAGGIORE	0.50
LAGO MINORE	0.50

NAME	Stage ft Navd88
LAKE BELMAR	0.50
LAKE LUCERNE CANAL	1.00
LAKE WARD	0.50
LAWRENCE WATERWAY	0.40
LIDO CANAL	0.50
LINDGREN CANAL	3.00
LINDGREN CANAL	4.00
LITTLE ARCH @ NE 119 ST	0.50
LITTLE ARCH CANAL	0.50
LITTLE ARCH CREEK	0.50
LITTLE ARCH DRAINAGE EASEMENT	0.50
LITTLE RIVER CANAL	0.50
LITTLE RIVER CANAL	1.00
LOOP CANAL	1.50
LUDLAM GLADES CANAL	1.80
LUDLAM GLADES LAKE	1.80
MARAL ESTATE CANAL	2.00
MARCO CANAL	2.00
MARINA DEL REY WATERWAY	0.25
MATHESON HAMMOCK DITCH	0.50
MAULES LAKE	0.25
MELROSE CANAL	1.50
METRO ZOO	4.00
MIAMI RIVER	0.50
MIAMI RIVER	1.50
MIAMI INTERNATIONAL AIRPORT	1.50
MIAMI SHORES BAY PARK ESTATES WATERWAY	0.50
MILITARY CANAL	0.60
MILITARY CANAL	0.75
MODEL LANDS	0.50
MODEL LANDS	1.00
MOWRY CANAL	2.50
MOWRY CANAL	0.75
MOWRY CANAL	3.50

NAME	Stage ft Navd88
MUD CANAL NW 137 AVE	3.00
MUD CREEK CANAL	3.00
MYSTIC POINTE MARINA	0.25
NARANJA CANAL	2.50
NE 197 ST TO OLETA	0.25
NE 37 AVE WATERSTONE DITCH	2.50
NE 5TH AVE DITCH	0.50
NE 6 AVE 151 ST DITCH	0.50
NEW ARCH CREEK	0.50
NORMANDY WATERWAY	0.50
NORTH BAY CREST CANAL	0.50
NORTH CANAL/POINT LAKE	0.50
NORTH CANAL	0.75
NORTH CANAL	0.75
NORTH DADE CANAL	1.00
NORTH DADE EXT. @ NW 215 ST	1.00
NORTH DADE GOLF @ TPX	1.00
NORTH DADE GOLF CANAL	1.00
NORTH FORK CANAL	0.50
NORTH LINE CANAL	1.50
NORTH LINE CANAL	3.00
NORTH WATERWAY	0.50
NW 107 AVE CANAL WEST	2.00
NW 107 AVE CANAL	2.00
NW 12 ST 117 AVE	3.00
NW 12 ST	3.00
NW 127 AVE	2.00
NW 127 ST CANAL	1.50
NW 150 ST SPUR BISC. PUMP	0.50
NW 17 AVE CANAL	2.00
NW 202 ST CANAL	2.00
NW 25 ST CANAL	1.50
NW 25 ST Canal	3.00
NW 27 AVE CANAL	1.00

NAME	Stage ft Navd88
NW 41 ST DITCH SOUTH	3.00
NW 5 AVE DITCH	0.50
NW 57 AVE CANAL	2.00
NW 58 ST CANAL	1.50
NW 67 AVE DITCH	2.00
NW 69 AVE DITCH MIA - C4	1.50
NW 87 AVE CANAL	1.50
NW 97 AVE CANAL	1.50
NW WELLFIELD CANAL	3.50
OCEANIA CANAL	0.25
OLD CARD SOUND DITCH	1.50
OLD CUTLER BAY WATERWAY	0.50
OLETA RIVER STATE REC AREA DITCH	0.25
OLETA RIVER STATE REC. AREA NORTH DITCH	0.25
OLETA RIVER STATE REC. AREA SOUTH DITCH	0.25
OLETA RIVER	0.25
OPA LOCKA AIRPORT DITCH	1.50
OPA LOCKA CANAL	1.50
OPA LOCKA CANAL	2.00
OPA LOCKA WEST AIRPORT DITCH	2.00
PALM CANAL	2.00
PALM SPRINGS CANAL	1.50
PALM SPRINGS NORTH CANAL	2.00
PELLICAN CANAL	0.50
PENNSUCO	3.50
PETER'S PIKE CANAL	1.50
PETER'S PIKE CANAL	2.00
POINCIANNA WATERWAY	0.25
POINT LAKE	0.50
PRINCETON CANAL	1.50
PRINCETON CANAL	3.50
PRINCETON CANAL	3.80
PRINCETON CANAL	4.00
PRIVATE DITCH	0.25

NAME	Stage ft Navd88
QUAIL ROOST TRAILER PARK CANAL	3.80
REAL SITE	2.00
RED ROAD CANAL	1.50
RED ROAD CANAL	2.00
REDLAND CANAL SECTION II	3.50
REDLAND CANAL	3.50
REPUBLIC LAKE CANAL	3.00
ROCK LAKE	2.00
ROCKMINE DITCH NW 117 AVE	2.00
ROYAL GREEN CANAL	3.00
RUSSIAN COLONY CANAL	2.00
RUSSIAN COLONY CANAL	3.50
SABAL LAKE	0.50
SANS SOUCI ESTATES WATERWAY	0.50
SCHARFS CANAL	0.50
SEABOARD ACRES DITCHES	0.50
SEABOARD ACRES NE 135 ST	0.50
SEABOARD ACRES NE 2 AVE	0.50
SFWMD PUMP STATION	3.00
SNAKE CREEK CANAL	0.25
SNAKE CREEK CANAL	1.00
SNAKE CREEK CANAL	2.50
SNAKE CREEK CANAL	6.00
SNAPPER CREEK CANAL	0.50
SNAPPER CREEK CANAL	0.75
SNAPPER CREEK CANAL	3.00
SNAPPER CREEK EXTENSION CANAL	3.00
SNAPPER CREEK EXTENSION CANAL	3.50
SNAPPER CREEK SERVICE PLAZA	4.00
SOUTH ARCH CREEK	0.50
SOUTH BAY CREST CANAL	0.50
SOUTH DADE LANDFILL E. DITCH	0.75
SOUTH WATERWAY	0.50
SOUTHERN ESTATES CANAL	3.00

NAME	Stage ft Navd88
SPUR #1 CANAL	1.50
SPUR #1 CANAL	2.00
SPUR #4 CANAL	0.50
SPUR 1 EXT. TO GOLF COURSE	1.50
SPUR DITCH NE 18 AVE	0.50
SR 836 @ TPX	3.00
SUNRISE HARBOUR WATERWAY	0.50
SUNSET PARK CANAL	3.00
SUNSWEPT ISLES DITCH (20-FOOT EASEMENT)	0.25
SUNSWEPT ISLES DITCH	0.25
SURPRISE WATERWAY	0.50
SW 101 AVE S. 344 ST FPL	0.50
SW 104 AVE DITCH	1.50
SW 104 ST DITCH 117 AVE	4.00
SW 107 AVE DITCH EAST	0.75
SW 107 AVE DITCH WEST	0.75
SW 107 AVE DITCH WEST	1.50
SW 110 AVE DITCH	0.75
SW 112 AVE DITCH EAST	0.75
SW 112 AVE DITCH WEST	0.75
SW 112 AVE DITCH WEST	1.50
SW 112 AVE DITCH	0.75
SW 114 AVE S. 344 ST	0.50
SW 117 AVE DITCH EAST	0.75
SW 117 AVE DITCH WEST	0.75
SW 117 ST DITCH EAST	0.75
SW 117 ST DITCH WEST	0.75
SW 121 AVE DITCH	0.75
SW 122 AVE CANAL	4.00
SW 122 AVE DITCH WEST	0.75
SW 122 AVE DITCH	4.00
SW 124 AVE S. 344 ST	0.75
SW 125 AVE DITCH	0.75
SW 127 AVE DITCH EAST	0.75

NAME	Stage ft Navd88
SW 127 AVE DITCH WEST	0.75
SW 127 AVE S. 344 ST	0.75
SW 129 AVE S. 344 ST	0.75
SW 130 AVE DITCH EAST	0.75
SW 130 AVE DITCH WEST	0.75
SW 132 AVE CANAL	3.00
SW 132 AVE DITCH EAST	0.75
SW 132 AVE DITCH WEST	0.75
SW 132 AVE DITCH	0.75
SW 134 AVE DITCH EAST	0.75
SW 134 AVE DITCH WEST	0.75
SW 137 AVE DITCH EAST	0.75
SW 137 AVE DITCH WEST	0.75
SW 137 AVE DITCH	0.75
SW 137 AVE MODEL LANDS	1.50
SW 137 AVE	1.50
SW 139 AVE DITCH EAST	0.75
SW 139 AVE DITCH WEST	0.75
SW 139 CT DITCH EAST	0.75
SW 139 CT DITCH WEST	0.75
SW 142 AVE DITCH EAST	0.75
SW 142 AVE DITCH WEST	0.75
SW 142 AVE DITCH	0.75
SW 144 AVE CANAL	3.00
SW 144 AVE DITCH EAST	0.75
SW 144 AVE DITCH WEST	0.75
SW 147 AVE 72 ST	3.00
SW 147 AVE DITCH EAST	0.75
SW 147 AVE DITCH WEST	0.75
SW 154 AVE 85 TERR	3.00
SW 156 AVE 80 ST DITCH	3.00
SW 157 AVE TRADEWINDS	3.00
SW 157 AVE	3.00
SW 167 AVE DITCH WEST	1.50

NAME	Stage ft Navd88
SW 167 AVE DITCH WEST	3.00
SW 168 ST DITCH NORTH	4.00
SW 168 ST DITCH SOUTH	4.00
SW 169 AVE DITCH	1.50
SW 169 AVE	3.00
SW 170 AVE CANAL	3.00
SW 172 AVE DITCH	1.50
SW 182 RD DITCH EAST	1.50
SW 182 RD DITCH WEST	1.50
SW 182 RD STAIRSTEP WEST	1.50
SW 187 AVE DITCH WEST	1.50
SW 187 AVE DITCH	0.80
SW 187 AVE DITCH	1.50
SW 192 AVE DITCH EAST	1.50
SW 192 AVE DITCH WEST	1.50
SW 204 ST	3.80
SW 237 AVE DITCH EAST (CONTEXT RD)	4.00
SW 240 ST DITCH @ TPX	0.80
SW 240 ST DITCH NORTH	0.80
SW 248 ST DITCH	1.50
SW 256 ST DITCH NORTH	1.50
SW 268 ST DITCH NORTH	0.75
SW 268 ST DITCH SOUTH	0.75
SW 272 ST DITCH	0.75
SW 276 ST DITCH	0.50
SW 280 ST DITCH NORTH	0.75
SW 280 ST DITCH SOUTH	0.75
SW 280 ST DITCH	0.50
SW 280 ST DITCH	0.75
SW 284 ST DITCH	0.50
SW 288 ST DITCH	0.50
SW 288 ST DITCH	0.75
SW 292 DITCH WEST OF 107 AVE	0.75
SW 292 ST DITCH	0.75

NAME	Stage ft Navd88
SW 296 ST DITCH NORTH	0.75
SW 296 ST DITCH SOUTH	0.75
SW 296 ST DITCH	0.50
SW 301 ST LEVEE DITCH S.	0.75
SW 304 ST DITCH NORTH	0.75
SW 304 ST DITCH	0.75
SW 308 ST DITCH NORTH	0.75
SW 308 ST DITCH W OF 112 AVE	0.75
SW 308 ST DITCH	0.50
SW 308 ST DITCH	0.75
SW 312 ST DITCH NORTH	0.75
SW 312 ST DITCH SOUTH	0.75
SW 312 ST DITCH	0.50
SW 312 ST DITCH	0.75
SW 312 ST DTICH NORTH	0.75
SW 316 ST DITCH NORTH	0.75
SW 318 ST DITCH	0.75
SW 320 ST DITCH NORTH	0.75
SW 320 ST DITCH SOUTH	0.75
SW 320 ST DITCH SOUTH	0.75
SW 320 ST DITCH	0.75
SW 328 ST DITCH SOUTH	0.75
SW 328 ST S./122 AVE DITCH	0.75
SW 336 ST DITCH NORTH	0.75
SW 336 ST DITCH SOUTH	0.75
SW 352 ST CANAL	1.50
SW 352 ST DITCH	1.50
SW 356 ST DITCH NORTH	1.50
SW 356 ST DITCH SOUTH	1.50
SW 356 ST DITCH	1.50
SW 360 ST DITCH NORTH	1.50
SW 360 ST DITCH SOUTH	1.50
SW 360 ST DITCH	3.00
SW 360 ST ROCKMINE DITCH	1.50

NAME	Stage ft Navd88
SW 368 ST DITCH	1.50
SW 382 ST DITCH NORTH	1.50
SW 384 ST DITCH NORTH	1.50
SW 392 ST DITCH NORTH	1.50
SW 392 ST DITCH SOUTH	1.50
SW 42 ST DITCH	3.00
SW 424 ST DITCH NORTH	1.50
SW 424 ST DITCH	1.50
SW 440 ST AEROJET	2.50
SW 440 ST CANAL	2.50
SW 56 ST MILLER CANAL	3.00
SW 60 ST CANAL	3.00
SW 60 ST GOLF CRS LAKES	3.00
SW 62 ST 139 AVE	3.00
SW 63 ST CANAL	3.00
SW 64 ST CANAL	3.00
SW 70 AVE CANAL	1.80
SW 70 AVE CANAL	2.00
SW 87 AVE CANAL	0.80
SW 92 AVE CANAL	3.00
SW 97 AVE CANAL	3.00
SW 97 AVE DITCH WEST	0.80
SW MANOR CANAL	3.00
SW MARAL ESTATES CANAL	2.00
TAMIAMI AIRPORT DITCH	4.00
TAMIAMI AIRPORT	4.00
TAMIAMI CANAL	0.25
TAMIAMI CANAL	3.00
TATUM WATERWAY	0.50
TPX DITCH @ i-75	2.00
TPX DITCH @ I-75	2.00
TPX DITCH @ SW 72 ST	3.00
TPX DITCH N AT SW 167 AVE	0.75
TPX DITCH WEST	0.75

NAME	Stage ft Navd88
TPX DITCH	2.00
TPX DITCH	2.50
TPX LAKE SW 152 ST	4.00
TPX RAMP DITCH @ CALDER	1.00
TPX RAMP TO SR 836	3.00
TURNBERRY ISLE MARINA YACHT CLUB	0.25
TURNPIKE TOLL STATION	2.00
TWIN LAKES CANAL	1.80
US1 MODEL LANDS	1.50
VENETIAN CANAL	1.50
WAGNER CREEK CANAL	0.50
WATERWAYS CANAL	0.25
WATERWAYS MARINA	0.25
WEST ANDOVER CANAL	1.00
WEST BROOK CANAL	3.00
WESTBROOK CANAL EXT.	3.00
WESTCHESTER CANAL	3.00
WESTWOOD LAKES CANAL	3.00
WILLIAMS ISLE MARINA	0.25
WILLIIAMS ISLE MARINA	0.25

Appendix E
Gated Structure Elevations

Structure	Gated elevation ft-NAVD88
G93	3.2
S118	5
S119	4.9
S123	5.4
S148	5
S165	6.5
S166	6.5
S167	6.5
S176	7
S177	5.5
S179	4.5
S18C	4
S20	4
S20A	4
S20F	4
S20G	4
S21	4.2
S21A	4
S22	4
S25B	4
S26	4
S27	4
S28	4
S29	4